

**FAILURE ANALYSIS OF SURFACE DEFECTS ON ALUMINIUM
EXTRUDATES**

CHONG CHEE HAO

**A project report submitted in partial fulfilment of the
requirements for the award of Bachelor of Engineering
(Honours) Mechanical Engineering**

**Lee Kong Chian Faculty of Engineering and Science
Universiti Tunku Abdul Rahman**

September 2020

DECLARATION

I hereby declare that this project report is based on my original work except for citations and quotations which have been duly acknowledged. I also declare that it has not been previously and concurrently submitted for any other degree or award at UTAR or other institutions.

Signature :



Name : CHONG CHEE HAO

ID No. : 16UEB00551

Date : 27 / 09 / 2020

APPROVAL FOR SUBMISSION

I certify that this project report entitled “**FAILURE ANALYSIS OF SURFACE DEFECTS ON ALUMINIUM EXTRUDATE**” was prepared by **CHONG CHEE HAO** has met the required standard for submission in partial fulfilment of the requirements for the award of Bachelor of Engineering (Honours) Mechanical Engineering at Universiti Tunku Abdul Rahman.

Approved by,

Signature

:



Supervisor

:

DR YEO WEI HONG

Date

:

30 / 09 / 2020

The copyright of this report belongs to the author under the terms of the copyright Act 1987 as qualified by Intellectual Property Policy of Universiti Tunku Abdul Rahman. Due acknowledgement shall always be made of the use of any material contained in, or derived from, this report.

© 2020, Chong Chee Hao. All right reserved.

ACKNOWLEDGEMENTS

First of all, I would like to express my sincere gratitude to my supervisor, Dr Yeo Wei Hong for providing me an interesting industrial research problem to work on. Dr Yeo Wei Hong has been an exceptional advisor, both academically and personally. His support, encouragement, suggestions, discussions and comments throughout my research were invaluable. I was fortunate to have the opportunity to work with him.

I also would like to thank everyone who had contributed to the successful completion of this project. I would like to express my gratitude to Press Metal Berhad for providing samples and some informations for the analysis in this research. This research definitely had widen my horizon on the extrusion and die design.

Also I would like to thank all the technicians and laboratory officers at Universiti Tunku Abdul Rahman (UTAR) for their patience and help in the research.

Finally, I would like to thank my parents and my friends for their assistant and encouragement during the research period.

ABSTRACT

In this investigation, there are two different aluminium alloy (AA6005) extrudate profiles provided to investigate surface defects and seek for any solutions to eliminate or minimise the defects. There were two surface defects found on the extrudates which are pick-up defect and die line defect. Pick-up defect has a teardrop shape and die line defect has black line streak appearance. These defects may be influenced by exit temperature of extrudate, process parameters, die bearing condition and billet quality. Effects of extrusion process parameters on the extrusion process were studied through finite element method (FEM) as the extrusion process parameters have significant effect on the die bearing wear and surface finish of aluminium extrudate. Also, a subroutine that calculate die wear depth based on modified Archard's wear model was developed and used to study die wear behaviour on the measured points. It is noted that the highest die wear depth is found at die bearing entrance, up to 63.18 % difference compared to lowest die bearing wear depth. This is due to largest billet deformation occurs in this area. Pick-up defect is temperature sensitive and extrudate's exit temperature cannot exceed its eutectic point (555 °C). Ram speed is suggested to reduce to below 3 mm/s or decrease initial billet temperature to below 480 °C according to the extrusion process parameters given by the company in order to ensure extrudate's exit temperature is below its eutectic point. On the other hands, die line defect is mainly due to imperfections of die bearing surface. This defect can be minimised by reducing ram speed to below 3 mm/s or increasing initial billet temperature to above 480 °C according to the extrusion process parameters given by the company to reduce extrusion force to below 1452.582 tons which can decrease chances of spalling of nitriding layer. However, changing initial billet temperature can affect extrusion force which would affect die bearing wear and surface finish of aluminium extrudate. Die bearing condition and billet quality were not investigated in this research but re-nitriding and polishing of die and using better aluminium billet quality are suggested to eliminate or minimise both defects.

TABLE OF CONTENTS

DECLARATION		i
APPROVAL FOR SUBMISSION		ii
ACKNOWLEDGEMENTS		iv
ABSTRACT		v
TABLE OF CONTENTS		vi
LIST OF TABLES		x
LIST OF FIGURES		xi
LIST OF SYMBOLS / ABBREVIATIONS		xvi
LIST OF APPENDICES		xviii
CHAPTER		
1	INTRODUCTION	1
1.1	General Introduction	1
1.2	Importance of the Study	2
1.3	Problem Statement	3
1.4	Aim and Objectives	3
1.5	Scope and Limitation of the Study	4
1.6	Contribution of the Study	5
1.7	Outline of the Report	5
2	LITERATURE REVIEW	7
2.1	Introduction to Aluminium Extrusion	7
2.1.1	Aluminium Extrusion Application	8
2.1.2	Aluminium Extrusion Process	9
2.2	Type of Metal Extrusion	10
2.2.1	Direct Extrusion	10
2.2.2	Indirect Extrusion	11
2.2.3	Hydrostatic Extrusion	11
2.2.4	Impact Extrusion	12
2.3	Characteristic of Extrusion Process	13

	2.3.1	Metal Flow Pattern	13
	2.3.2	Pressure Distribution on Die Surface	13
	2.3.3	Temperature Control	15
2.4		Main Components of Metal Extrusion Machine	18
	2.4.1	Ram	18
	2.4.2	Dummy Block	18
	2.4.3	Die	19
2.5		Characteristics of Die	19
	2.5.1	Type of Die	19
	2.5.2	Die Design	21
	2.5.3	Die Material	23
	2.5.4	Die Hardening Treatment	24
	2.5.5	Die Hardness	26
	2.5.6	Die Correction	27
	2.5.7	Die Wear	27
	2.5.8	Die Fatigue Failure	29
2.6		Aluminium Extrudate Surface Defects	31
	2.6.1	Pick-up Defect	31
	2.6.2	Die Line Defect	32
	2.6.3	Blister	33
	2.6.4	Tearing	33
2.7		Summary	34
3		METHODOLOGY AND WORK PLAN	35
	3.1	Introduction	35
	3.2	Surface Defects Analysis of Extrudate Samples	35
	3.2.1	Degreasing	37
	3.2.2	Etching	38
	3.2.3	Desmutting	39
	3.2.4	Cutting	40
	3.2.5	Microscopy Analysis	41
	3.2.6	Energy Dispersive X-Ray (EDX) Analysis	41
	3.3	Numerical Simulation of Extrusion Process	43

3.3.1	3D Model of Extrudate and Extrusion Die	43
3.3.2	Bearing Length Optimisation	45
3.3.3	Mesh Generation of Whole Numerical Model	48
3.3.4	Process Definition	50
3.3.5	Development of User-Defined Wear Subroutine	52
3.3.6	Extrusion Force Formula	54
4	RESULTS AND DISCUSSION	55
4.1	Introduction	55
4.2	Microscopy Analysis	55
4.2.1	Pick-up Defect	55
4.2.2	Formation Mechanisms of Pick-up Defect	60
4.2.3	Die Line	62
4.2.4	Formation Mechanism of Die Line Defect	64
4.3	Mesh Convergence Test	65
4.4	Simulation Results	66
4.5	Effect of Ram Speed	68
4.5.1	Temperature Distribution	68
4.5.2	Average Temperature of Billet and Die	69
4.5.3	Pressure Distribution	71
4.5.4	Extrusion Force	72
4.5.5	Wear Coefficient and Die Hardness	73
4.5.6	Die Wear Behaviour	74
4.5.7	Maximum Extruded Profile Length	76
4.6	Effect of Initial Billet Temperature	79
4.6.1	Extrusion Force	79
4.6.2	Die Wear Behaviour	80
4.7	Effect of Initial Die Temperature	82
4.7.1	Extrusion Force	82
4.7.2	Die Wear Behaviour	83

4.8	Causes and Preventions of Pick-up Defect	85
4.9	Causes and Prevention of Die Line Defect	87
4.10	Summary	89
5	CONCLUSIONS AND RECOMMENDATIONS	90
5.1	Conclusions	90
5.2	Recommendations for future work	91
	REFERENCES	93
	APPENDICES	99

LIST OF TABLES

Table 2.1: SKD 61 Chemical Composition.	24
Table 3.1: Defined Number of Mesh of 4823 Die and 4824 Die for Mesh Convergence Analysis.	50
Table 3.2: Chemical Composition (%) of aluminium alloy AA6005.	50
Table 3.3: Extrusion Process Parameters given from the Local Aluminium Extrusion Company.	51
Table 3.4: Process Parameters Defined in the Simulation to Study the Effect of Ram Speed on Extrusion Process and Die Wear Behaviour.	51
Table 3.5: Process Parameters Defined in the Simulation to Study the Effect of Initial Billet Temperature on Extrusion Process and Die Wear Behaviour.	52
Table 3.6: Process Parameters Defined in the Simulation to Study the Effect of Initial Die Temperature on Extrusion Process and Die Wear Behaviour.	52
Table 4.1: Wear Coefficient and Die Hardness of 4823 Die at Different Ram Speed.	74
Table 4.2: Wear Coefficient and Die Hardness of 4824 Die at Different Ram Speed.	74
Table 4.3: Results Verification for Own-developed Equations.	77
Table 4.4: Maximum Extruded Profile Length for 4823 Die.	78
Table 4.5: Maximum Extruded Profile Length for 4824 Die.	78

LIST OF FIGURES

Figure 1.1: Basic Components in the Extrusion Process (Bombac, et al., 2013).	1
Figure 1.2: Depiction of Different Area Occurring on the Die Bearing Surface (Bombac, et al., 2013).	2
Figure 2.1: Global Market Share for Aluminium Extrusion Products, by Region, 2017 (%) (Market Research Future, 2019).	8
Figure 2.2: Multiport Tube Aluminium Extruded Profile for Heat Exchanger in Air Conditioning (Trumony Aluminium Limited, 2020).	9
Figure 2.3: Direct Extrusion Process (Kalpakijian and Schmid, 2010).	10
Figure 2.4: Indirect Extrusion Process (Kalpakijian and Schmid, 2010).	11
Figure 2.5: Hydrostatic Extrusion Process (Kalpakijian and Schmid, 2010).	12
Figure 2.6: Impact Extrusion Process (Kalpakijian and Schmid, 2010).	12
Figure 2.7: Different Metal Flow Patterns in Extrusion (Clode and Sheppard, 1990).	13
Figure 2.8: Pressure Distribution on Die Surface (Mori, et al., 2002).	14
Figure 2.9: Graph of Extrusion Pressure versus Ram Stroke (Mori, et al., 2002).	15
Figure 2.10: Temperature on the die at different distances from the bearing surface (TC 1 = 0.19 mm, TC 2 = 0.95 mm, TC 3 = 1.28 mm, TC 4 = 1.68 mm) (Terčelj, et al., 2005).	16
Figure 2.11: Direct Extrusion with Dummy Block (Saha, 2000).	18
Figure 2.12: Solid Die (Oamar, Pervez and Chekotu, 2018).	20
Figure 2.13: Hollow Die (Oamar, Pervez and Chekotu, 2018).	20
Figure 2.14: Semi Hollow Die (Oamar, Pervez and Chekotu, 2018).	21
Figure 2.15: Unbalanced Profile of Extruded Product (Butdee, Noomtong and Tichkiewitch, 2008).	22
Figure 2.16: Microstructure of Nitried Steel die (Terčelj and Kugler, 2017).	26

Figure 2.17: Relationship between Compound Layer Thickness and Wear Rate (Krishnaraj, et al., 1997).	26
Figure 2.18: Wear of die surface: (A) Formation of crack, (B) Removed nitride layer, (C) Formation of crater, (D) Formation of furrow (Bombac, et al., 2013).	29
Figure 2.19: Simulation Results of Von Mises maximum Stress and Maximum Principle Strain using Abaqus (Tong, et al., 2013).	31
Figure 2.20: Pick-up Defect (Fourmann, 2017).	32
Figure 2.21: Die Line Defect (Fourmann, 2017).	32
Figure 2.22: Blister (Fourmann, 2017).	33
Figure 2.23: Tearing (Fourmann, 2017).	34
Figure 3.1: Aluminium Extruded Products: (a) 4823, (b) 4824.	35
Figure 3.2: Flowchart of Workplan.	37
Figure 3.3: Aluminium Extruded Product (4824) Immersed in Acetone Solution.	38
Figure 3.4: Aluminium Extruded Product (4824) Immersed into Etching Solution (10% Sodium Hydroxide and 60% Distilled Water).	39
Figure 3.5: Aluminium Extruded Product (4824) Immersed into Desmutting Solution (40% Nitric Acid and 60% Distilled Water).	40
Figure 3.6: Cutting Saw.	40
Figure 3.7: Optical Microscope.	41
Figure 3.8: Holders for Scanning Electron Microscope (SEM) with Energy Dispersive X-ray (EDX) Analysis.	42
Figure 3.9: Scanning Electron Microscope (SEM) with Energy Dispersive X-ray (EDX) Analysis.	42
Figure 3.10: Three-dimensional Shape of Extruded Profile (4823).	43
Figure 3.11: Three-dimensional Shape of Extruded Profile (4824).	44
Figure 3.12: Three-dimensional Shape of Mandrel (a) and Die (b) (4823).	45

Figure 3.13: Three-dimensional Shape of Mandrel (a) and Die (b) (4824).	45
Figure 3.14: Optimised 3D Drawing of Bearing of 4823 Die.	46
Figure 3.15: Optimised 3D drawing of Bearing of 4824 Die.	46
Figure 3.16: Relative Exit Speed Difference of Before (a) and After (b) Bearing Length Optimisation for 4823 Die.	47
Figure 3.17: Relative Exit Speed Difference of Before (a) and After (b) Bearing Length Optimisation for 4824 Die.	47
Figure 3.18: Mesh Generation of Whole Numerical Model for 4823 Die.	49
Figure 3.19: Mesh Generation of Whole Numerical Model for 4824 Die.	49
Figure 4.1: Location of Pick Up Defect on 4824 Extrudate Surface.	56
Figure 4.2: Appearance of Pick-up Defect on 4824 Extrudate Surface at Location 1 Before (a) and After (b) Etching Treatment.	56
Figure 4.3: Optical Microscope Showing Pick-up Defect on 4824 Extrudate Surface at Location 1.	57
Figure 4.4: Appearance of Pick-up Defect on 4824 Extrudate Surface at Location 2 (upper) and 3 (bottom) Before (a) and After (b) Etching Treatment.	57
Figure 4.5: Optical Microscope showing Pick-up Defect on 4824 Extrudate Surface at Location 2.	58
Figure 4.6: Optical Microscope showing Pick-up Defect on 4824 Extrudate Surface at Location 3.	58
Figure 4.7: Appearance of Pick-up Defect on 4824 Extrudate Surface at Location 4 Before (a) and After (b) Etching Treatment.	59
Figure 4.8: Optical Microscope showing Pick-up Defect on 4824 Extrudate Surface at Location 4.	59
Figure 4.9: EDX Analysis at Pick-up Defect Location.	60
Figure 4.10: Cross Section of Die and Extrudate During Extrusion Process When Pick-up Defect was formed (Peris, 2007).	61

Figure 4.11: Cross Section of Extrudate Flowing on the Die Bearing Surface (Peris, 2007).	62
Figure 4.12: Location of Die Line on 4823 Extrudate Surface.	62
Figure 4.13: Die Line Appearance on 4823 Extrudate Surface Before (a) and After (b) Etching Treatment.	63
Figure 4.14: Optical Microscope showing Die line on 4823 Extrudate Surface.	63
Figure 4.15: EDX Analysis at Die Line Defect.	64
Figure 4.16: Cross Section of Die and Extrudate During Extrusion Process When Die Line Defect was formed (Peris, 2007).	65
Figure 4.17: Mesh Convergence Analysis for 4823 Die.	66
Figure 4.18: Mesh Convergence Analysis for 4824 Die.	66
Figure 4.19: Measured Points on Metal Flow in Die 4823.	67
Figure 4.20: Measured Points on Metal Flow in Die 4824.	67
Figure 4.21: Temperature of Measured Points on 4823 Die at Different Ram Speed.	69
Figure 4.22: Temperature of Measured Points on 4824 Die at Different Ram Speed.	69
Figure 4.23: Average Temperature on Billet and Die Temperature at Different Ram Speed (4823 Die).	70
Figure 4.24: Average Temperature on Billet and Die Temperature at Different Ram Speed (4824 Die).	70
Figure 4.25: Pressure on the Measured Points at Different Ram Speed (4823 Die).	71
Figure 4.26: Pressure on the Measured Points at Different Ram Speed (4824 Die).	72
Figure 4.27: Extrusion Force at Different Ram Speed (4823 Die).	73
Figure 4.28: Extrusion Force at Different Ram Speed (4824 Die).	73
Figure 4.29: Distribution of Die Wear Depth on Measured Points at Different Ram Speed (4823 Die).	75

Figure 4.30: Distribution of Die Wear Depth on Measured Points at Different Ram Speed (4824 Die).	76
Figure 4.31: Extrusion Force at Different Initial Billet Temperature for 4823 Die.	80
Figure 4.32: Extrusion Force at Different Initial Billet Temperature for 4824 Die.	80
Figure 4.33: Distribution of Die Wear Depth on Measured Points at Different Initial Billet Temperature (4823 Die).	81
Figure 4.34: Distribution of Die Wear Depth on Measured Points at Different Initial Billet Temperature (4824 Die).	82
Figure 4.35: Extrusion Force at Different Initial Die Temperature for 4823 Die.	83
Figure 4.36: Extrusion Force at Different Initial Die Temperature for 4824 Die.	83
Figure 4.37: Maximum Die Wear Depth at Different Initial Die Temperature for 4823 Die.	84
Figure 4.38: Maximum Die Wear Depth at Different Initial Die Temperature for 4824 Die.	85
Figure 4.39: Phase Diagram for Aluminium Alloy AA6xxx with Magnesium Content (Total Materia, 2014).	86

LIST OF SYMBOLS / ABBREVIATIONS

T	temperature, K
r	radius, m
λ	heat conductivity, W/m
A	heat transfer coefficient, W/m ³ K
S	depth, m
O	offset, m
P	pressure, MPa
b	fatigue strength exponent
c	fatigue ductility exponent
E	modulus of elasticity
N_f	number of fatigue cycle
σ_{max}	maximum stress, MPa
σ_a	stress amplitude, MPa
σ_m	mean stress, MPa
σ'_f	fatigue strength coefficient, MPa
ε_a	strain amplitude
ε'_f	fatigue ductility coefficient
FEM	finite element method
ALE	arbitrary lagrarian-eulerian
SEM	scatter electron microscope
XRD	X-ray diffraction
Al	aluminium
Mg_2Si	magnesium silicide
C	carbon
S	sulphur
P	phosphate
Mn	manganese
V	vanadium
Cr	chromium
Mg	magnesium
NaOH	Sodium Hydroxide

W	wear, m
K	wear coefficient
H	die hardness
L	relative length between extrudate and die
A_o	area of billet before extrusion, m^2
A_f	area final profile, m^2
F	extrusion force, N
x	number of extrusion cycle
T_{max}	maximum tolerance, m
W_{max}	maximum wear depth, m
$L_{extruded}$	maximum extruded length
L_{billet}	metal billet length
R	extrusion ratio
SEM	scanning electron microscope
EDX	energy dispersive x-ray spectroscopy

LIST OF APPENDICES

APPENDIX A: Graphs for Effect of Initial Billet Temperature (4823 Die).	99
APPENDIX B: Graphs for Effect of Initial Billet Temperature (4824 Die).	103
APPENDIX C: Tables of Maximum Extruded Length Under Various Initial Billet Temperature (4823 Die and 4824 Die).	107
APPENDIX D: Graphs for Effect of Initial Die Temperature (4823 Die).	108
APPENDIX E: Graphs for Effect of Initial Die Temperature (4824 Die).	112
APPENDIX F: Tables of Maximum Extruded Length Under Various Initial Die Temperature (4823 Die and 4824 Die).	116

CHAPTER 1

INTRODUCTION

1.1 General Introduction

Extrusion is a very common manufacturing process due to its versatility for producing products with various complex design of products, while having achieving desired mechanical property and cosmetics goals especially for aluminium alloy. Extrusion is a metal forming process where the heated metal billet will be pushed by a hydraulic press with ram towards the die (refer to Figure 1.1). Die has a distinct shape that can shape the metal billet into desired profile shape when metal billet is pushed through opening profile of the die. Aluminium extruded products are used in many industries such as construction, aerospace, automotive and so on. Some of the extruded products were manufactured for decoration purpose. Hence, surface defects formed on the extruded products have been a concern as it could degrade the aesthetic look of the products, while some may affect the mechanical properties of the products (Clode and Sheppard, 1990).

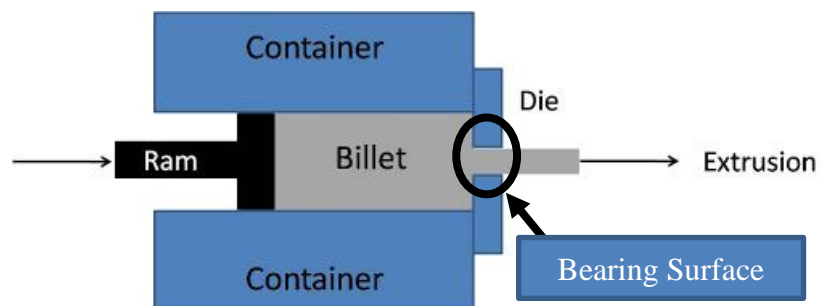


Figure 1.1: Basic Components in the Extrusion Process (Bombac, et al., 2013).

The surface defects could be found on the extruded products are die line, pick-up, tearing, blistering and so on. The defects formed on products are mainly due to the extrusion process and die bearing condition. Despite the surface defects found on the aluminium extrudate has been a major problem in the extrusion process, there is very little documented technical literature or systematic study on the surface defects. The most prevalent surface defects could be found on the extruded products are pick-up and die line in aluminium

alloy (Arif, et al., 2002). Clode and Sheppard (1990) pointed out that the surface defects formed on the extrudate are due to the interaction of adhering aluminium layer on die bearing condition and die bearing surface (die land) during extrusion process (refer to Figure 1.2).

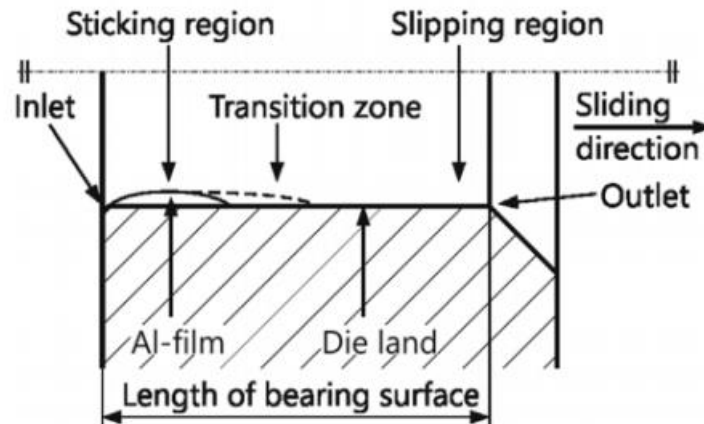


Figure 1.2: Depiction of Different Area Occurring on the Die Bearing Surface (Bombac, et al., 2013).

1.2 Importance of the Study

Despite the surface defects found on the aluminium extrudate has been a major problem in the extrusion process, there is very little documented technical literature or systematic study on the surface defects. In order to minimise the surface defects on the aluminium extrudate, it is very important to understand the surface defects' formation of origin and their formation mechanism. Some investigators had proposed that extrusion process parameter is the main cause to the die wear and results in poor surface finish of products (Peris, 2007). This is due to the light of extrusion processes such as temperature, pressure and so on have significant impact on the die bearing wear and surface finish of the aluminium extrudate. Therefore, this study will investigate the effect of extrusion process parameters on the extrusion process to minimise the surface defects formed on the extrudate during extrusion process. This is because process parameters have great effect on the temperature and pressure in the extrusion process. Also, formation mechanism of the surface defects is studied as well to understand origin of formation and minimise the surface defects.

1.3 Problem Statement

Most of the surface defects found on that aluminium extruded products occurs during aluminium hot extrusion process. The appearance of surface defects on the products could affect the aesthetic look of the products while some would affect the products' mechanical properties. Due to these issues, these products will be rejected by customers and disposed. Therefore, it can affect production of the products because it takes time to do the die correction or review the extrusion process to eliminate or minimise the defects on the extrudate. In addition, surface finish of the products can have direct impact on the cost or profitability of the company because there is waste of resources and it takes energy and costs to recycle the products back into billet.

There are numerous surface defects could be found on the extrudate. The most serious defects that could normally found on the aluminium alloy AA6xxx series are pick-up defect and die line defects (Clode and Sheppard, 1990). There are a lot of researches about die wear to improve die construction and prolong the die service lifetime (Bombac, et al., 2013). However, there is very little documented technical literature on the origin of defects formation. There are some literature reported that die wear condition that causes surface defects on extrudate (Bombac, et al., 2013). Some reported that it could be due to quality of billet, which has inadequate homogenization (Matienzo, et al., 1983). While some investigators had proposed that extrusion process parameter is the main cause to the die wear and results in poor surface finish of products (Peris, 2007). The extrusion process parameters not only can affect die bearing condition but also affect the surface quality of the extrudate.

Therefore, it is important to identify the formation mechanism of the defects found on the extrudate. Also, effect of extrusion process parameters on the quality of extrudate will be investigated as the process parameters have significant effect on the temperature and pressure in the extrusion process.

1.4 Aim and Objectives

The aim of this research is to investigate surface defects found on the aluminium extrudates in relation to the process parameters. The extrusion process simulation and surface defects found on the aluminium alloy extrudate

are investigated to seek a possible origin to the defects. The objective of this research:

- i) To identify defects formation mechanism on the aluminium alloy extrudate surface.
- ii) To investigate the effect of extrusion process parameters on the quality of the extrudate.
- iii) To propose suitable improvement measures can be done to eliminate or minimize surface defects on extrudate.

1.5 Scope and Limitation of the Study

Microstructural analysis was carried out to examine the surface defects of extrudate samples given under optical microscope. Before the examination, degreasing, etching and desmutting are needed to clean the grease and remove oxide layer on the extrudate surface after anodising process, in order to have clear image of surface defects under optical microscope. The surface defects found on the extrudate surface was identified and studied on the origin formation.

In this research, study on the effect of process parameter on the extrusion process was done by using finite element method (FEM). The extrusion process is simulated by means of Inspire Extrude Metal Student Edition Simulation software (formerly known as HyperXtrude). Through the series of numerical results, effect of ram speed, effect of initial metal billet temperature and initial die temperature on the extrusion process, such as temperature distribution, extrusion force, pressure distribution and so on are investigated to seek any improvements could be done to eliminate or minimise the defects. In addition, a subroutine that calculate die wear depth based on modified Archard's wear model was developed and used to study die wear behaviour on the measured points. With this model, sections with severe wear could be identified and some improvement could be done to improve the die service lifetime. Also, with the calculated die wear depth, maximum extrusion length can be predicted as well before unacceptable dimension tolerance is reached where the dimension is beyond scope.

There are some limitations in this project. Since dies are not given in this project, there is no investigation on the die bearing surface condition. Die

bearing surface is the main part where the flowing material has direct contact with and surface defects are caused by the wear of the bearing surface. In addition, properties of the aluminium billet are not investigated as well. Although there are some limitations in this research, any possible improvement of the die bearing condition and properties of aluminium billet could be proposed to eliminate or minimise the surface defects formed on the aluminium alloy extrudate.

1.6 Contribution of the Study

There are a lot of investigations of die wear on the bearing surfaces of nitrided dies for aluminium hot extrusion to prolong the die service lifetime. However, there is little documented research in the technical literature on the origin of defects formation. In this research, surface defects found on the aluminium extrudate samples are identified and characterized. Formation mechanisms of these defects are identified as well. In addition, effect of extrusion process parameters on the quality of extrudate is evaluated and improvements on the extrusion process are suggested to minimise the defects. Therefore, practical extrusion process can be evaluated.

1.7 Outline of the Report

In this paper, there are five chapters:

Chapter 1 discusses general introduction of aluminium alloy extrusion, problem statement that had been facing before this research, objectives, scope and limitations of this study and contribution of the study.

Chapter 2 is about literature review of this research, including introduction to aluminium extrusion, type of metal extrusion, characteristics of metal extrusion, surface defects on the aluminium alloy extrudate and so on. All the information was solely based on article and research papers of professionals.

Chapter 3 is about methodology has been carried out for this research. This chapter reveals all the geometric modelling information, material properties, process parameter defined in the simulation process as well as meshing generation information. In addition, process about degreasing, etching, desmutting are explained and done for preparation of examination under optical microscope.

Chapter 4 is about results obtained from simulation and experiments. This chapter will reveal the results obtained from extrusion process simulation and surface defects observed under optical microscope. Next, formation of surface defects found on aluminium alloy extrudate will be discussed in relation to the process parameter and any other methods that could eliminate the defects.

Chapter 5 is about conclusion of the whole research with the results obtained through extrusion process simulation and laboratory experiments. The conclusion made is based on objective to accomplish in this research. Also, future works or study will be discussed for this research.

CHAPTER 2

LITERATURE REVIEW

2.1 Introduction to Aluminium Extrusion

Metal extrusion is a very famous and multi-faceted manufacturing process. The extruded materials could be aluminium, copper, steel, magnesium and lead. However, aluminium is the most common material used for metal extrusion due to its versatility and durability and aluminium extrusion is the main topic in this paper. The market for aluminium-extruded products is growing rapidly around the world for over past 10 years and it still growing steadily until today. According to Market Research Future (2019), the global market demand for aluminium-extruded products was valued at around USD 44001.1 million in 2018 and it is expected to grow 6.5 % every year, reaching USD 68.5 billion by 2025. The automotive industry has the most use of aluminium-extruded products due to factors such as intention on reducing the weight cars which will save the consumption fuel and the introduction various initiatives from government to attract foreign direct investments (Industry Research, 2019).

The surging demand of aluminium-extruded products in construction in the emerging countries of Asia- Pacific is expected to boost the global market growth during forecast period (Market Research Future, 2019). Recently, China has dominated more than 40% of the global market share, expected to have 8 % growing rate (Industry Research, 2019). In addition, India is also fledging market for aluminium extrusion as the infrastructure is having major overhaul and aluminium-extruded products has their main choice to meet strict geometric, mechanical property, cosmetic goals and cost-effective goal.

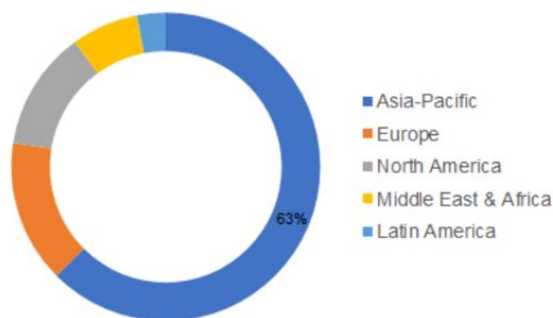


Figure 2.1: Global Market Share for Aluminium Extrusion Products, by Region, 2017 (%) (Market Research Future, 2019).

2.1.1 Aluminium Extrusion Application

Due to aluminium's versatility and durability properties, aluminium-extruded products are widely applied in various industries such as aerospace, automotive and construction sectors. These products are usually come in long size such as rods, tubes, wire and complicated shape profile. By far, building and construction industries have the greatest volume of usage of aluminium-extruded products in the form of frames and decorative trim. Aluminium has been the best material used in construction sector` due to distortion resistance towards extreme weather and building movement. It has great flexibility under load which can spring back from an impact. Aluminium has also a naturally formed thin film, known as aluminium oxide which makes it corrosion resistance towards extreme weather (Davis, 2011).

In automotive industry, strength-to-weight ratio material is highly desired (Davis, 2011). Aluminium extrusion has been their ideal material and it is usually used for engine block, transmission housing, car chassis and as well as components part for vehicle. Having lightweight material, vehicle could also reduce fuel consumption to produce more power to carry the weight, resulting in reducing emission. It has been the main reason why aluminium extrusion is growing extensively in these years. Besides, aluminium has also great thermal conductivity, its thermal conductivity is three times higher than steel (Davis, 2011). This property makes the aluminium extrusion is applied for automobile radiator, air conditioner, condenser tube, nuclear reactor, pharmaceutical thawing units, and heating and cooling device used in electronic devices.

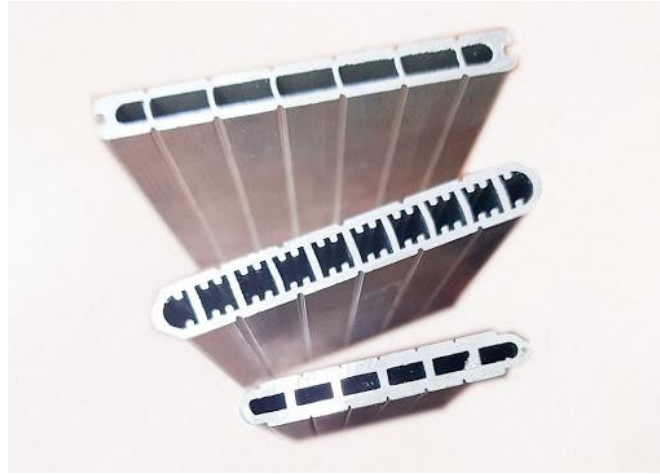


Figure 2.2: Multiport Tube Aluminium Extruded Profile for Heat Exchanger in Air Conditioning (Trumony Aluminium Limited, 2020).

2.1.2 Aluminium Extrusion Process

Extrusion is a plastic deformation process where a metal billet placed in the container and being pressed by hydraulic press by a ram or steam towards die profile opening and final product shape will be produced in this way depending on the die profile (Schey, 1999). Each billet is extruded individually, thus extrusion is a batch or semi-continuous operation. Depending on the required ductility of the material, the extrusion process can be carried out at room temperature (known as cold extrusion) or elevated temperature (known as hot extrusion). In hot extrusion process, the aluminium billet is usually preheated at between 450 °C and 500 °C and will pass through the die profile opening where exit profile speed at between 5 m/min and 100 m/min (Shahriar, Torgeir and Sigurd, 1996). This process could cause bearing surface of die temperature could reach up to 600 °C by the deformation that follows the extreme area reduction when a profile is formed out of a massive metal billet (Bjork, Westegard and Hogmark, 2001). In order to carry out the process smoothly and produce a flawless, a study on the temperature, chemical composition of the metal to be extruded, extrusion ratio of die, ram/stem speed, material flow through the die, profile shape, die design, dimension should be studied which will significantly influence service lifetime of the die.

2.2 Type of Metal Extrusion

Extrusion can be carried out in different process and condition depends on the desired product's properties, its complicity and flow characteristics of extruded product. There are basically four mechanisms used for metal extrusion; direct extrusion (forward extrusion), indirect extrusion (backward extrusion), hydrostatic extrusion and impact extrusion (pressing extrusion) and will be explained briefly in the following sections.

2.2.1 Direct Extrusion

In direct extrusion (Figure 2.3), also known as forward extrusion, metal billet is placed in a container and pushed towards opening die by hydrostatic press (Schey, 1999). The billet is usually preheated. The die opening could be round or any other shape, depending on desired profile shape. The dummy block is used to protect tip of pressing stem, especially in hot extrusion. During the process, part of the extrusion load applied will be used to deal with the friction occurs between the metal billet and container wall due to shear effect acting on inner materials on the slower moving material to the container wall (Tempelman, Shercliff and Eyben, 2014). This friction will lead to heat generation, which will affect mechanical properties and surface finish of the extruded product. If the friction between the container wall and metal billet is significant, it will result the central region of metal billet will flow at higher speed towards die than material flowing near to the container wall due to friction, inhomogeneous flow will occur (Guo and Yang, 2014). Therefore, a proper research should be done for this type of extrusion to get optimal operation, includes die design, temperature, ram speed and so on.

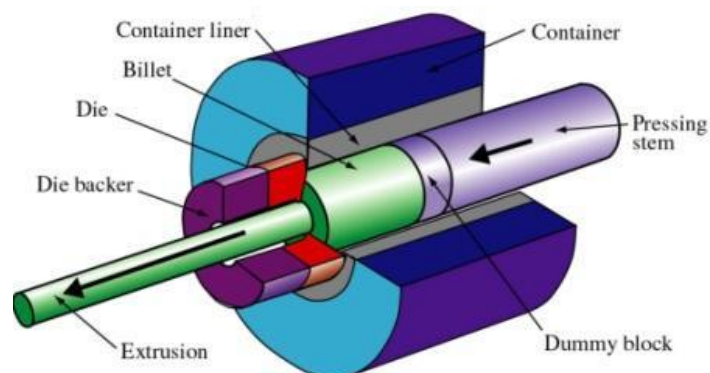


Figure 2.3: Direct Extrusion Process (Kalpakijian and Schmid, 2010).

2.2.2 Indirect Extrusion

In indirect extrusion (Figure 2.4), also known as reverse, inverted or backward extrusion, die moves towards unextruded metal billet (Schey, 1999). The billet is usually preheated. Unlike the direct extrusion, indirect injection doesn't have friction occurs between billet and container wall problem. Additionally, it has several advantages over direct injection. Lower extrusion load is required for process, thus smaller cross section product can be done. Since there is no occurrence of friction in this process, there is heat generation which leads to rise in temperature and the metal flow will be more uniform, thus less tendency to have defects in extruded products and prolongs tool service lifetime (Guo and Yang, 2014). This process is usually done in hot working as well.

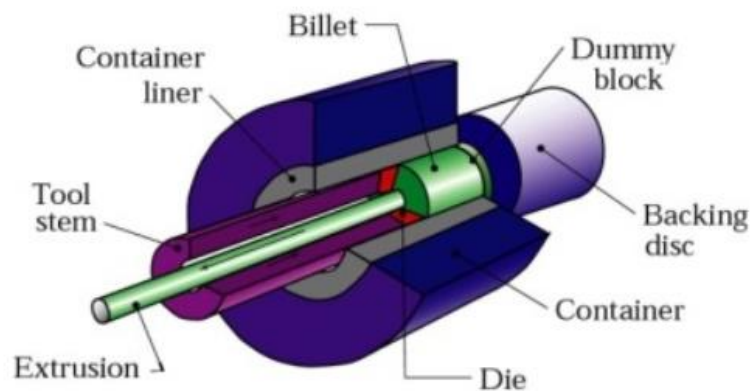


Figure 2.4: Indirect Extrusion Process (Kalpakijian and Schmid, 2010).

2.2.3 Hydrostatic Extrusion

In hydrostatic extrusion (Figure 2.5), the metal billet is immersed in fluid filled in container and it has smaller in diameter than the container, and pressure is transmitted to the fluid by ram, so there is no direct contact between billet and container wall (Schey, 1999). Since the container is filled with fluid, there is no chafing between billet and container wall. As the billet is applied with uniform hydrostatic pressure, it doesn't get upset when filling the bore of the container, resulting in large length to diameter ratio or it may have irregular section (Guo and Yang, 2014). The extruded products usually will have good surface finish and great dimension accuracy.

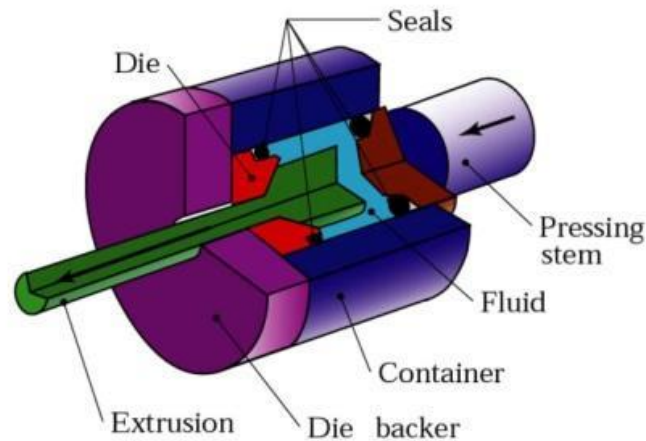


Figure 2.5: Hydrostatic Extrusion Process (Kalpakijian and Schmid, 2010).

2.2.4 Impact Extrusion

In impact extrusion (Figure 2.6), products are formed at high pressure and high efficiency. The billet is typically is not preheated and this process is carried at room temperature. In this process, lubricated slug is placed in the die cavity and punch will press against the metal billet, resulting in flow back of metal and wrap around the punch via opening between the die and the punch (Guo and Yang, 2014). The material to be extruded in this process is usually softer in nature such as tin, aluminium and lead. The product usually is small in size and in cylindrical shape.

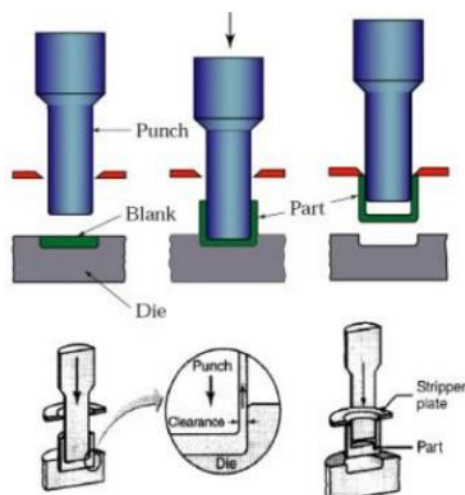


Figure 2.6: Impact Extrusion Process (Kalpakijian and Schmid, 2010).

2.3 Characteristic of Extrusion Process

In extrusion, there are some characteristics should be taken into considerable while carrying out the process as these parameters will affect the surface quality and mechanical properties of the products.

2.3.1 Metal Flow Pattern

It is important to study the metal flow pattern in the extrusion process as it implies friction between billet and container wall that would affect the quality of the extruded product. Pearson and Parkins (1960) had done investigation on this metal flow pattern in extrusion using gridded, spilt billet method and result in quasi-static flow patterns that are categorised into four classes: S, A, B and C (Figure 2.7). Flow pattern S is found in a condition where no chafing between billet and container wall is found during homogenous material whereas the flow pattern occurs in a condition where friction at the interface only (Qamar, 2010). Flow pattern A has separate metal zone (dead metal zone) found at the corner where of the leading of billet is formed at die face and container wall, there is friction either at container wall or die (Qamar, 2010). Flow pattern B is formed when there is friction at both container and die, resulting in extended dead metal zone, whereas, flow pattern c can be found when the inhomogeneous material is extruded at non-uniform temperature condition.

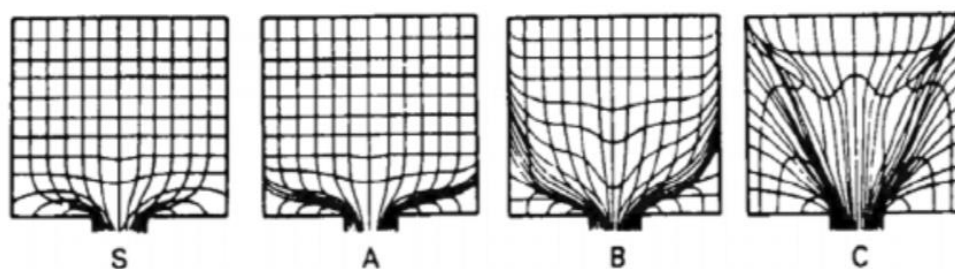


Figure 2.7: Different Metal Flow Patterns in Extrusion (Clode and Sheppard, 1990).

2.3.2 Pressure Distribution on Die Surface

It is important to understand the pressure distribution on the die surface as it may affect extrusion die accuracy, leading to defect in product quality. However, study pressure distribution on extrusion die surface in hot extrusion is difficult

because it involves high temperature and pressure. There are some researchers done on this matter using the semiconductor-strain-type pressure sensor to study the effect of metal flow on the pressure distribution on the die surface. Mori, et al. (2002) proposed the non-dimensional pressure to describe pressure distribution to avoid difference of measured pressure in experiment and they found out that the pressure decreases with increasing distance of from die centre due to friction force acting between billet and container wall (Figure 2.8). Also, the pressure remains constant when decreasing distance from die centre (Mori, et al., 2002).

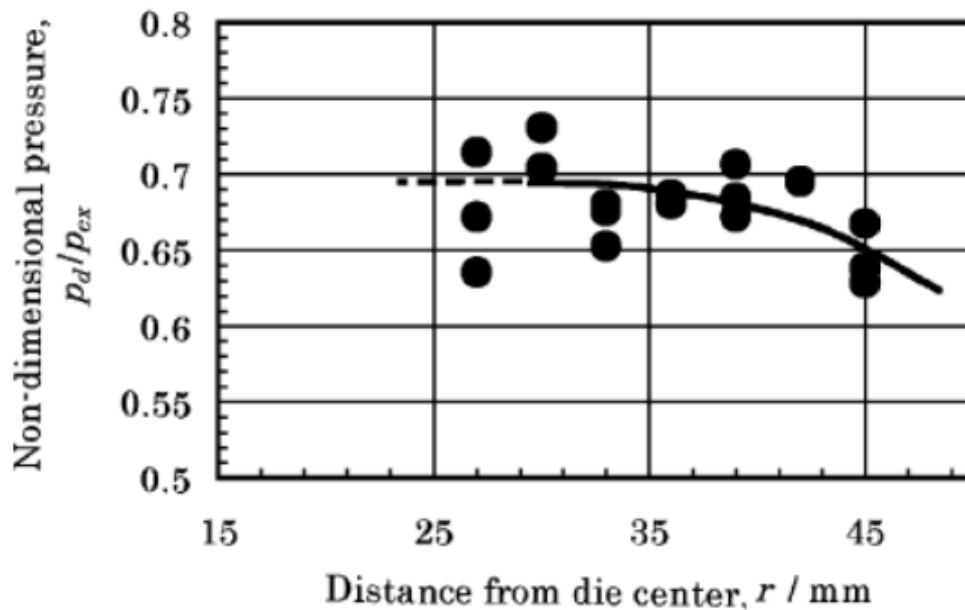


Figure 2.8: Pressure Distribution on Die Surface (Mori, et al., 2002).

In addition, Mori, et al. (2002) had done study on relationship between extrusion pressure and ram stroke as well (Figure 2.9). Both extrusion pressure and pressure on die surface increase in the initial stage of extrusion process. The pressure on die surface remains relatively constant for a specific range of ram stroke after the initial stage of extrusion process, while the extrusion pressure increases slightly. Then, the extrusion pressure decreased gradually after reaching maximum pressure. This is due to the light of friction force between metal billet and container (Mori, et al., 2002).

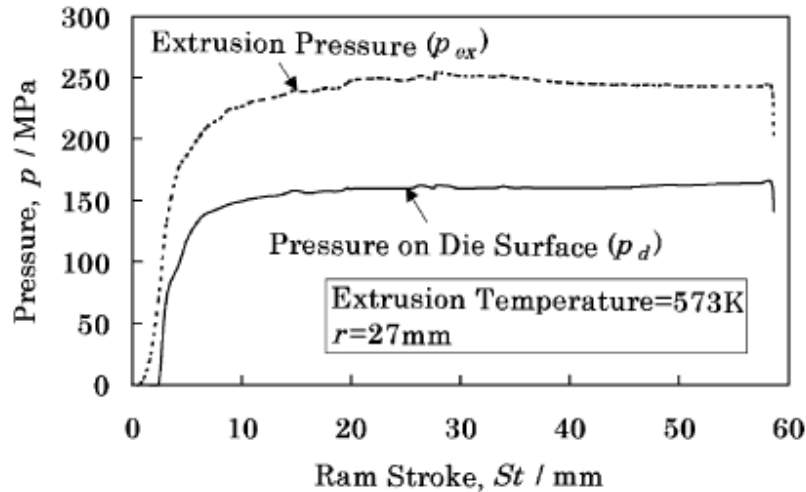


Figure 2.9: Graph of Extrusion Pressure versus Ram Stroke (Mori, et al., 2002).

2.3.3 Temperature Control

Temperature varies in extrusion process depends on extrusion speed, preheated metal billet temperature, heat transfer between container and billet, and heat generation due to deformation and friction. These heats would affect the mechanical properties, quality of the product and die service lifetime. Therefore, having a great knowledge of controlling the temperature on the die's bearing surface is very important from the viewpoint of economy of the process, which is able to high volume of product, yet prolong die service lifetime (tribology aspect). A precise knowledge on controlling temperature on bearing surface could help in Finite Element Method (FEM) simulation in getting optimal conditions for the process (Lefstad and Reiso, 1996).

Terčelj, et al. (2005) had done experiments using thermocouple welded on the bearing surface that would not cause unstable fraction condition during extrusion to investigate temperature on the die's bearing surface at different point. Referring to Figure 2.10, we can note that at stage 1 (billet upsetting) the temperature on bearing surface increases due to ram moving forwards and the billet filled the space in small diameter. At stage 2, the temperature drops due to ram having short-term recurring movement to remove the air. At stage 3, the temperature increases constantly where the extrusion process reaches stable state.

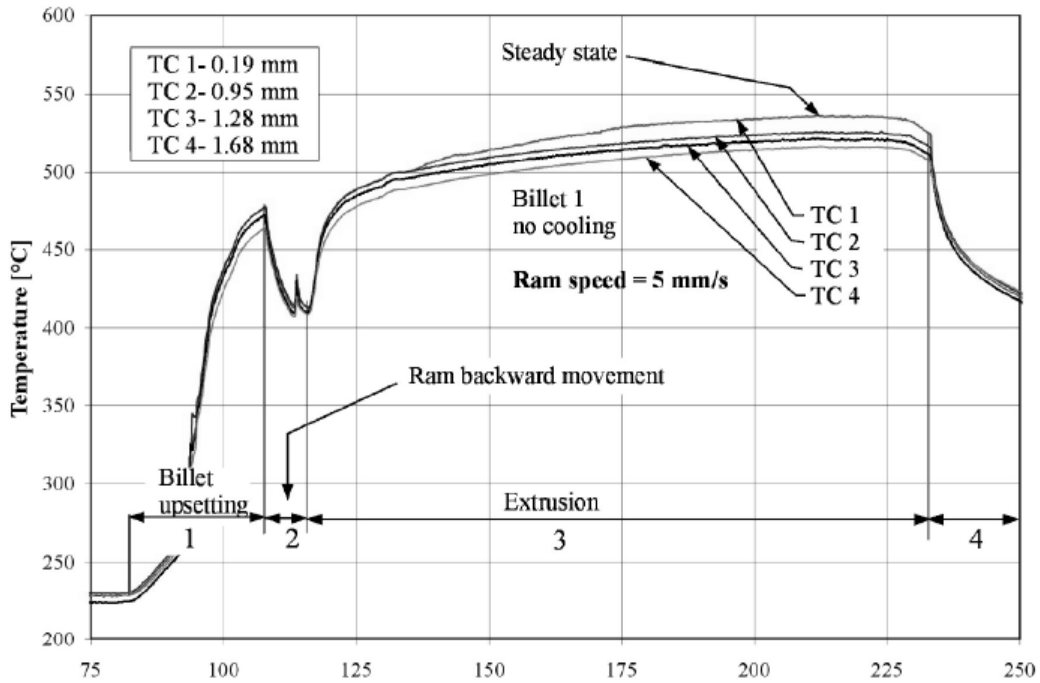


Figure 2.10: Temperature on the die at different distances from the bearing surface (TC 1 = 0.19 mm, TC 2 = 0.95 mm, TC 3 = 1.28 mm, TC 4 = 1.68 mm) (Terčelj, et al., 2005).

Terčelj, et al. (2005) had done experiments with various extrusion and different temperature of preheated billet and they found out that increasing extrusion speed would cause greater temperature and oscillation of temperature in stage 3 unlike in the graph above. The oscillation of temperature is mainly caused by different friction coefficient and heat consequently generated (Terčelj, et al., 2005). Also, increasing temperature will result in melting of eutectic Magnesium Silicide (Mg_2Si) occurs on the surface of the extrudate when temperature reaches 591 °C and this would result in deterioration in the extrude profile surface (Lefstad and Reiso, 1996). Magnesium Silicide is a particle that could be found on surface of extrudate. Lefstad and Reiso (1996) reported there are two limiting temperature, 591 °C and 612 °C for aluminium billet AA6063 in the extrusion process to prevent melting of eutectic Mg_2Si .

The temperature and heat transfer coefficient and temperature field could be described by the Laplace equation:

$$\Delta^2 T = 0 \quad (2.1)$$

For cylindrical geometry can be described as follow:

$$\frac{1}{r} \frac{\partial}{\partial r} \left(r \frac{\partial T}{\partial r} \right) + \frac{1}{r^2} \frac{\partial^2 y}{\partial \phi^2} + \frac{\partial^2 y}{\partial Z^2} = 0 \quad (2.2)$$

The thermocouple may not be able to detect temperature in z direction and the dependence z can be neglected, where the equation for the boundary condition would be

$$\frac{d}{dr} \left(r \frac{dT}{dr} \right) = 0 \quad (2.3)$$

The heat flow through the die is proportional to the temperature difference between the extrudate surface and die bearing surface. The temperature on the bearing surface is prescribed. Therefore:

$$\lambda \frac{dT}{dr} \Big|_{r=r_D} = -A(T_o - T(r_0)) \text{ and } T(r_1) = T_1 \quad (2.4)$$

Where the λ is the heat conductivity of the die and A is the heat transfer coefficient between die and extrudate. The solution of the above equation for such boundary condition is:

$$T(r) = T_1 + \frac{(T_o - T_1)}{\ln\left(\frac{r_o}{r_1}\right) - \frac{\lambda}{r_o A}} \ln \frac{r}{r_1} \quad (2.5)$$

To calculate the temperature of the bearing surface of die, with the boundary condition, the equation could be written in:

$$T(r) = T_1 + (T_o - T_1) \frac{\ln\left(\frac{r}{r_1}\right)}{\ln\left(\frac{r_o}{r}\right)} \quad (2.6)$$

2.4 Main Components of Metal Extrusion Machine

There are some components should be known in the metal extrusion machine such as ram, dummy block and die.

2.4.1 Ram

During metal extrusion process, the metal billet is placed in the container or chamber. The ram a tool placed in horizontal orientation and exert force on one side of the billet and pushes towards the die (refer to Figure 2.11). The extrudate will be formed on the other side and its flow direction is same as where the force is exerted. It is important to study the ram speed and it will exert different amount of pressure applied on the billet and it would affect die service lifetime and extruded product surface quality.

2.4.2 Dummy Block

During extrusion process, there will be chafing between the billet and container's wall that would affect the metal flow pattern and force applied on the billet especially in hot extrusion. This is because, during hot working, aluminium is reactive with oxygen gas and it will form oxide layer that would affect the extrusion operation and product surface quality. Therefore, a dummy block should be placed ahead the ram (refer to Figure 2.11) to avoid negative effect to the operation. Dummy block is usually smaller in size, so the outermost billet is not extruded and leaving behind in the container. The leftover is called as skull. Skull is the oxide layer formed from the reaction between aluminium and oxygen gas.

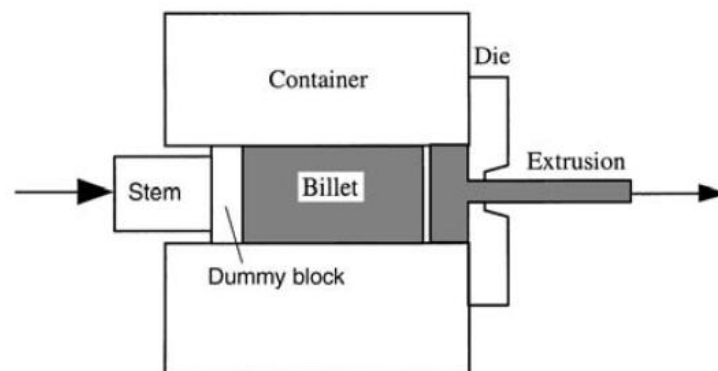


Figure 2.11: Direct Extrusion with Dummy Block (Saha, 2000).

2.4.3 Die

The core component in metal extrusion is die. Die is like a mould, has own distinct shape that will shape the metal billet into desired shape of the product. There are some tools required to provide sufficient support to the die against the pressure applied by the ram during extrusion process. The die ring is used to hold the die components together. The purpose of the feeder plate is to ensure the metal can flow smoothly and continuously without breaking. Bolster is applied to transfer the pressure load from the die to the ring and pressure will be transferred to the press plate and guards the against bolster deflection.

2.5 Characteristics of Die

Die is the main component in the metal extrusion. There are few criteria to be considered while design the extrusion die to achieve smooth and flawless products. Reducing cost is also associated with this process, where increasing lifetime of the extrusion die has been the most importance factor. The cost of die may reach as much as 17 % the product produced (Terčelj, et al., 2007)

2.5.1 Type of Die

There are three basic types of aluminium extrusion di: solid die, hollow die and semi hollow die. A solid profile product usually needs single die to work, while hollow or semi hollow need two pieces of die to work known as cap and mandrel (Oamar, Pervez and Chekotu, 2018). For solid die (Figure 2.12), it usually has weld-plate style die, where two die are combined. A die may have larger cavity than the product's profile. This cavity can help in controlling metal flows by controlling the contour and spread of aluminium (Butdee, Noomtong and Tichkiewitch, 2008). If the profile of the product is small enough, four same profile of product can be extruded using one set of die. However, the extruded product should not be rubbing with each other as it would bend the product behind (Butdee, Noomtong and Tichkiewitch, 2008).

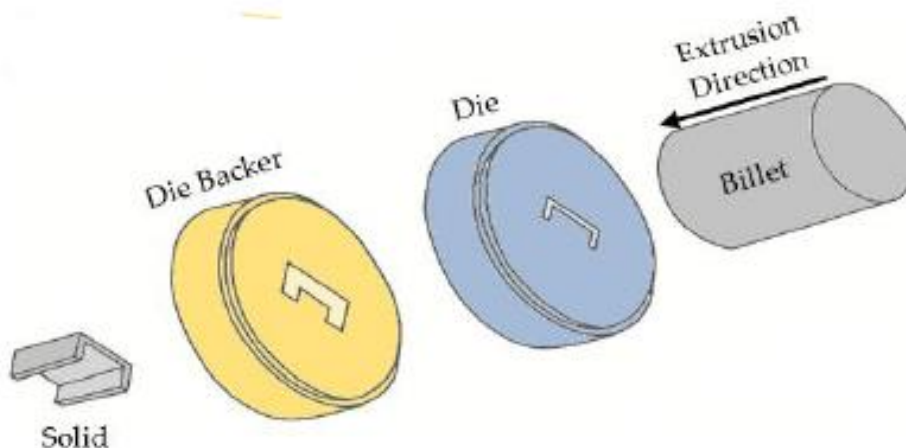


Figure 2.12: Solid Die (Oamar, Pervez and Chekotu, 2018).

For the hollow die (Figure 2.13), a porthole die is commonly used, which comprises two pieces of die known as cap and mandrel and it doesn't have backer or back plate. The mandrel has multiple portholes and the metal will be separated by bridge into portholes and the metal will join together in the weld chamber before entering cap or die (Butdee, Noomtong and Tichkiewitch, 2008). Webs, also known as bridge, used to support the core section, separate the porthole. The cap is used to create the external profile of the product which is the rejoin metal flow from mandrel (Butdee, Noomtong and Tichkiewitch, 2008).

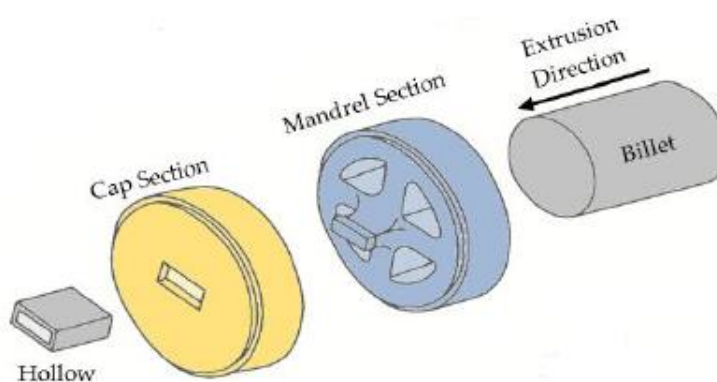


Figure 2.13: Hollow Die (Oamar, Pervez and Chekotu, 2018).

For semi-hollow die (Figure 2.14), it has the same portholes and bridge as the hollow die but without core to make a void of section. The semi hollow

classification can be derived from ratio of the partially enclosed void area to square of the size of gap (Butdee, Noomtong and Tichkiewitch, 2008). This ratio ($area/gap^2$) is known as tongue ratio. This ratio will determine whether the die should be constructed into weld-plate, porthole or even flat style.

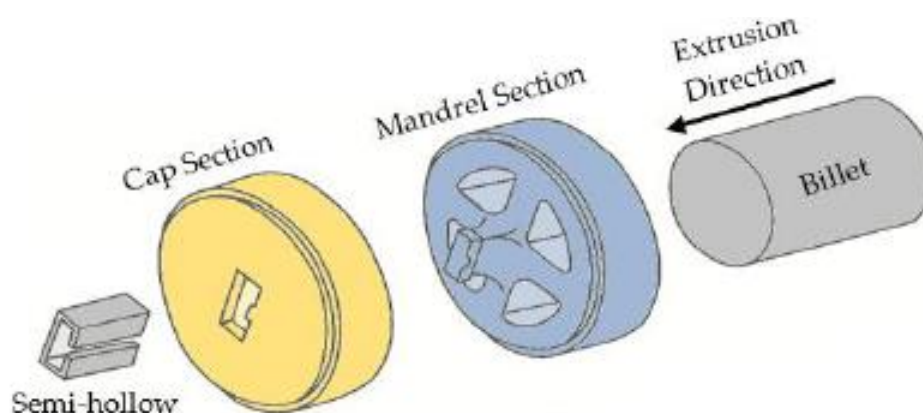


Figure 2.14: Semi Hollow Die (Oamar, Pervez and Chekotu, 2018).

2.5.2 Die Design

Die design has been the most important factor to yield cost-effective operation. The design could determine scrap production and production speed, which will affect production and efficiency of the process, and results difference in profit margin of the company. In traditional, die design is based on knowledges and experience of the designer. The designers learn and yield knowledge by doing trial and error practice. However, this practice could cost a lot to the company. Nowadays, most of the designers are relying on the finite element method (FEM) to evaluate the design.

During die design process, the designer must have calculated all the possible shrinkage points on profile section, determining porthole shapes, dimensional die orifice, bearing length to control the metal flow and exit velocity during extrusion process (Butdee, Noomtong and Tichkiewitch, 2008). In order to have high productivity die, the design process should focus on the shape factor, extrusion ratio, extrude ability and so on which may affect the service lifetime of the die. Furthermore, metal flow pattern playing significant role in prolonging the service lifetime of the die. The designer must imagine the metal flow pattern in order to make decision on the die feature such as die orifice and die length which have directly impact to the metal flow velocity. According

to Butdee, Noomtong and Tichkiewitch (2008), the velocity should be balance at every points of the profile when exit, which can be manipulated by the bearing length. Otherwise, the extruded product may have twist pattern (Figure 2.15).

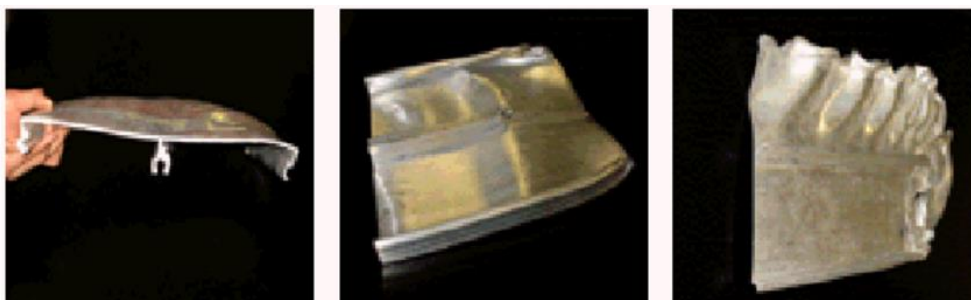


Figure 2.15: Unbalanced Profile of Extruded Product (Butdee, Noomtong and Tichkiewitch, 2008).

In this full of advanced technologies era, die designer tends to use Finite Element Method (FEM) to predict the metal flow pattern and the result of extruded product's profile before applying into practice. This method could save a lot of resource and cost in fabricating the die and testing. Implementing this method, the designer can predict the how significant the contact motion between the aluminium flow and the container that would result in non-uniform flow of aluminium, metal flow pattern and so on (Ouwerkerk, 2009). If unsatisfied results obtained, the designer could further study the geometry of die and modify it to control exit velocity and overcome the any possible die failure.

Ouwerkerk (2009) had tried to run isothermal simulations of the AA6063 aluminium alloy with an ALE description to investigate the pressure with container effect (distance of the profile cavity to the centre of the die). He found that the pressure is irrelevant to the variation in cavity thickness, T and the relationship can be described as:

$$P(O, R, S, T) = c_1 T^{n_1} + c_2 R^{n_2} + c_3 S T^{n_3} O^{c_4} T^{n_4} \quad (2.7)$$

Where

S = depth,

O = Offset,

R = distance from the point on profile to die centre

$c_{1...4}$ and $n_{1...4}$ = constants were fitted to the numerical results.

There are some factors are not included in this formula such as extrusion ratio, pre-heat billet temperature, bearing length, and ram/stem speed (Ouwerkerk, 2009).

Furthermore, Ouwerkerk (2009) found out the minimum bearing length of die could be calculated with the average inflow pressure difference from the previous formula. The formula for calculating minimum bearing length b_i is:

$$b_i = c_1 \cdot b_{min} \left(\frac{P_{max}}{P_i} \right)^{c_2} \quad (2.8)$$

Where

P_i = pressure for the point,

P_{max} = maximum pressure when smallest bearing length is chosen (b_{min}),

c_1 and c_2 = constant.

Bearing angle is also another important parameter in design the die as it should affect the inflow pressure that would affect the metal flow pattern and friction between the die and metal. Having parallel inlet bearing would result in unstable metal flow pattern and affect the service lifetime of the die. Thus, having bearing angle could help in productivity of die and reduce the resistance flow. Choke angle is recommended to ensure the aluminium stays in contact with the die during extrusion and the resistance flow is greatly reduced. This would result in absent of imperfections of surface quality of extruded product. The critical choke angle was found to be approximately at 0.5° based on real extrusion process from an experiment known as Akeret's experiment (Ouwerkerk, 2009)

2.5.3 Die Material

Material chosen for the extrusion process is very important. The chosen material should be able to withstand high thermal and mechanical loading, great wear resistance and failure. Bjork, Westegard and Hogmark (2001) pointed out that wear resistance is playing the major in extrusion die as it would affect

technological and economical aspect because it would affect surface quality of the extruded product. Tool steel is the material widely used for industrial purpose and is a highly alloyed steels that can be hardened and tempered to have guaranteed hardening characteristics to improve strength and wear resistance (Budinski and Budiskin, 2002). Aluminium extrusion process is done in hot working process and the temperature may achieve in average range of 560 °C – 600 °C during the extrusion process and the most frequently used die material worldwide is AISI H13 (Saha, 2000). In this project, SKD 61 steel tool is used for the extrusion die and research purpose. SKD61 is found in JIS G4404 standard, Japan Standard. The JIS G4404 steel is applied in hot rolled application and alloy tool steel that was built for forging, and this standard is also most stipulation from ISO 4957 standard. SKD 61 tool steel with the few chemical composition (refer to Table 2.1) and Fe balance the rest chemical composition for the die material. Whereas, H13 is found in standard ASTM A681, America Standard, which covers the all fields of requirements (chemical, mechanical and physical requirement) for available various types of alloy tool steel products. Both H13 and SKD61 have almost the same chemical compositions and properties, but they are from different standard.

Table 2.1: SKD 61 Chemical Composition.

Chemical	C	Si	Mn	P	S	Cr	Mo	V
Content (wt%)	0.35- 0.42	0.8- 1.2	0.25- 0.50	0.03 (max)	0.02 (max)	4.8- 5.5	1.0- 1.5	0.8- 1.5

2.5.4 Die Hardening Treatment

Saha (2000) pointed out that surface finish of the product is relying on many factors, and wear mechanism of the bearing surface of the die is playing the major role. In order to prolong die service lifetime and produce flawless products in long term, the die needs to undergo hardening treatment. This treatment could help enhance die's wear resistance and save tooling costs.

The extrusion can have extended lifetime by enhancing die surface bearing surface wear resistance by nitriding treatment such as gas nitriding treatment, ion nitriding treatment and salt bath furnacing method or by any new die material application. There are alternative methods to increase the die

surface wear resistance for extrusion, such as CVD (which has TiC +TiN) or PVD coating (which has CrN, TiN, TiAlN or Duplex treatment) and so on, but gas nitriding is found to be the most common method (90 % - 95 %) for surface hardening treatment. This is due to the light of this approach is very effective for narrow surface with deep gaps, which is represented in majority extrusion die profile (Bjork, Westegard and Hogmark, 2001). Typically, salt bath furnace nitrocarburizing hardening treatment is applied for the aluminium extrusion die. The difference between salt bath furnace nitrocarburizing hardening treatment and gas nitriding is salt bath furnace nitrocarburizing hardening treatment uses heated cyanide salt mixture in the bath, whereas gas nitrocarburizing is using nitrogen gas and the heat requirement for salt bath furnace nitrocarburizing is lower than gas nitrocarburizing (P´erez and Belzunce, 2016). Also, salt bath furnace method is also effective in producing uniform nitride layer through surface contact between substrate and liquid salt for narrow and deep gap.

Before salt bath furnace nitrocarburizing hardening treatment, the aluminium extrusion die is polished and preheated at 400 °C for 1.5 hours to 2 hours. Then, the die is transfered to salt bath furnace filled with cyanide mixture at temperature of 580 °C – 680 °C for 2 hours. The cyanide mixture comprises alkali cyanates (CNO^- , 36 ± 2 %), alkali carbonates (CO_3^{2-} , 18 ± 2 %) and cyanide (CN^- , < 0.8 %) (Krishnaraj, et al., 1997). After that, the die undergoes quenching process by placing it into a tank fill with low temperature salt for one hour to further harden the steel. The die is then transfered into water tank to further decrease the temperature for 1.5 hours.

With this treatment, a compound layer can be found on top of the steel surface, which is known as chromium nitride layer (refer to Figure 2.16). After 8 hours, the layer can be a thick layer with maximum thickness at $6 \mu m - 8 \mu m$, where inner layer comprised of columnar grains and outer thin layer has equiaxed grains (Ohta, Sugimoto and Arai, 1992). This is result of the nitrogen atoms tends to diffuse deeper into the metal, establishing a competition between inward and outward of nitrogen flexes (Arai, 2015). The limit of the thickness is restricted by available amount of nitrogen atoms as in substrate which can determine the composition of the compound layer and diffusion zone developing during nitriding process (Arai, 2015).

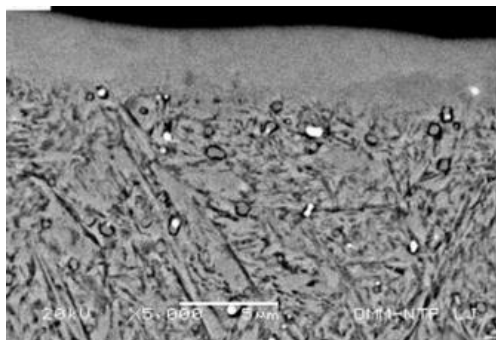


Figure 2.16: Microstructure of Nitried Steel die (Terčelj and Kugler, 2017).

2.5.5 Die Hardness

Some people argued that greater nitride layer or compound layer will lead to greater wear resistance. Hence, some engineers tend to do the treatment for several times in order to further enhance the tensile strength and wear resistance by increasing the compound layer thickness. However, having too thick of compound layer would bring negative effect on the wear resistance as the compound has brittle property that would cause spalling of the surface.

Also, increasing hardening treatment temperature and period will help in building up thicker compound layer and microstructure of the die (Krishnaraj, et al., 1997). Having thicker compound layer can have greater hardness and wear resistance (refer to Figure 2.17). However, achieving greater hardness by increasing the treatment temperature and period may lead to loss of core strength to unacceptable level, and can result in die fail to maintain dimensional accuracy due to occurrence of deformation (Krishnaraj, et al., 1997).

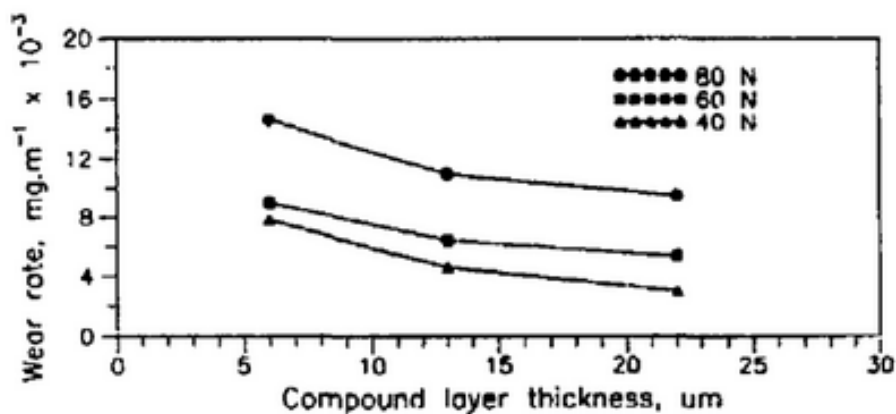


Figure 2.17: Relationship between Compound Layer Thickness and Wear Rate (Krishnaraj, et al., 1997).

Therefore, an optimal compound layer thickness by nitriding treatment should be predicted depends on the loading modes and the magnitude of the loading such as contact pressure to obtain optimum service lifetime.

2.5.6 Die Correction

As mentioned in the previous section, proper condition of die is playing vital role in product excellent surface quality of product and increase productivity. Therefore, die correction should be done frequently either before service or service to ensure the die is in tiptop condition. Basically, there are two types of die correction should be done, which are pre-service correction and post-service of the die. Pre-service correction is usually carried out after initial run of new die, prior placing them into regular service and this correction concerns on adjusting the geometry or feed design, if minor adjustment is needed (Oamar, Pervez and Chekotu, 2018). Post-service correction is referring to correcting maintenance of the die every time after the die is dismounted from the machine. This correction is determining any damage, wear, fracture, deflections and loss of hardness done to the die (Oamar, Pervez and Chekotu, 2018).

2.5.7 Die Wear

Die wear can be explained as progressive loss or removal of material from the die surface. Die wear can bring massive impact to the productivity as well as surface quality of the extruded product as the wear can affect the process, size and shape of the die. Wear basically alter the surface topography and may result in severe surface damage. There are few types of die wear could be found such as adhesive, abrasive, corrosion, fatigue, erosion, fretting or impact wear.

According to Borowski and Wendland (2015), the most common wear on the die's bearing surface and its cause are identified:

- Cracks and spalling are caused by thermomechanical fatigue. Thermomechanical fatigue is mainly caused by cyclic temperature fluctuation resulting in imposed cycling strain.
- Corrosion pit is caused by cleaning by cleaning/etching of the die in a sodium hydroxide solution. Cleaning is an interoperation to reveal the condition of its surface, and it is always performed before the die

regeneration process.

- Abrasive wear on the bearing surface, material removal and spalling occur, which could initiate cracks in the die surface later.

Adhesive wear occurs because of aluminium attachment on the die surface, and it may cover the whole surface. This development depends on many factors: temperature of the die, ram speed, geometry of the die, bearing length and so on (Saha, 2000). The temperature is the most important factor as the aluminium will be more reactive at elevated temperature and stick on die surface which is results from friction of the bearing. This developed layer can affect the metal flow pattern and surface quality of the extruded product. When the pressure is high enough, the deposition of aluminium can be removed together with the die material or compound layer, leading to formation of crater (Refer to Figure 2.18(C)). If the operation continues, a narrow line, known as furrow (Refer to Figure 2.18(D)) will be formed due to continuous die material removal in longitudinal direction.

Abrasion wear occurs when the force applied or the friction on the bearing surface is too violent. Abrasion wear is a result of cracking surface on the die surface. This wear may be attributed to over-nitriding effect at the exit edge area (Refer to Figure 2.18(B)) that would reduce the wear resistance as it is brittle. Cracking and adhesive removal of die material may occur as well. In addition, having high friction stress and continuous testing on the die may lead to chipping and formation of craters on the bearing surface and finally shallow furrows. These furrows could continue if the operation continues. With these formations of damage, the shear strength of the nitride surface will be decreased and this will facilities adhesive removal of die material in longitudinal direction (Bombac, et al., 2013). Eventually, crack would occur (Refer to Figure 2.18(A)) and the crack growth will be accelerated with oxidation of crack surface and transfer to aluminium along the grain boundaries (Bombac, et al., 2013).

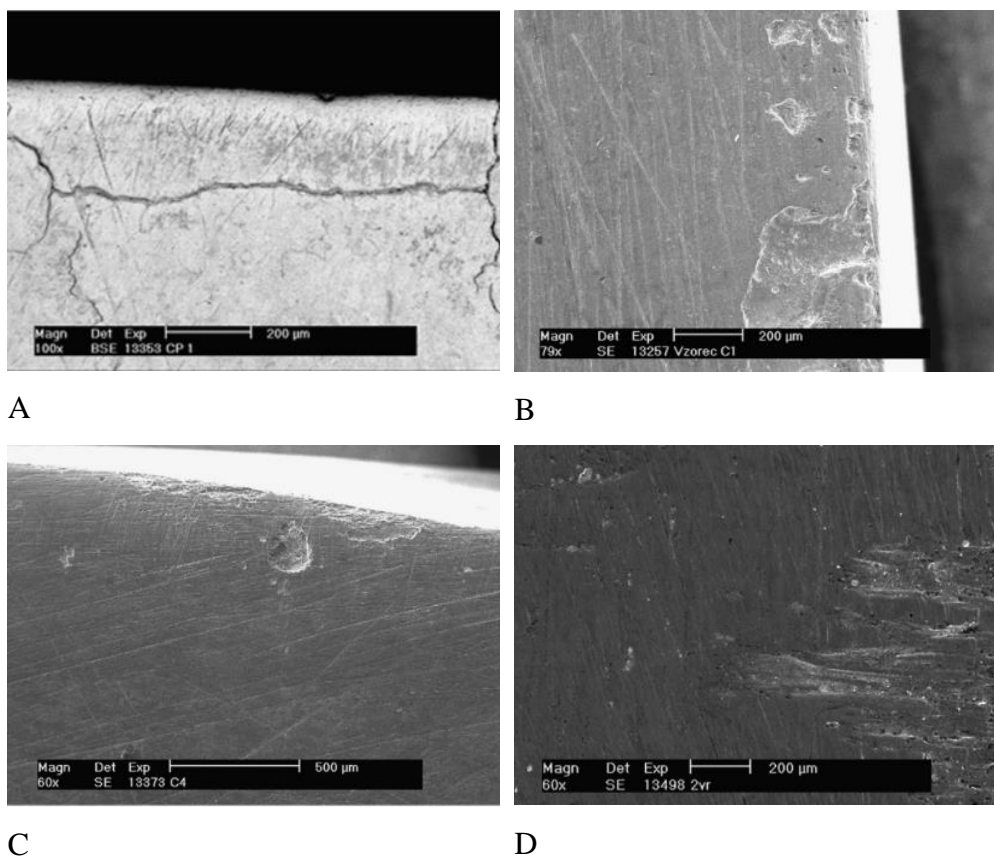


Figure 2.18: Wear of die surface: (A) Formation of crack, (B) Removed nitride layer, (C) Formation of crater, (D) Formation of furrow (Bombac, et al., 2013).

2.5.8 Die Fatigue Failure

Die fatigue failure is a process of premature failure or damage of the die due to cyclic stress in the extrusion service. It is difficult to predict the fatigue failure as the process just takes few seconds to complete and difficult to control the parameter such as temperature and pressure applied (Tong, et al., 2013). Besides, the die and other parts have complicated three-dimensional (3D) geometry which make the prediction even difficult to calculate. However, with the aid of Finite Element Method (FEM), this analysis on fatigue failure could be easier but it may not be very accurate as there are some discrepancies in defining parameter such as extrusion ratio, stress definition, different friction coefficient and so on.

The following equations can be used for the prediction of fatigue life cycle of aluminium extrusion die:

Morrow's stress life approach:

$$\sigma_a = 2N_f(\sigma'_f - \sigma_m)^b \quad (2.9)$$

Morrow' strain life approach:

$$\varepsilon_a = \frac{\sigma'_f}{E} \left(1 - \frac{\sigma_m}{\sigma'_f}\right) (2N_f)^b + \varepsilon'_f \left(1 - \frac{\sigma_m}{\sigma'_f}\right)^{\frac{c}{b}} (2N_f)^c \quad (2.10)$$

Where

σ_{max} is the maximum stress,

σ_a is stress amplitude,

σ_m is mean stress,

ε_a is strain amplitude,

σ'_f is fatigue strength coefficient,

ε'_f fatigue ductility coefficient,

b is fatigue strength exponent,

c is fatigue ductility exponent,

E is modulus of elasticity.

Both equations are used to describe the relationship between maximum stress-strain conditions and number of cycles to initiate crack (Akhtar and Arif, 2009). These equations is in uniaxial and it is difficult to handle parameters and design change will affect the multiaxial stress-strain state under loading (Akhtar and Arif, 2009). Furthermore, Akhtar and Arif (2009) found the critical fatigue location is at fillet radius or nearby regions by using FEM based on maximum effective von Misses stress criteria values and maximum principle strain values (refer to Figure 2.19). Besides, this failure is associated with metal flow stress. High flow stress will result in high die stress/strain which will lead to shorter die service lifetime (Akhtar and Arif, 2009). This problem can be resolved by increasing preheated billet temperature, but should be at optimal temperature.

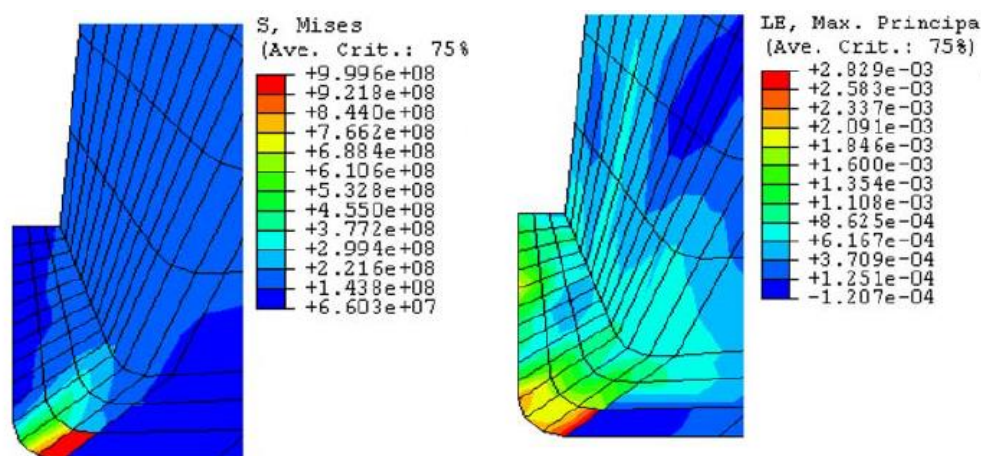


Figure 2.19: Simulation Results of Von Mises maximum Stress and Maximum Principle Strain using Abaqus (Tong, et al., 2013).

2.6 Aluminium Extrudate Surface Defects

Many aluminium extruded products are rejected due to defects found on the product surface. The most common defects could be found on the products' surface are die line and pick up (Clode and Sheppard, 1990). These defects could degrade the aesthetic look of the products, while some may affect mechanical properties of the product.

2.6.1 Pick-up Defect

Pick up defect has an appearance of comet tail or tear drop shape as shown in Figure 2.20. This defect has a maximum length at about 0.5 mm to 3.0 mm and width could reach up to $330 \mu m$ (Peris, 2007). Observation by our naked eyes, the defects looked like scratches along the aluminium alloy extrudate surface. However, this defect is different from the scratches done by equipment during transport. The defect has a constant comet tail-like shape along the aluminium alloy extrudate surface. Matienzo and Holub (1983) pointed out that aluminium deposition and transfer of oxide on the die bearing surface has been the main cause. The severity of pick-up defect on the extruded products is also depending on homogenization of the aluminium billet before extrusion, process parameter and die bearing condition (Matienzo and Holub, 1983). Arif, et al. (2002) believed this defect is sensitive to temperature. This defect could be easily found when the exit temperature of extrudate reaches eutectic point where liquid can be found in the extrudate.



Figure 2.20: Pick-up Defect (Fourmann, 2017).

2.6.2 Die Line Defect

Die line defect is a black line or longitudinal depression formed on the aluminium extrudate surface (refer to Figure 2.21). This defect is mainly due to imperfections of on the die surface (Clode, 1987). Imperfections of the die surface may be due to spalling of nitride layer. Thus, the interaction between extrudate and die bearing land is the major cause of the die line formation. Die line can be minimized by reducing the bearing length in order to have choke condition at die throat (Clode, 1987). However, at choke condition and highly polished surface, die line still could be found but it is called as micro die line. The formation of die line can affect effectiveness of anodizing process (Peris, 2007).

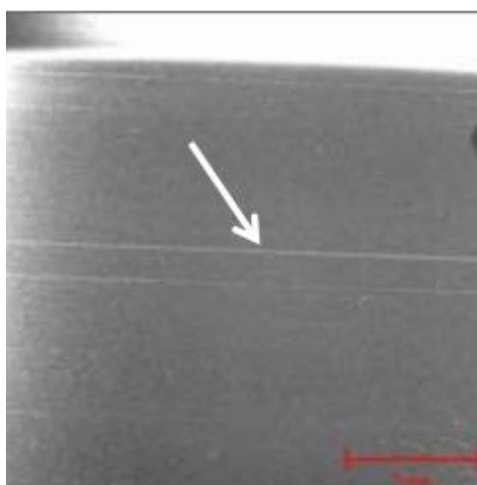


Figure 2.21: Die Line Defect (Fourmann, 2017).

2.6.3 Blister

Figure 2.22 is showing top view of the blister formed on a aluminium extrudate. This defect is caused by entrapment of air during billet loading or upsetting in the extrusion process (Arif, et al., 2015). It starts with the lubricant stuck at boundary of dead metal zone and particles of gases will be moving vigorously at the location due to high temperature, forming a pop-out appearance on the extrudate surface (Arif, et al., 2015). The blister may not appear on immediately on the extrudate at the die exit and may be formed during subsequent heat treatment.



Figure 2.22: Blister (Fourmann, 2017).

2.6.4 Tearing

Tearing defect has an appearance of cracking on the aluminium extrudate as shown in Figure 2.23. This defect can be formed when the temperature of the extrudate reaches eutectic points where liquid phase may be formed during extrusion (Peris, 2007). At this point, the adhering aluminium layer could have lower cohesive strength to adhere to die bearing surface and frictional force will be too high for the extrudate to flow through. The high frictional force is sufficient enough to pull the extrudate when flowing on the die bearing surface and resulting in tearing. Peris (2007) pointed that this tearing formation could extend up to $100 \mu m$ from the extrudate surface.

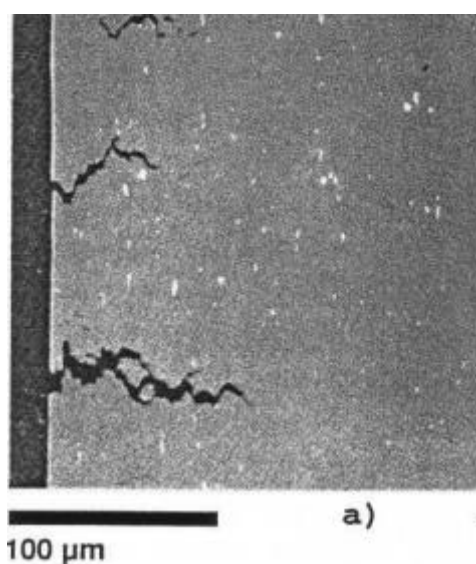


Figure 2.23: Tearing (Fourmann, 2017).

2.7 Summary

Surface defects on aluminium extrudate may degrade the aesthetic look of the product while some may affect mechanical properties of the aluminium extrudate. The most common surface defects could be found on extrudate are pick-up defect, die line defect, blister and tearing. Pick-up defect and die line defect are mainly caused by the interaction between extrudate and die bearing surface. Blister and tearing are due to inappropriate preparation for the extrusion process. In short, these surface defects occur during hot extrusion process. Therefore, the extrusion process parameters should be studied in order to obtain satisfied surface finish of product such as temperature, pressure, extrusion force and so on. Despite the surface defects found on the aluminium extrudate has been a major problem in the extrusion process, there is very little documented technical literature or systematic study on the surface defects. Thus, this study will investigate the effect of extrusion process parameters on the extrusion process by using FEM to minimise the surface defects formed on the extrudate during extrusion process. This is because process parameters has great effect on the temperature and pressure in the extrusion process. Also, formation mechanisms of the surface defects is studied as well to understand origin of formation and minimise the surface defects.

CHAPTER 3

METHODOLOGY AND WORK PLAN

3.1 Introduction

This chapter details about experiment setup to investigate the surface defects on the extruded products from the respective industrial die and simulation is done to investigate the extrusion process by applying various extrusion parameter including changing in ram speed, preheat billet temperature and die temperature to study the process parameters that would result in the surface defects found on the aluminium extruded product samples. The process parameters and industrial die designs were given by a local aluminium extrusion company.

3.2 Surface Defects Analysis of Extrudate Samples

In this study, two aluminium alloy extruded products as shown in Figure 3.1 are given by a local aluminium extrusion company to investigate the root causes of the surface defects on the extrudate. The surface defects are usually noticeable by our naked eyes. These surface defects could be streak defects, die lines, pick up defects, corrosion and so on due to various reasons such as process parameters, metal billet quality and so on. In order to have better visualization on the surface defects found on the samples, the samples will be placed under optical microscope to examine the microstructure. Before examining the defects under optical microscope, the samples have to undergo few processes: degreasing, etching and desmutting to have clearer image of surface defects.

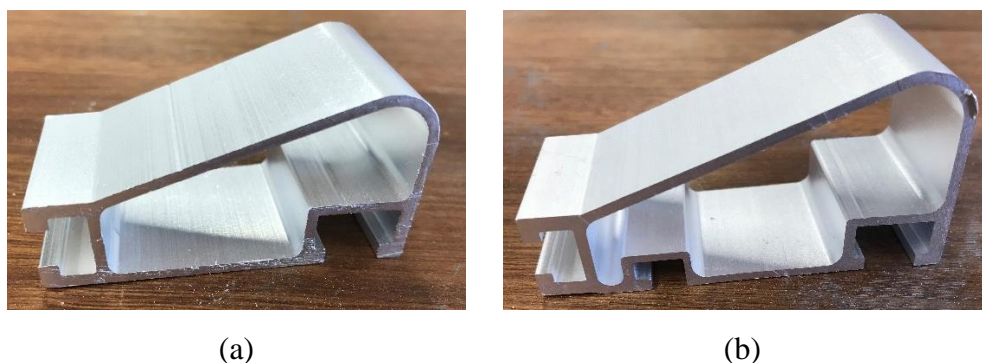


Figure 3.1: Aluminium Extruded Products: (a) 4823, (b) 4824.

The experiment was started with cutting the samples into desired length, at 3 cm by using abrasive cutting saw, so that the samples can fit into laboratory equipment given. After cutting, chemical solutions were needed to carry out etching process and desmutting process. In etching process, etching solution was used to remove adhesive bonding of oxide layer results from anodizing process. The etching solution is an alkaline solution which comprises 10% sodium hydroxide ($NaOH$) and 90% water (H_2O) to etch the samples. On the other hands, in desmutting process, desmutting solution was used to remove excess alloy metals from the extrudate surface which would enhance the build-up oxide layer on the extrudate later in anodizing process. The desmutting solution used for this research comprises of 40% nitric acid and 60% water.

Prior proceeding to conduct surface treatment to the aluminium extrudate, all lab safety procedures should be read and understood as the solution is corrosive and safety equipment should be worn at all time while conducting the experiment. The experiment was carried out in a sequence: degreasing, etching and desmutting (refer to Figure 3.2). After every step was done, the extrudate has to be rinsed with distilled water to remove the remaining solution adheres to the extrudate surface and prevent mixing with another solution. After these steps, cutting saw was used to cut the aluminium extrudates into smaller pieces which could be fit on the stage of optical microscope. Then, the surface defects on the extrudate surface were captured under optical microscope for further analysis. In addition, scanning electron microscope (SEM) with energy dispersive x-ray (EDX) analysis was used to analyse material elements on the surface defects. Detailed explanation on every steps of the experiment are explained in the following sub-sections.

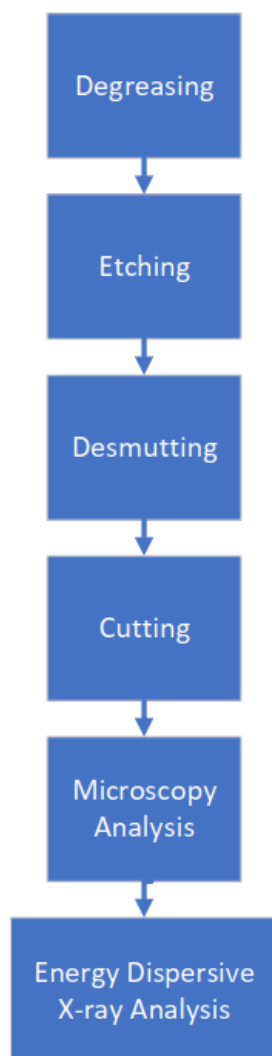


Figure 3.2: Flowchart of Workplan.

3.2.1 Degreasing

Degreasing is a process to remove all the oils and grease stained on the extrudate surface. It was found that for aluminium alloy extruded, solvent washing using acetone solution is suitable for degreasing on aluminium extruded surface (Bishop, 2005). Acetone solution is a common solution used to remove nails polish and widely used in textile industry. The aluminium extruded products were fully immersed into acetone solution to ensure every corner and sections can be degreased (refer to Figure 3.3). For safety considerations, nitrile gloves and safety goggles were worn at all the time as the solution may cause irritation to human's skin and stayed away from heat while carrying out the experiment because acetone solution is flammable.



Figure 3.3: Aluminium Extruded Product (4824) Immersed in Acetone Solution.

3.2.2 Etching

Etching is a destructive process to remove the adhesive bonding of oxide layer on the extrudate surface. The oxide layer can be formed naturally when the aluminium surface is exposed to oxygen-filled environment. The oxide layer can also be further enhanced through anodizing process where thicker oxide layer can be formed to enhance corrosion resistance. However, oxide layer on the extrudate may be an excess element in this research as it will cover some of the surface defects and the defects may not be so clear under our eye's observation. In order to remove the oxide layer on the extrudate, an alkaline etching solution was used which comprises 10% sodium hydroxide ($NaOH$) and 90% water (H_2O). The extrudate samples were fully immersed into alkaline etching solution for around 5 minutes to remove the oxide layer on the extrudate surface as shown in Figure 3.4. This process was carried out in fume cupboard as hydrogen gas will be emitted and may make us having difficulties in breathing and choking. Also, nitrile gloves and safety goggles were worn at all the time as the solution is corrosive. After that, a shiny extrudate without oxide layer should be produced and rinsed with distilled water.

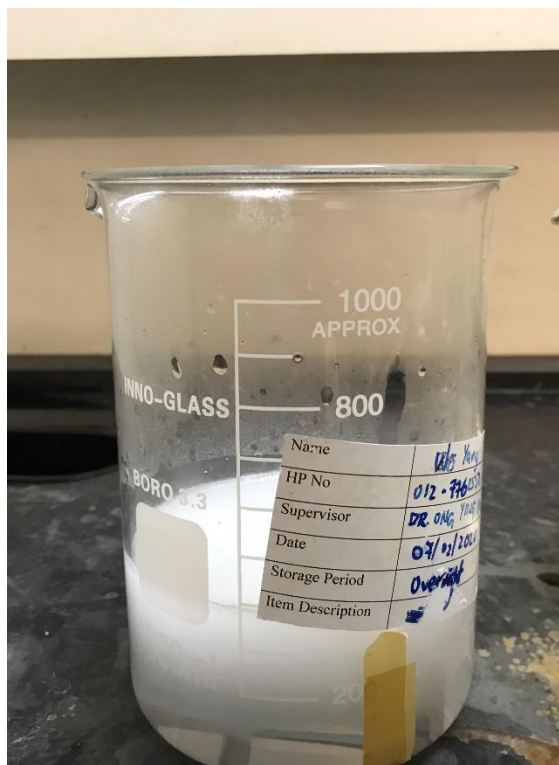


Figure 3.4: Aluminium Extruded Product (4824) Immersed into Etching Solution (10% Sodium Hydroxide and 60% Distilled Water).

3.2.3 Desmutting

Desmutting is a process to remove excess alloy element from the extrudate's surface. The alloy elements could be magnesium, silicon and so on. This process is usually carried out after etching process and before anodizing. Eliminating the excess alloy element on the extrudate surface can ensure the built up oxide layer will be more constant and effective during the anodizing process. The desmutting solution comprises 40% nitric acid and 60% water. The extrudate samples were fully immersed into the solution for around 1 minutes to remove excess alloy elements as shown in Figure 3.5. After that, the extrudate samples were rinsed with distilled water to remove the remaining solution adheres to the samples. For safety precautions, nitrile gloves and safety goggles were worn at all the time as the solution is corrosive.



Figure 3.5: Aluminium Extruded Product (4824) Immersed into Desmutting Solution (40% Nitric Acid and 60% Distilled Water).

3.2.4 Cutting

Cutting was carried out to cut the sample into piece, so that the aluminium extrudate sample can be put under optical microscopy for surface defect examination. The samples were clamped tightly on bench vice swivel table bench and had been cut into pieces by using cutting saw as shown in Figure 3.6.



Figure 3.6: Cutting Saw.

3.2.5 Microscopy Analysis

Optical microscope (refer to Figure 3.7) was used for microscopy analysis. It was used to view the microstructure of the samples especially surfaces with defects. The optical microscope has objective lens that can capture images of 5 to 100 times zoom. The captured image can be saved into computer as well.

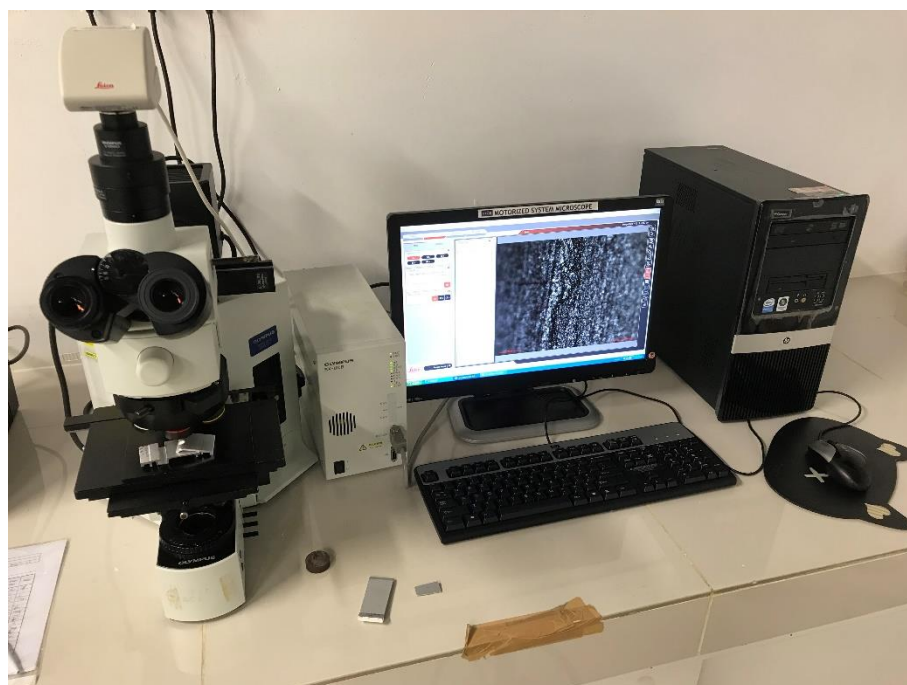


Figure 3.7: Optical Microscope.

3.2.6 Energy Dispersive X-Ray (EDX) Analysis

Energy dispersive x-ray (EDX), also known as energy dispersive x-ray spectroscopy (EDS) uses X-rays technique to identify the chemical composition or material element on the surface of interest. The X-ray can focus on specific point or area to analyse the chemical composition of targeted area. This analysis was used to analyse the material elements on the surface defects and identify the source of formation of mechanisms of the surface defects. The aluminium extrudates to be examined were stucked on the holders (circular metal) by using double-sided tape as shown in Figure 3.8. Then, the holder with aluminium extrudates were placed into the scanning electron microscope (SEM) with energy dispersive x-ray (EDX) analysis to analyse material elements on the surface defects.

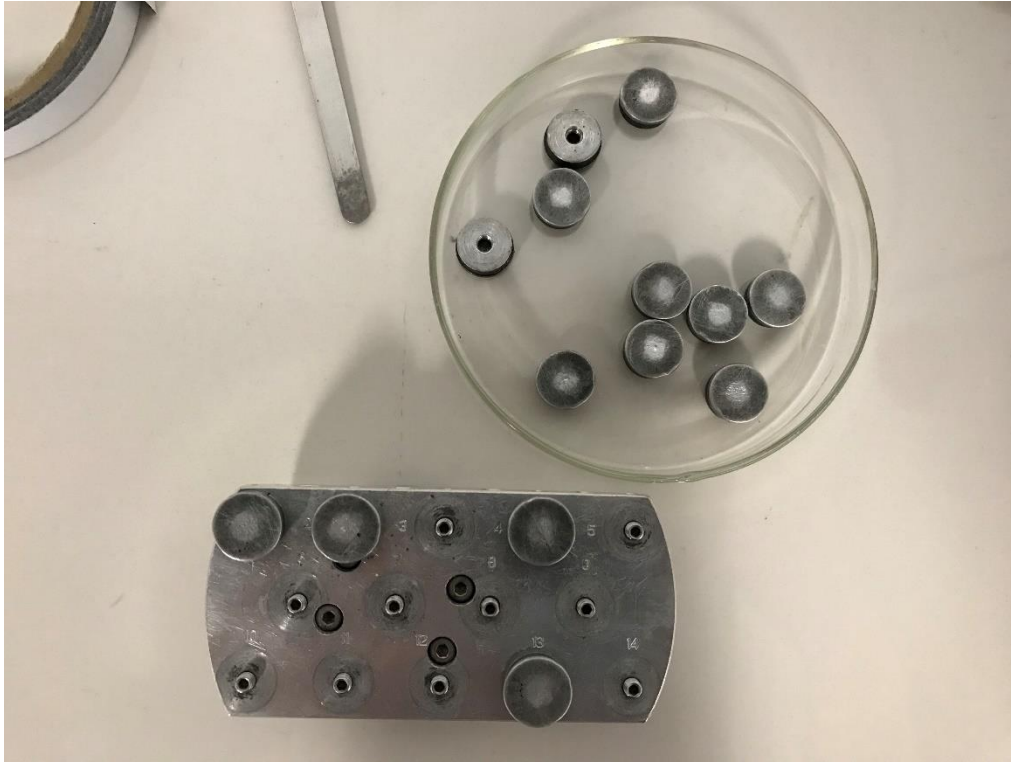


Figure 3.8: Holders for Scanning Electron Microscope (SEM) with Energy Dispersive X-ray (EDX) Analysis.



Figure 3.9: Scanning Electron Microscope (SEM) with Energy Dispersive X-ray (EDX) Analysis.

3.3 Numerical Simulation of Extrusion Process

In this research, the Inspire Extrude Metal (formerly known as HyperXtrude) Student Edition software of steady state finite element simulations based on Arbitrary Lagrangian-Eulerian (ALE) Adaptive remeshing technology is used on analogue simulation of aluminium extrusion processing. ALE formulation is a combination of Lagrangian and Eulerian methods. With this combination, the mesh is not attached to the material particle and not like fixed at specific space, it can move arbitrarily (Zhang, et al., 2011). Thus, for large deformation like extrusion process, ALE is an effective approach. This approach can also avoid mesh distortion and the difficulty on free surface tracking.

3.3.1 3D Model of Extrudate and Extrusion Die

In this study, there are two industrial dies provided by a local aluminium extrusion company for the analysis: Die 4823 and Die 4824. Therefore, there are two different geometries of extrudate and dies will be discussed in this project. Three-dimensional shape of the extruded profiles from the industrial dies are shown in Figure 3.10 and Figure 3.11. Both extruded products are made of aluminium AA6005-T5. The wall thickness is not equal at all sections for both products.

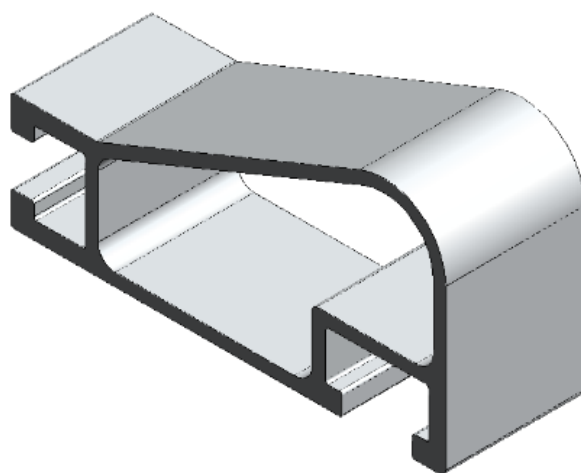


Figure 3.10: Three-dimensional Shape of Extruded Profile (4823).

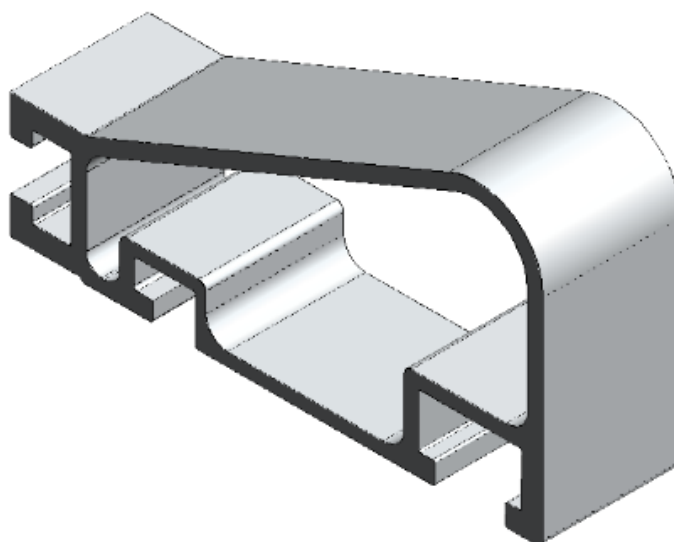


Figure 3.11: Three-dimensional Shape of Extruded Profile (4824).

The extrusion dies are designed according to the geometric characteristics of the profile, to ensure the metal flow smoothly throughout the extrusion process. Also, the design must produce balanced exit velocity of the extruded profile at all sections, to prevent twisting of the extruded profile. In this work, the extrusion dies are designed in such a way for the production of the geometric characteristic profile which are shown in Figure 3.12 and Figure 3.13. This kind of extrusion die has two dies combined together known as mandrel (upper die) and die (lower die). Both upper die 4823 and 4824 have dimension of $\text{Ø}220 \text{ mm} \times 70 \text{ mm}$. Both lower die 4823 and 4824 have dimension of $\text{Ø}230 \text{ mm} \times 80 \text{ mm}$. Both upper dies have three portholes that ensure metal flow evenly throughout the sections of the profile as shown in Figure 3.12(a) and Figure 3.13(a). Between the portholes, there is port bridge to separate the billet when billet flows through the mandrel. The main purpose of the mandrel is to create inner contour or hollow profile and it is supported by the bridges.

The lower die of both 4823 and 4824 have two-step weld chamber to balance the metal flow (Figure 3.12(b) and Figure 3.13(b)). Weld chamber is a region where the metal is bonded together after spitted by the bridge. The total weld chamber length is 18 mm; the length of first-step weld chamber is 15 mm and length of second-step weld chamber is 3 mm. High hydro-pressure in the

weld chamber could push the metal towards the die orifice and it could affect surface finish of the extruded product (Zhang, et al., 2012).

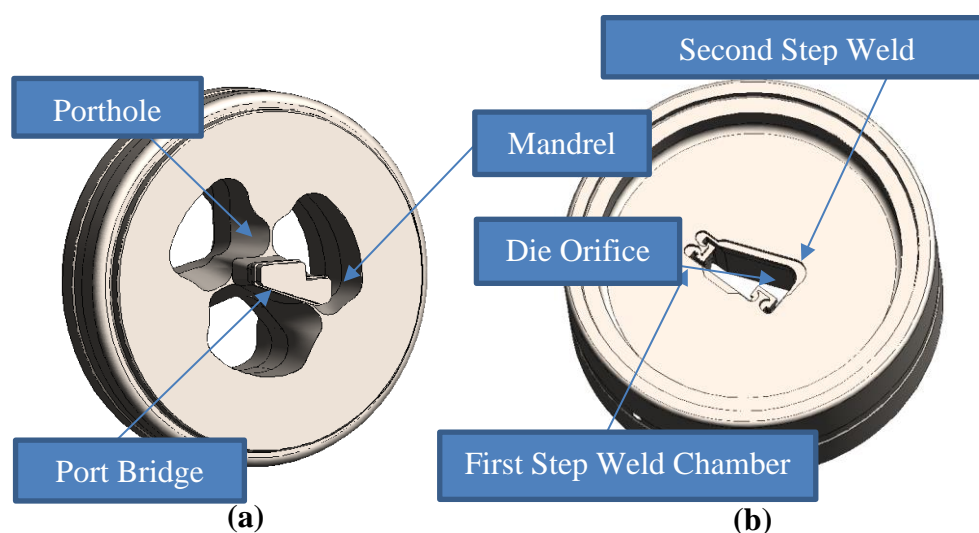


Figure 3.12: Three-dimensional Shape of Mandrel (a) and Die (b) (4823).

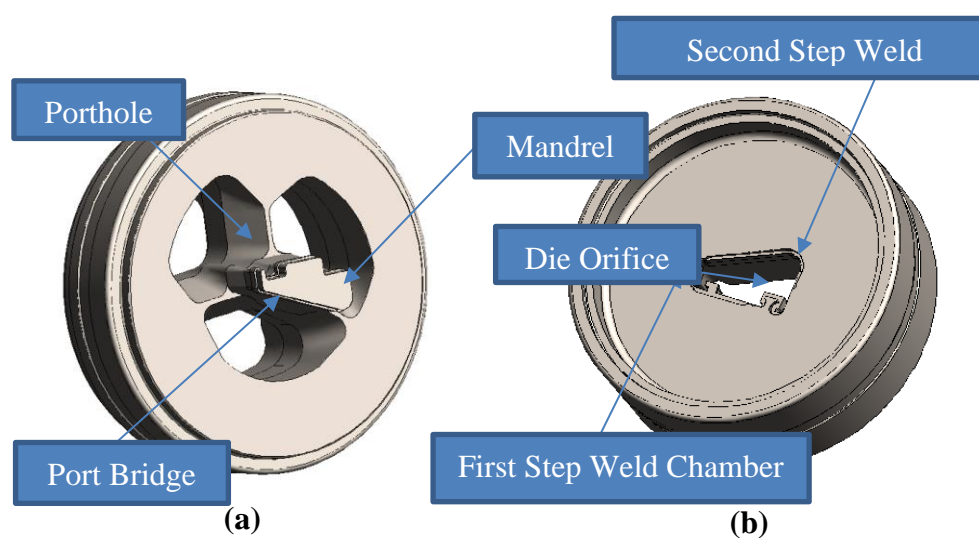


Figure 3.13: Three-dimensional Shape of Mandrel (a) and Die (b) (4824).

3.3.2 Bearing Length Optimisation

There are bearing lands for both upper and lower dies. Bearing land is the region where the extruded product comes in contact with the die surface before exiting the die. The friction or heat generation happens at the bearing land. The friction can affect the velocity distribution for all extrudate section. Thus, it is crucial to have optimised bearing length to ensure the extrudate at all sections flowing out from the die orifice at same speed. Hence, the bearing length may be different

at different sections of the profile to balance the velocity distribution at all sections. Longer bearing length can have higher resistance for the metal to flow and vice versa. Sections with thicker profile usually have greater metal flow speed and it can be slowed down with longer bearing length to match the metal flow speed at sections with thinner profile. Therefore, bearing length should be determined carefully for all profile sections before fabricating the die and putting into production. Since the drawings provided by the local aluminium extrusion company don't provide the bearing length of the dies for every sections, trial and error on the bearing length optimization were done to ensure the velocity distribution is more uniform for all sections. Figure 3.14 and Figure 3.15 show the optimised 3D drawing bearing length for both profiles extruded from respective die.

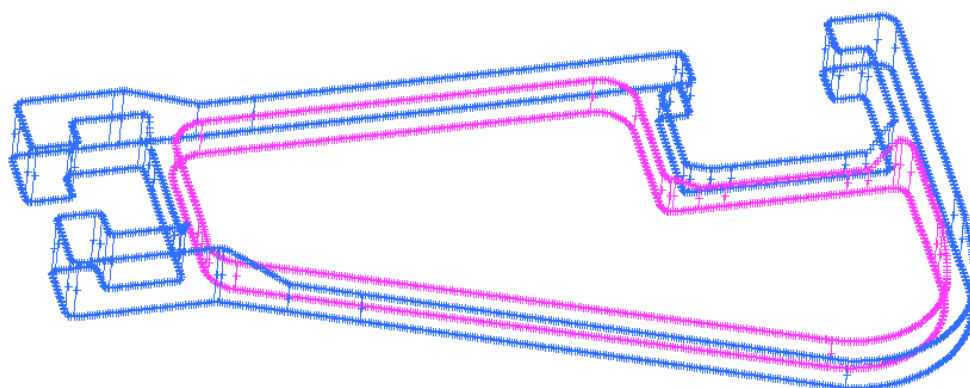


Figure 3.14: Optimised 3D Drawing of Bearing of 4823 Die.

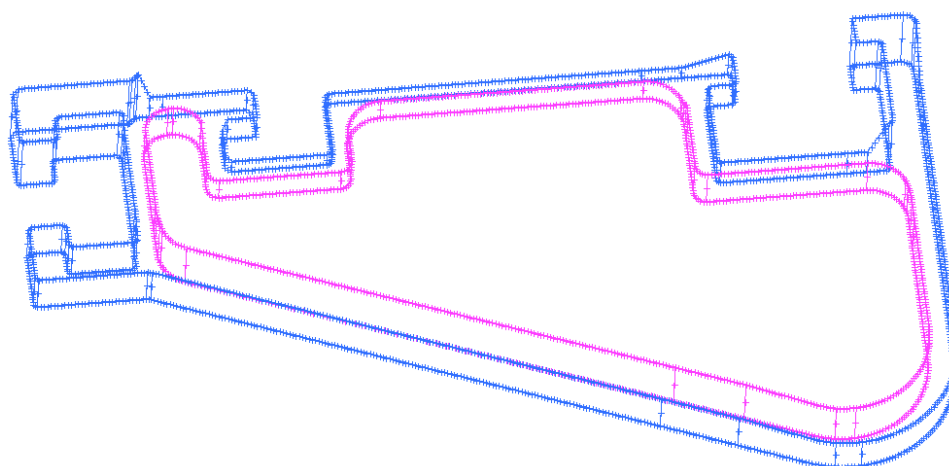


Figure 3.15: Optimised 3D drawing of Bearing of 4824 Die.

Imbalance flow of exit velocity at die exit will lead to poor quality of extruded profile such as twisted or deflected pattern, as shown in Figure 3.16(a) and Figure 3.17(a) . This imbalance exit velocity of extruded profile will also make the research difficult in determine the temperature, flow stress in the die and so on. Thus, it is important to have uniform exit velocity of extruded profile before any studies are carried out. Metal flow in hollow die extrusion is highly complex process and bearing length optimisation was studied and done in few weeks. The relative exit speed difference for both was reduced to maximum 5 % . After bearing length optimisation, the exit speed difference for both profile are balanced and the deflection of profile had been eliminated, as shown in Figure 3.16(b) and Figure 3.17(b).

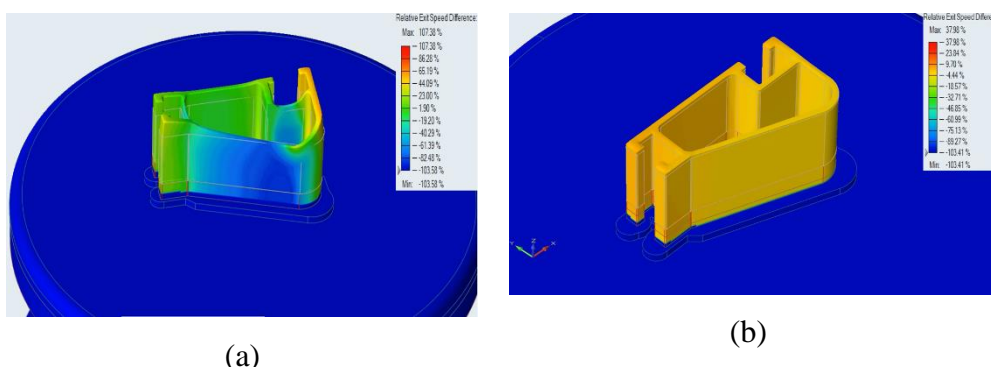


Figure 3.16: Relative Exit Speed Difference of Before (a) and After (b) Bearing Length Optimisation for 4823 Die.

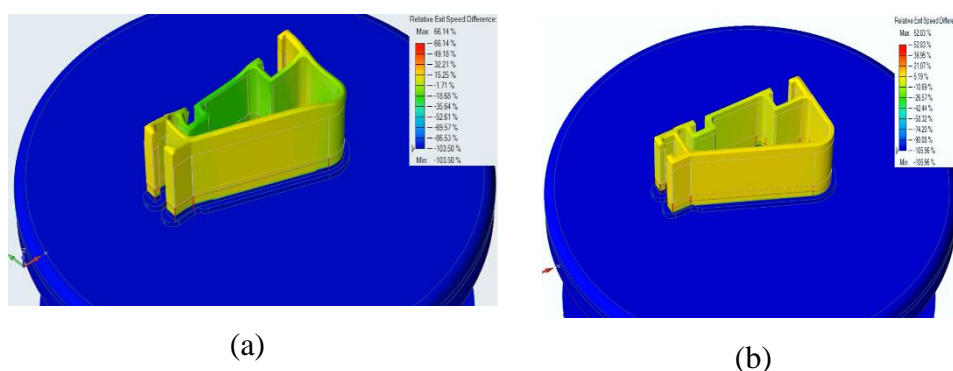


Figure 3.17: Relative Exit Speed Difference of Before (a) and After (b) Bearing Length Optimisation for 4824 Die.

3.3.3 Mesh Generation of Whole Numerical Model

To simulate the extrusion process in the simulation software, all the domains that material flows through are extracted and meshed. In order to ensure the simulation can be carried out smoothly, there are some amendments done for the die geometry. This amendment could greatly influence the size and quality of the mesh generation in the meshing stage. In this simulation, the model is separated into five parts: billet, porthole, welding chamber, bearing and profile for convenient in creating boundary conditions and meshing (refer to Figure 3.18 and Figure 3.19).

Number of elements and size of elements in meshing have great impact on the simulation accuracy and time taken for processing. The smaller the size of elements can result in higher number of elements in mesh generation and giving more accurate simulation result but longer processing time is required. Sections where metal billet experiences greater deformation should have smaller element size in order to have more accurate results especially bearing area. Considering these complex hollow profiles to be extruded, meshing is challenging. Fortunately, the simulation software allows to set different size of element and type for every domain. To enhance the accuracy of the result, elements density should be varied in the model. As discussed earlier, sections where metal billet experiences large deformation should have finer to higher density of elements especially at bearing area where the final profile shape will be formed. Hence, finer elements should be applied towards the bearing area as shear deformation increases towards bearing area. The meshes of the weld chamber, bearing, profile, porthole and billet are shown in Figure 3.18 and Figure 3.19.

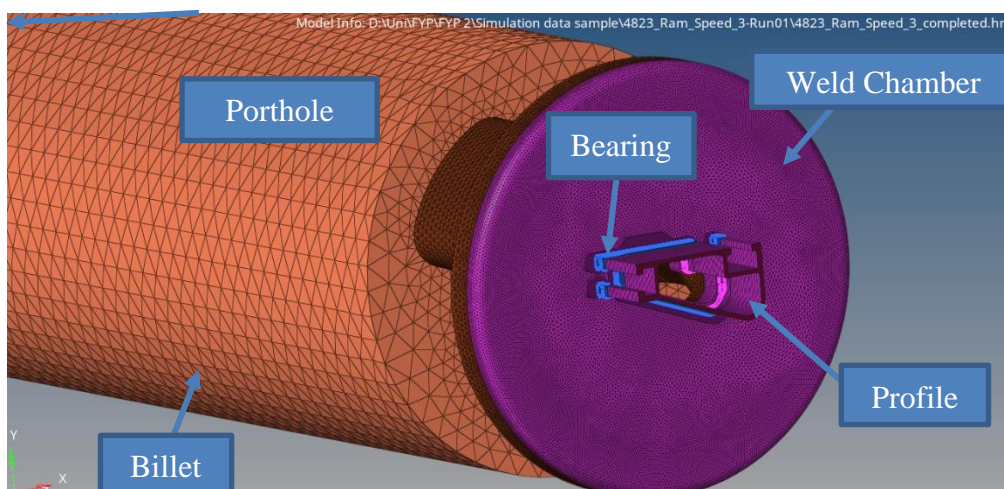


Figure 3.18: Mesh Generation of Whole Numerical Model for 4823 Die.

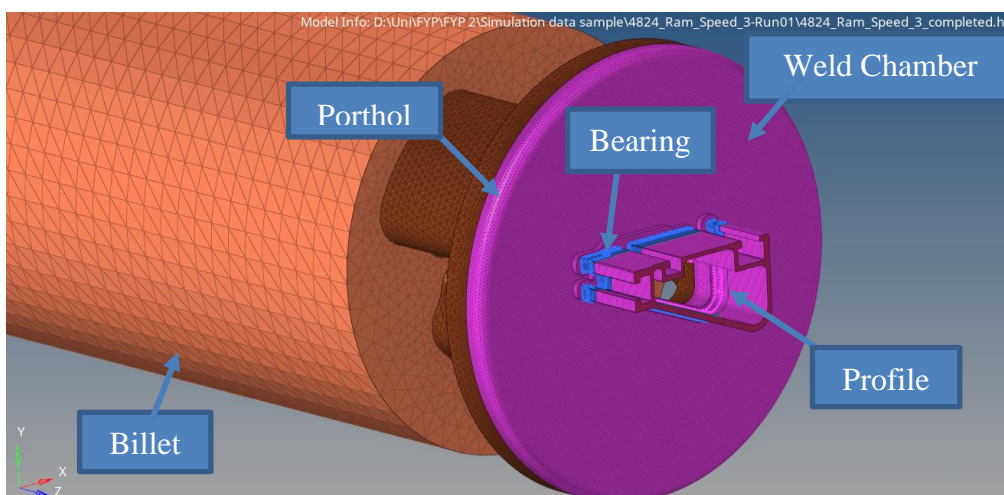


Figure 3.19: Mesh Generation of Whole Numerical Model for 4824 Die.

To further enhance the simulation results, mesh convergence analysis is carried out to determine appropriate number of elements which can give the accurate results. It is very important to perform this analysis as elements size has significant impact on output (Ahmad, Ismail and Mat, 2013). For this analysis, at least three convergence runs are required to plot a curve to indicate where convergence is achieved, or how many of elements are required to get accurate results. If two runs with different number of elements, give same results, convergence is achieved and the number of elements or mesh density is appropriate for the FEM. In this study, there are five runs with different number of elements are carried out for mesh convergence analysis for both dies. Different number of mesh to be tested for both dies are listed in Table 2.1.

Table 3.1: Defined Number of Mesh of 4823 Die and 4824 Die for Mesh Convergence Analysis.

Run	Number of Mesh (4823 Die)	Number of Mesh (4824 Die)
1	625681	634884
2	775155	767244
3	906662	811718
4	956653	962122
5	1049151	1217388

3.3.4 Process Definition

The die material for both dies are JIS SKD61 tool steel (also known as H13) and the chemical composition is presented in Table 2.1. On the other hand, the metal billet is in cylindrical shape and the material is aluminium alloy AA6005 for both dies. Aluminium alloy AA6005 chemical composition is presented in Table 3.2.

Table 3.2: Chemical Composition (%) of aluminium alloy AA6005.

Element	Cr	Cu	Fe	Mg	Mn	Si	Ti	Zn	Al
Content (wt%)	0.04 (max)	0.2 (max)	0.30 (max)	0.52-0.57	0.1-0.2	0.58-0.63	0.1 (max)	0.1 (max)	Balance

For 4823 die, the aluminium alloy billet has diameter of 177.8 mm (7 inch) and 650 mm in length. For 4824 die, the aluminium alloy billet has diameter of 177.8 mm (7 inch) and 670 mm in length. The extrusion ratio for 4823 die and 4824 die is about 74 and 46 respectively. The initial temperature for billet, die and container defined in simulation are 480 °C, 450 °C and 480 °C respectively. There are some extrusion process parameters were not given from local aluminium extrusion company, such as initial die temperature and container temperature (refer to Table 3.3). Thus, there are some assumptions made for process parameters.

The initial die temperature is assumed at 450 °C which is 30 °C lower than initial billet's temperature because the temperature difference can create temperature gradient where the heat can be dissipated from billet to die due to

friction. This method may help in reducing extrudate's temperature as too high temperature may result in poor surface quality. The initial container temperature was assumed to be same as initial billet temperature because this can ensure the billet has appropriate softness prior deformation enter entering die and avoid hardening when exposed to lower temperature environment.

In this project, there are three extrusion process parameters to be investigated which are ram speed, initial billet temperature and initial die temperature to study the effect on the extrusion process and wear behaviour. These extrusion process parameters have significant effect on the exit temperature of extrudate, pressure and die wear. Therefore, it is important to study the effect of these extrusion process parameters to investigate the impact on the surface quality of extrudate. From these studies, improvements on the extrusion process parameters can be proposed to eliminate or minimise the surface defects formed on extrudate. The process parameters defined in the simulation to study effect of ram speed, initial billet temperature and initial die temperature on extrusion process and die wear behaviour are listed in Table 3.4, Table 3.5 and Table 3.6 respectively.

Table 3.3: Extrusion Process Parameters given from the Local Aluminium Extrusion Company.

Die Material	Metal Billet	Ram Speed (mm/s)	Initial Billet Temperature (°C)	Billet Length (mm)
Tool Steel SKD61	Aluminium Alloy AA6005	3	480	650 (4823 Die), 670(4824 Die)

Table 3.4: Process Parameters Defined in the Simulation to Study the Effect of Ram Speed on Extrusion Process and Die Wear Behaviour.

Initial Die Temperature (°C)	Initial Container Temperature (°C)	Ram Speed (mm/s)	Initial Billet Temperature (°C)	Initial Die Temperature (°C)
450	480	1,2,3,4,5	480	450

Table 3.5: Process Parameters Defined in the Simulation to Study the Effect of Initial Billet Temperature on Extrusion Process and Die Wear Behaviour.

Initial Die Temperature (°C)	Initial Container Temperature (°C)	Ram Speed (mm/s)	Initial Billet Temperature (°C)	Initial Die Temperature (°C)
450	440	3	440	410
	460		460	430
	480		480	450
	500		500	470
	520		520	490

Table 3.6: Process Parameters Defined in the Simulation to Study the Effect of Initial Die Temperature on Extrusion Process and Die Wear Behaviour.

Initial Die Temperature (°C)	Initial Container Temperature (°C)	Ram Speed (mm/s)	Initial Billet Temperature (°C)	Initial Die Temperature (°C)
450	480	3	480	390,420,480,510

3.3.5 Development of User-Defined Wear Subroutine

Traditional Archard wear model is widely applied to analyse wear behavior of dies, as shown in equation (3.1). In this traditional model, it shows the wear depth, W (m) is directly proportional to the wear coefficient, K , contact pressure, P (MPa) and relative length between die and billet, L (m), and it is inversely proportional to the die hardness, H (HB).

$$W = \frac{KLP}{H} \quad (3.1)$$

However, this model describes the wear depth by assuming the wear coefficient and die hardness is constant throughout the extrusion process for every sections. In fact, the material properties like wear coefficient and die hardness for this case can change significantly during hot extrusion process, especially when the process temperature is higher than 400°C (Li, et al., 2013).

In order to have more accurate calculation, Kang, et al. (1999) had tried modifying the model by considering the wear coefficient and die hardness are functions of temperature as the material will be softened when the temperature increased, as shown in equation (3.2). Kang, et al. (1999) had done numerous experiments to verify this model by carrying out experiment numerically. With this model, the wear coefficient and die hardness can be determined for every point where the temperature may vary along the die bearing surface.

$$W = \frac{K(T)LP}{H(T)} \quad (3.2)$$

Furthermore, Lee and Jou (2003) had also further modified the model based on tool steel H13 used in metal forming operation. They had come out wear coefficient and die hardness equation in function of temperature for tool steel H13 to describe the relationship between temperature, wear coefficient and die hardness as shown in equation (3.3) and equation (3.4):

$$K(T) = [29.29 \times \ln T - 168.73] \times 10^{-6} \quad (3.3)$$

$$H(T) = 9216.4 \times T^{-0.505} \quad (3.4)$$

Li, et al. (2013) pointed out that the interface pressure, temperature and velocity field will vary with relative position between die and metal billet during the extrusion process. Hence, the equation below can be further modified as shown in equation (3.5). Subscript i^{th} of the parameter is describing the forming position and subscript j^{th} of parameter is at the time increment. The temperature and pressure for every position obtained and recorded in simulation software. Thus, die wear depth can be calculated using the data obtained from the simulation.

$$\Delta W_{ij} = k_{ij}(T) \frac{L_{ij}P_{ij}}{H_{ij}(T)} \quad (3.5)$$

3.3.6 Extrusion Force Formula

Extrusion force is a term to indicate how much force is required to extrude the billet out of the die at desired speed. Extrusion force can be calculated by applying the equation (3.6). F is the extrusion force (N), A_o is the area of billet before extrusion (m^2), A_f is the area of the profile to be extruded (m^2) and Y_{avg} is the average true stress of the billet, (N/m^2). A_o/A_f is actually extrusion ratio.

$$F = A_f Y_{avg} \ln \frac{A_o}{A_f} \quad (3.6)$$

Average true stress of the billet can be determined based on the metal used and the temperature of the billet. It also depends on many factors such as strength of billet, friction generated during extrusion process, flow stress and process parameters such billet temperature and ram speed (Kalpakjian and Schmid, 2010). When there is increasing of friction and deformation rate during extrusion process, average true stress will increase and lead to higher extrusion force required.

CHAPTER 4

RESULTS AND DISCUSSION

4.1 Introduction

This chapter starts with microscopy analysis which discusses about the surface defects identified on the aluminium extrudate and their formation mechanism. Next, result and discussion about the effect of extrusion process parameters on the extrusion process based on FEM results. Last section will discuss the causes and preventions for the surface defects identified on the aluminium extrudates.

4.2 Microscopy Analysis

This section will discuss about the surface defects found on aluminium 4823 extrudate samples and aluminium 4824 extrudate samples that were collected and etched for microscopy analysis. Pick-up defects and die line are mainly found on the samples' extrudate surface. These defects have a specific appearance and characteristics which will be revealed in following sub-sections. From these samples, die line defects can be found on 4823 extrudate surface and pick-up defects are found mostly on 4824 extrudate surface.

4.2.1 Pick-up Defect

Pick up defect has an appearance of comet tail or tear drop shape. The defect has a maximum length at about 2.5 mm and width could reach up to $330 \mu\text{m}$ (Peris, 2007). Figure 4.1 is showing the location of pick-up defect found on 4824 extrudate surface. Observation by our naked eyes, the defects look like scratches along the aluminium alloy extrudate surface as shown in Figure 4.2, Figure 4.4 and Figure 4.7 at respective location on 4824 aluminium alloy extrudate surface. However, this defect is different from the scratches that were done by equipment or mishandling during transport. The defect has a constant comet tail-like shape along the aluminium alloy extrudate surface. Figure 4.3, Figure 4.5, Figure 4.6 and Figure 4.8 are showing pick-up defect under optical microscope at location 1,2,3 and 4 respectively. Figure 4.3 and Figure 4.5 have rather blur visualisation on the defect because it was captured on the curve surface.

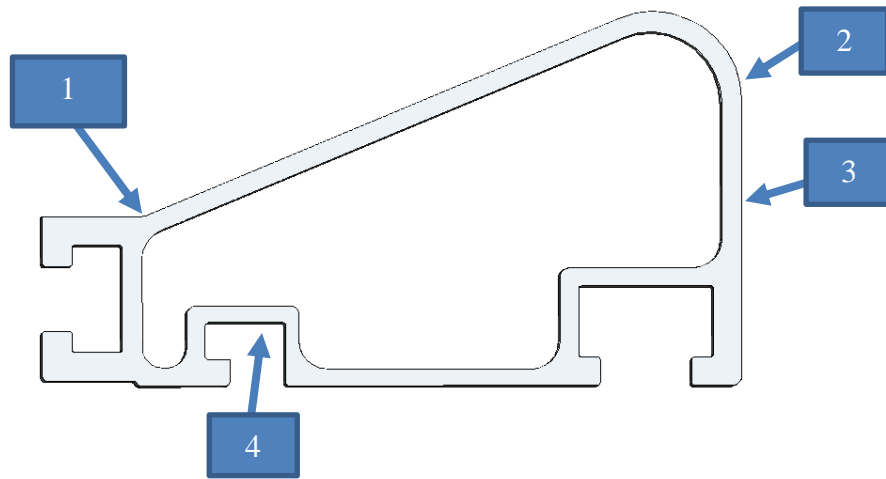


Figure 4.1: Location of Pick Up Defect on 4824 Extrudate Surface.

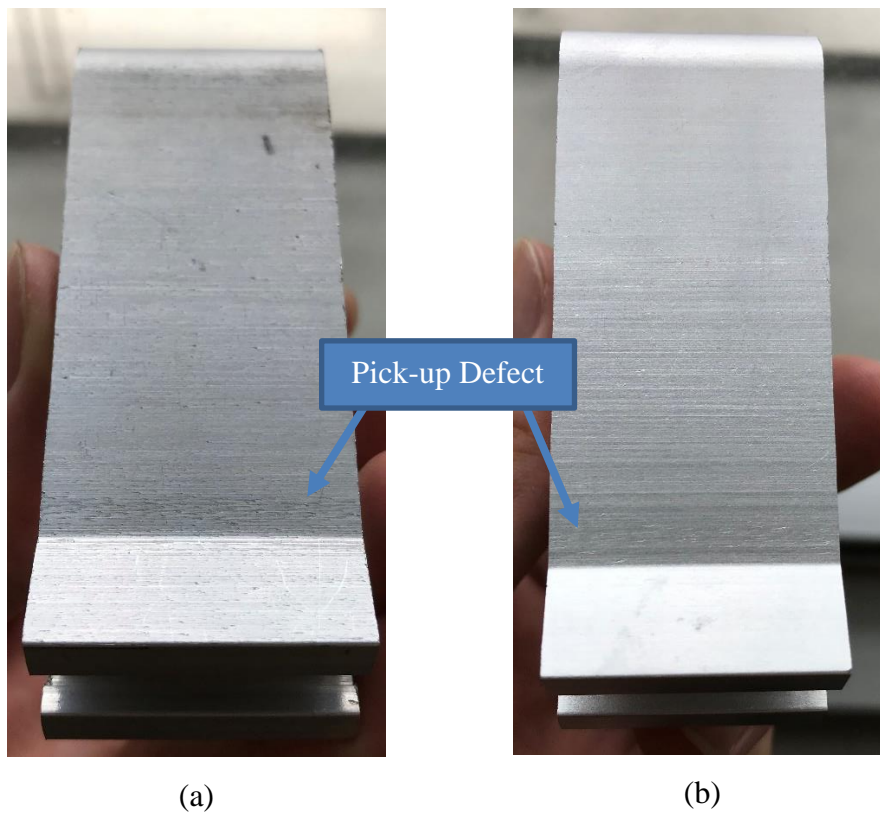


Figure 4.2: Appearance of Pick-up Defect on 4824 Extrudate Surface at Location 1 Before (a) and After (b) Etching Treatment.

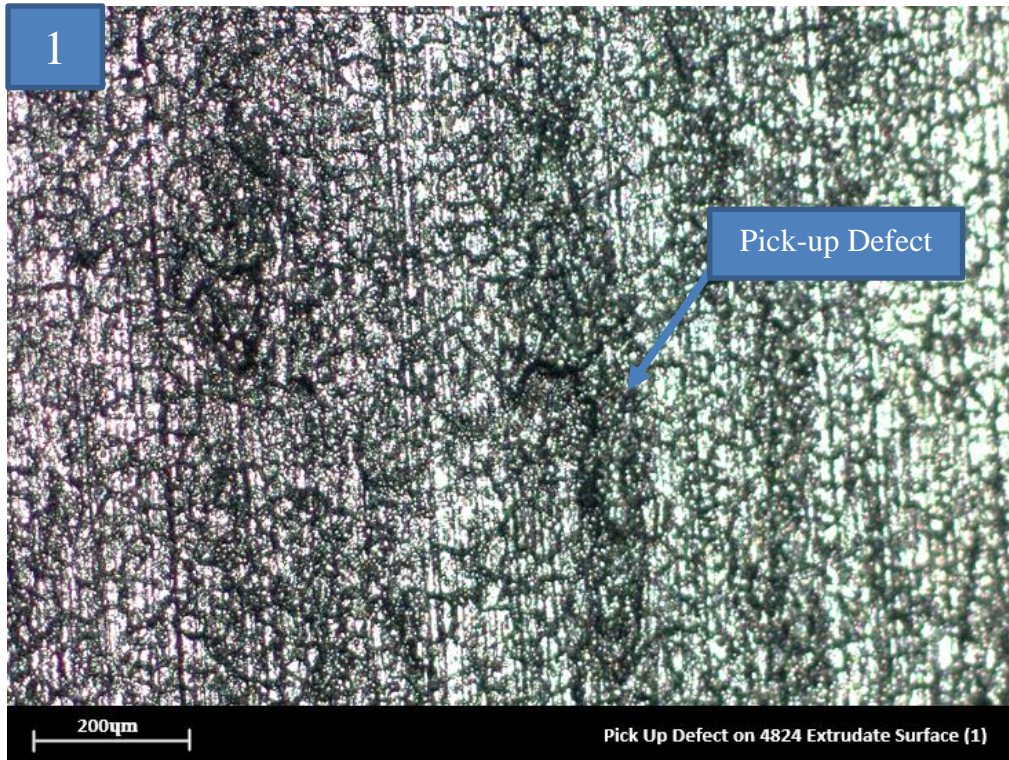


Figure 4.3: Optical Microscope Showing Pick-up Defect on 4824 Extrudate Surface at Location 1.

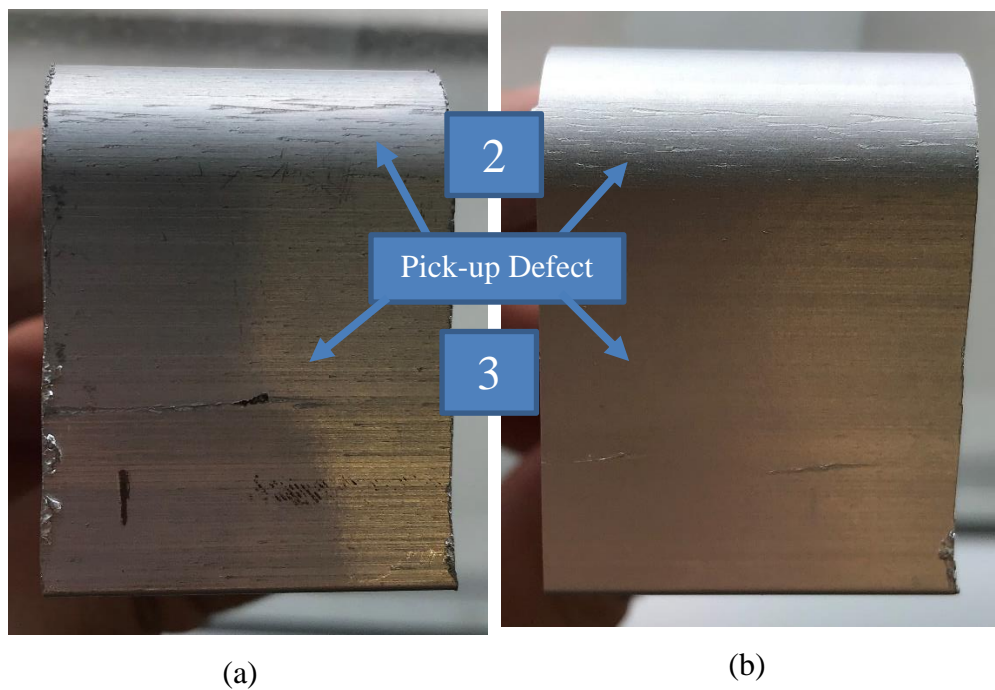


Figure 4.4: Appearance of Pick-up Defect on 4824 Extrudate Surface at Location 2 (upper) and 3 (bottom) Before (a) and After (b) Etching Treatment.

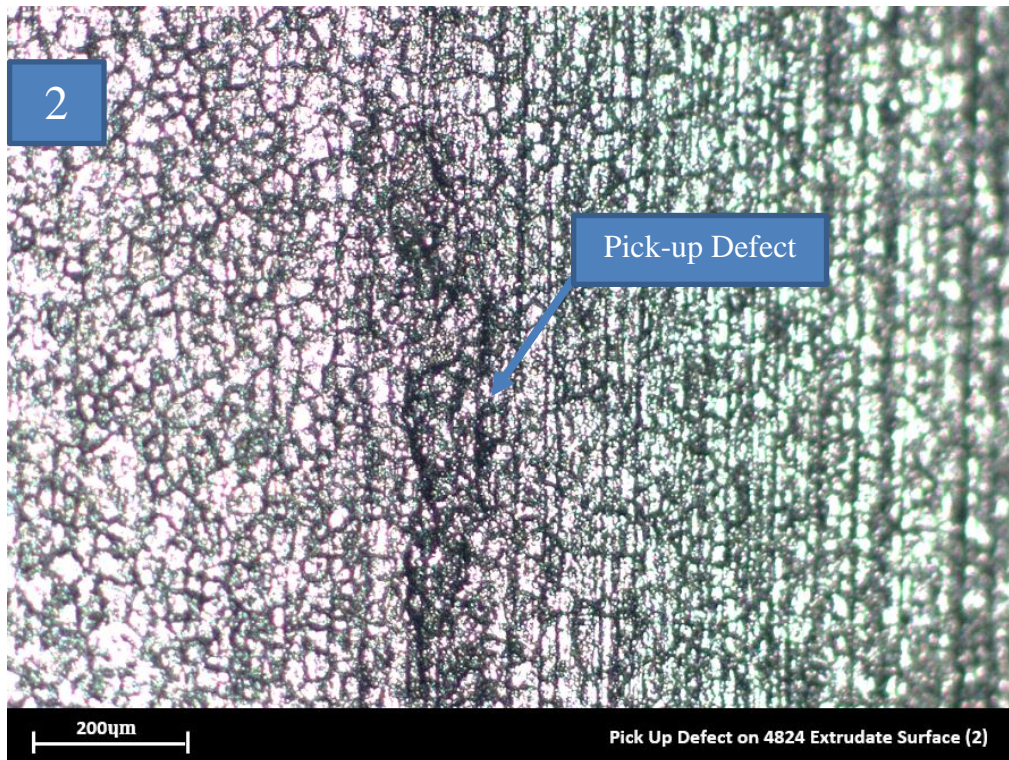


Figure 4.5: Optical Microscope showing Pick-up Defect on 4824 Extrudate Surface at Location 2.

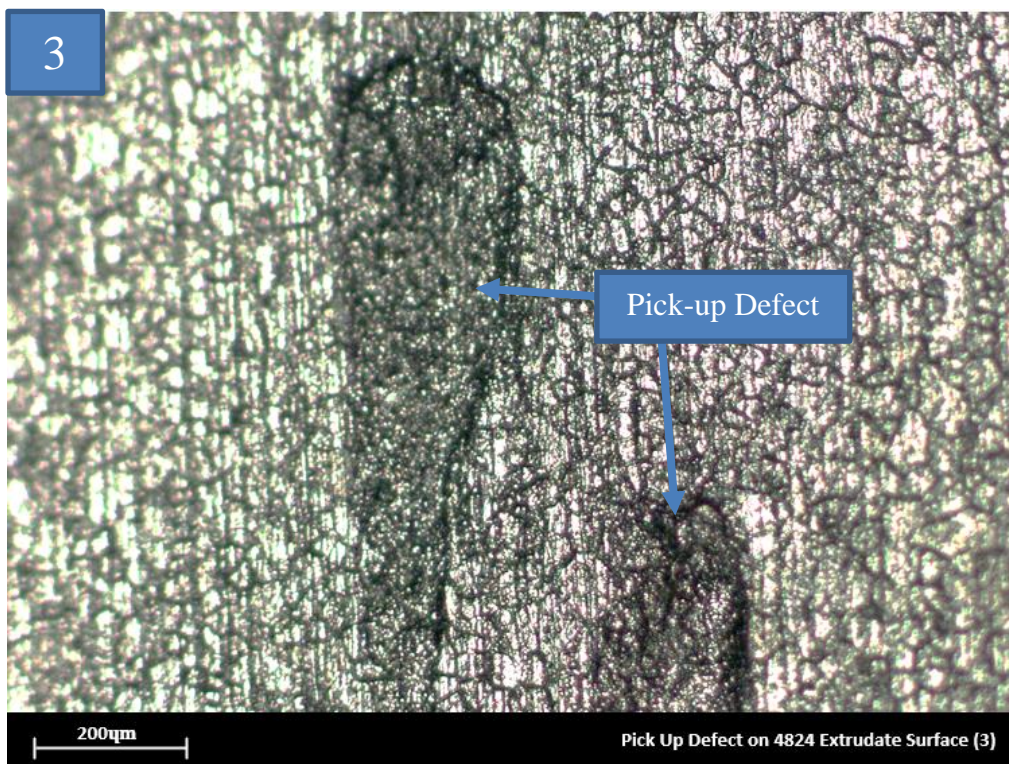


Figure 4.6: Optical Microscope showing Pick-up Defect on 4824 Extrudate Surface at Location 3.

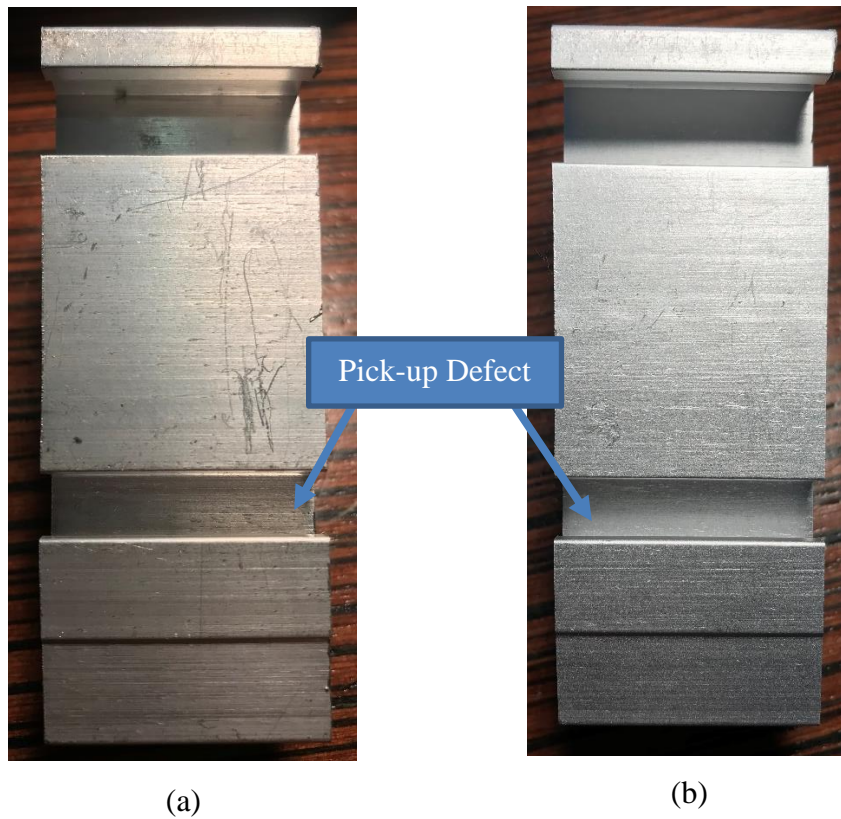


Figure 4.7: Appearance of Pick-up Defect on 4824 Extrudate Surface at Location 4 Before (a) and After (b) Etching Treatment.

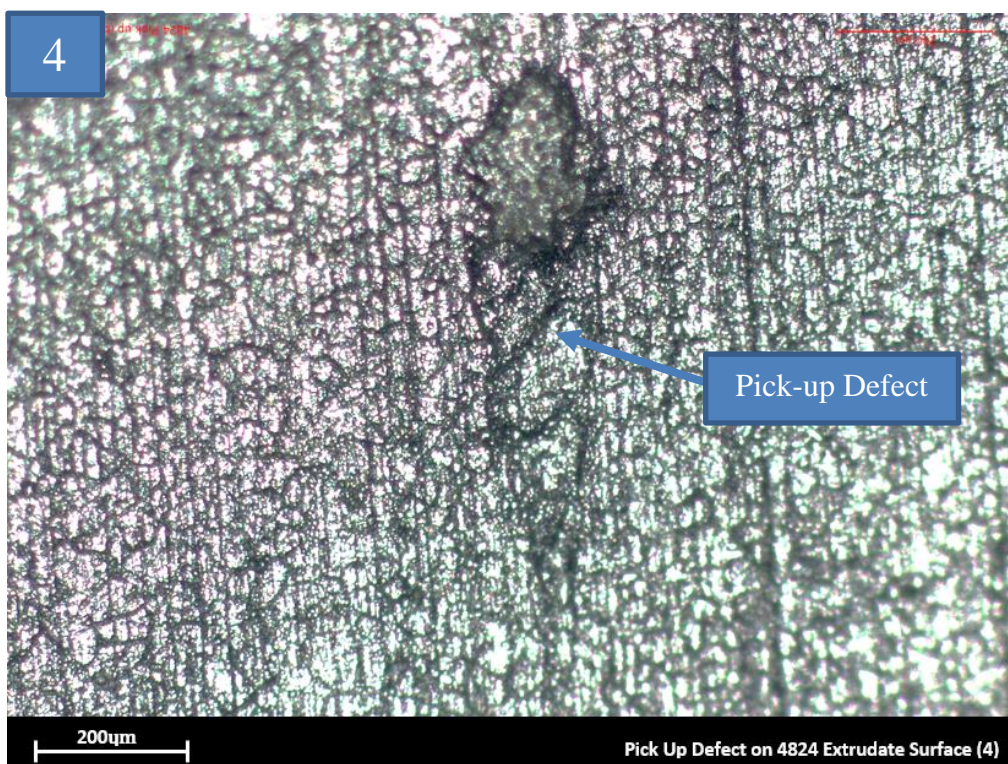


Figure 4.8: Optical Microscope showing Pick-up Defect on 4824 Extrudate Surface at Location 4.

After identifying the surface defects on the 4824 extrudates, EDX analysis was carried out to analyse material elements on the surface defects. It is found that most of the chemical content on the pick-up defect is aluminium as shown in Figure 4.9. Peris (2007) also found that most of the chemical content on the pick-up defect is aluminum by X-Ray spectroscopy (EDS). In addition, Matienzo, et al. (1983) had done numerous extrusion process and found out that there is no trace of iron oxide from die surface to cause pick-up defect. Thus, it can be said that this defect was mainly caused by aluminium adhered on the die bearing surface. The formation mechanism will be discussed in next section.

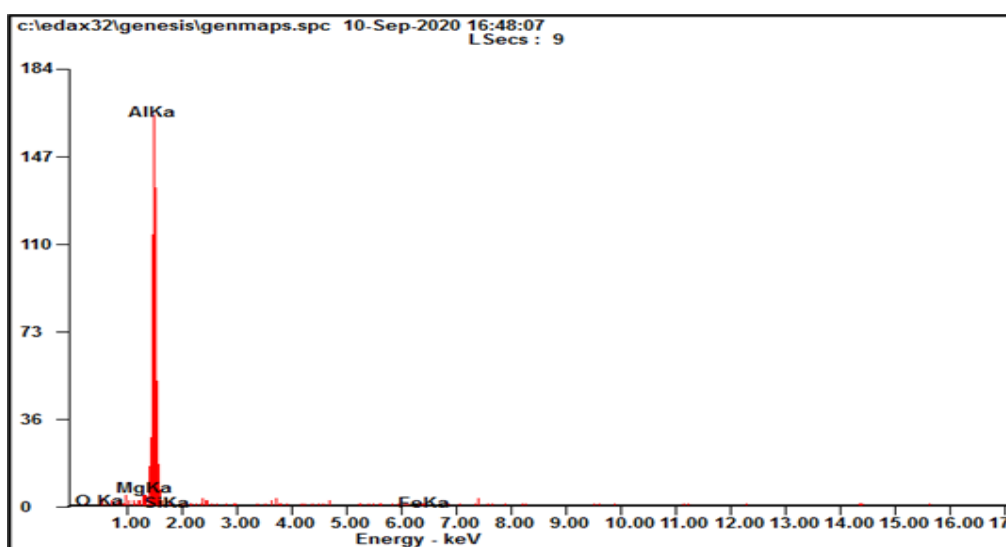


Figure 4.9: EDX Analysis at Pick-up Defect Location.

4.2.2 Formation Mechanisms of Pick-up Defect

Figure 4.10 is depicting cross section of die and extrudate during extrusion when pick-up defect was formed. In this research, the dies material is JIS SKD 61 and the dies have undergone surface treatment, known as nitriding to enhance wear resistance and hardness. Decarburized layer is a layer formed when carbon is diffused out of the die material during heat treatment for nitriding. After nitriding treatment, nitriding layer is formed on top of the decarburizing layer and it is very hard. However, this nitriding layer is not stable at elevated temperature and nitride may diffuse out of die material to react with aluminium during extrusion process. This reaction will form aluminium nitride (AlN), known as intermetallic layer on top of nitriding layer.

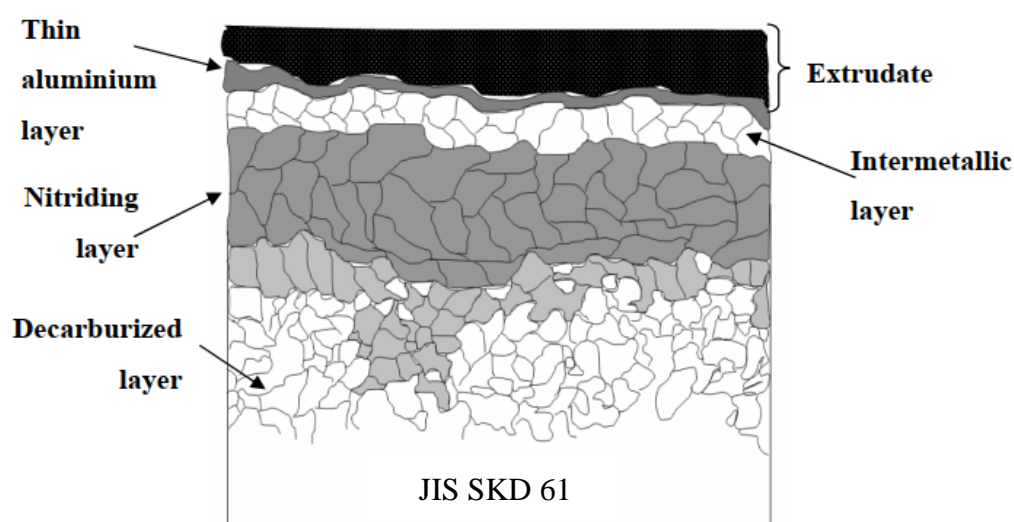


Figure 4.10: Cross Section of Die and Extrudate During Extrusion Process When Pick-up Defect was formed (Peris, 2007).

In fluid mechanic, the fluid flows near to the surface boundary will have lower speed than actual speed due to friction. This theory can be applied in extrusion process as well because extrudate is flowing like a fluid in die. The cross section of the extrudate flowing on the die bearing surface is illustrated in Figure 4.11. During extrusion process, aluminium alloy which is flowing near to the intermetallic layer has lower flowing speed compared to actual flowing speed and this layer is known as adhering aluminium layer. Adhering aluminium could have formed as aluminium oxide (Al_2O_3) particles when there is presence of oxygen gas in the extrusion environment. When the aluminium alloy extrudate flows through the aluminium oxide particles, the extrudate may be scratched. Due to the velocity different, shearing effect can be introduced from high flow speed on the low flow speed. Also, high pressure, high strain rate and high temperature can be introduced during extrusion. These factors could be enough to reduce cohesive strength of adhered aluminium oxide particles on the bearing surface. The reduced cohesive strength of aluminium oxide can result in tearing and chipping of the adhered aluminium layer. Thus, pick-up defect occurs at interface of adhered aluminium oxide layer and moving extrudate during extrusion process due to sticking condition and reduced cohesive strength of aluminium.

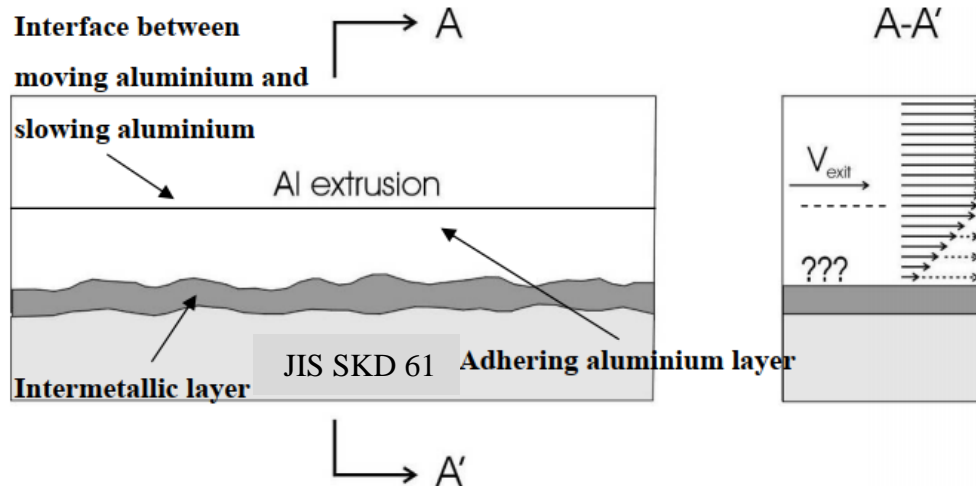


Figure 4.11: Cross Section of Extrudate Flowing on the Die Bearing Surface (Peris, 2007).

4.2.3 Die Line

Die line defect can only be found on 4823 extrudate surface and the location is indicated in Figure 4.12. Die line is a black line or longitudinal depression formed on the aluminium extrudate surface as shown in Figure 4.13. Figure 4.14 is showing the die line at the location under optical microscope. The die line found on 4823 extrudate surface is considered as serious surface defect as the width of the die line is quite wide. This is defect is usually formed due to imperfections of die bearing surface.

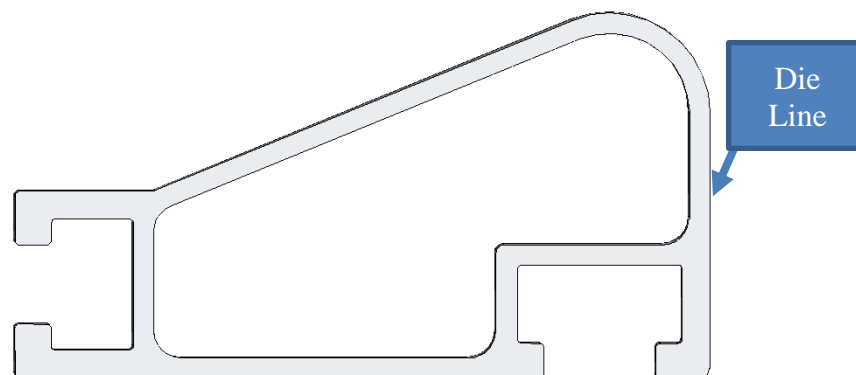


Figure 4.12: Location of Die Line on 4823 Extrudate Surface.

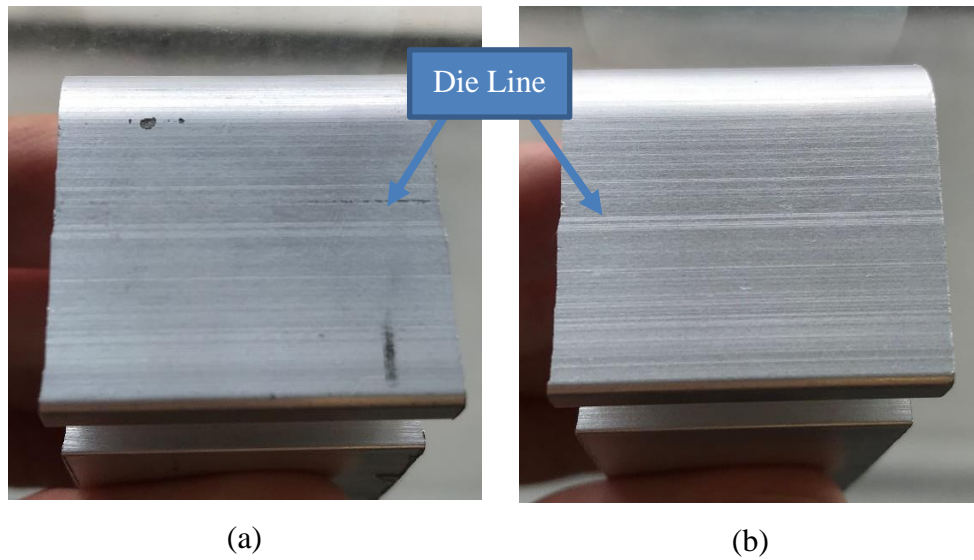


Figure 4.13: Die Line Appearance on 4823 Extrudate Surface Before (a) and After (b) Etching Treatment.

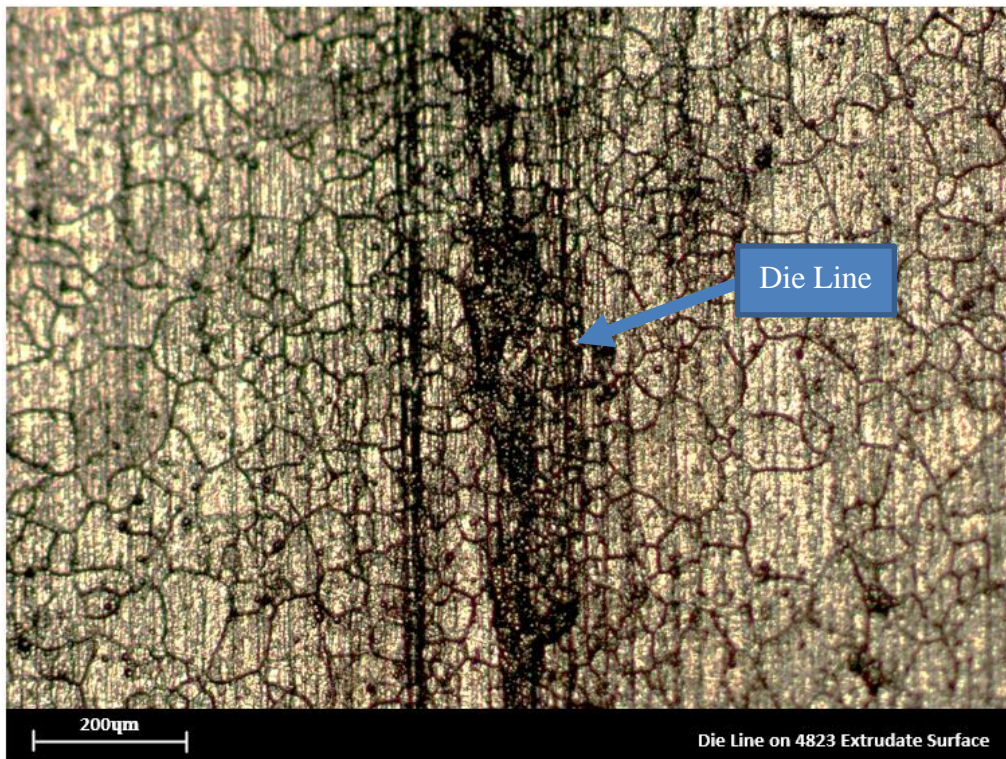


Figure 4.14: Optical Microscope showing Die line on 4823 Extrudate Surface.

After identifying the surface defects on the 4823 extrudates, EDX analysis was carried out to analyse material elements on the surface defects. It is found that most of the chemical content on the die line defect is aluminium

and there is small amount of iron content as shown in Figure 4.15. However, Peris (2007) found that high content of iron (Fe) can be found on the die line defect. There is low iron content found at die line in this work because most of iron attached at die line defect was removed during desmutting process. It is believed that the formation of die line is related to deterioration of nitride layer and pick-up of die material. The formation of die line will be discussed in next section.

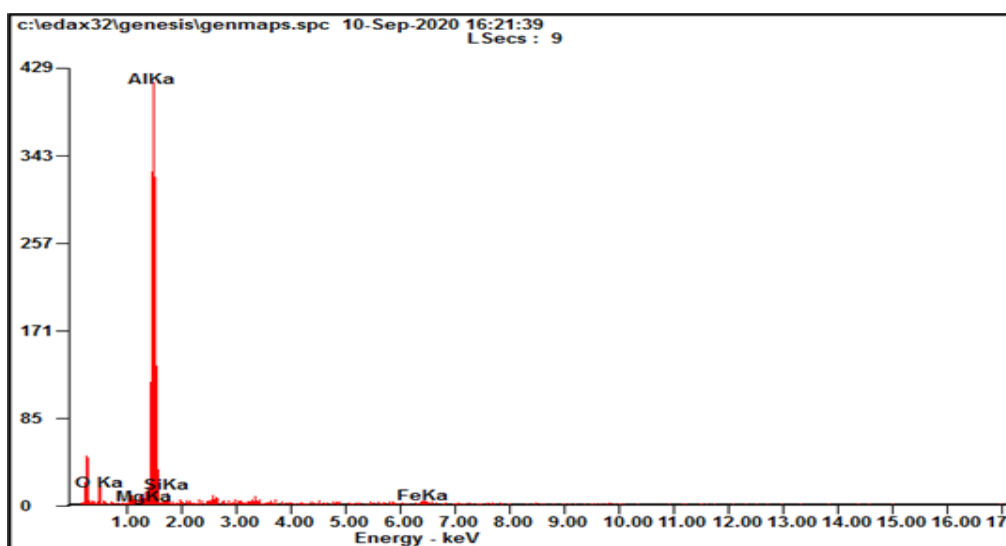


Figure 4.15: EDX Analysis at Die Line Defect.

4.2.4 Formation Mechanism of Die Line Defect

Figure 4.16 is depicting cross section of die and extrudate during extrusion process when die line is formed. Unlike formation mechanisms of pick-up defects, intermetallic particle doesn't form as a layer on top of nitriding layer but as a cluster and has a cauliflower appearance. These intermetallic particles formed make the bearing surface looks uneven, resulting in poor smoothness for the metal flow during extrusion process. The velocity flow profile of the aluminium alloy is similar discussed in Formation Mechanisms of Pick-up Defect (refer to Figure 4.11). Thus, shearing effect can be introduced and shear force or pressure would be sufficient enough to remove the intermetallic particle and nitriding layer from the bearing surface, causing die material exposes to the aluminium alloy. This wear mechanism is known as abrasive wear. Aluminium alloy extrudate will be scratched by the die material when extrudate is flowing through it. From the EDX analysis, there is some traces of

iron. Thus, it is believed that die line happens when there is spalling of nitriding layer and causing local tearing and chipping.

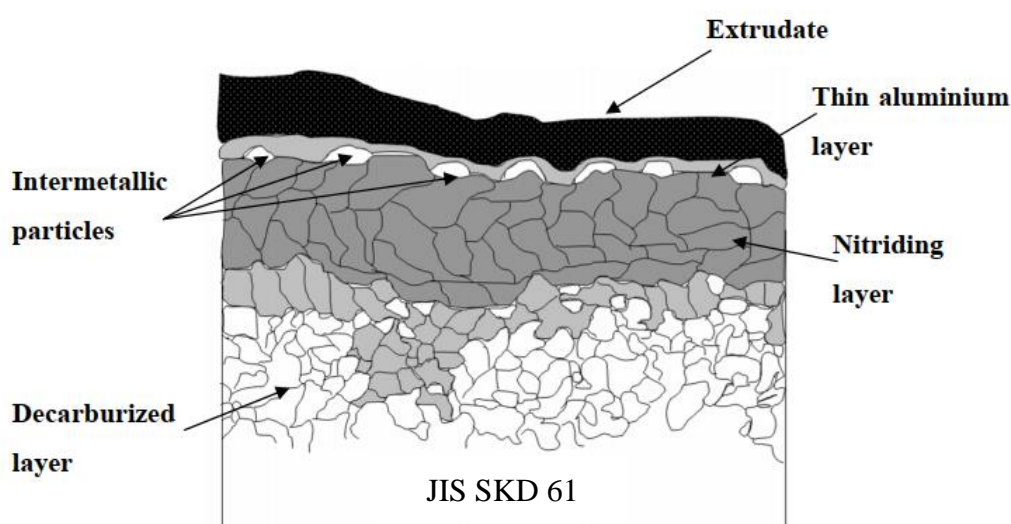


Figure 4.16: Cross Section of Die and Extrudate During Extrusion Process When Die Line Defect was formed (Peris, 2007).

4.3 Mesh Convergence Test

Meshing is a very important step for simulation to compute. The number of elements has a great effect on the accuracy of the results. Hence, it is necessary to carry out mesh convergence test to determine the appropriate number of elements needed for this study. In this study, the extrusion force is recorded and compare the results with different number of elements for both dies.

Figure 4.17 and Figure 4.18 show the extrusion force obtained from FEM with various number of elements in mesh for 4823 die and 4824 die respectively. It is noted that the extrusion force for 4823 die drops when the number of elements in mesh is increased from 625681 to 906662 and the extrusion force remains relative constant when number of elements in mesh is further increased from 906662 to 1049151. On the other hand, the extrusion force for 4824 die drops when the number of elements in mesh is increased from 634844 to 767244 and the extrusion force remains relative constant when the number of elements in mesh is further increased from 767244 to 1217388. The convergence is achieved when the extrusion force is remains relative constant as the number of elements in mesh has very little effect on the simulation result. Therefore, the mesh for 4823 die and 4824 die should have total elements

number for the whole model of 906662 and 767244 respectively because it is the number of elements in mesh that achieve convergence first. With this analysis, it is able to obtain more accurate result from the simulations by using FEM with the least time.

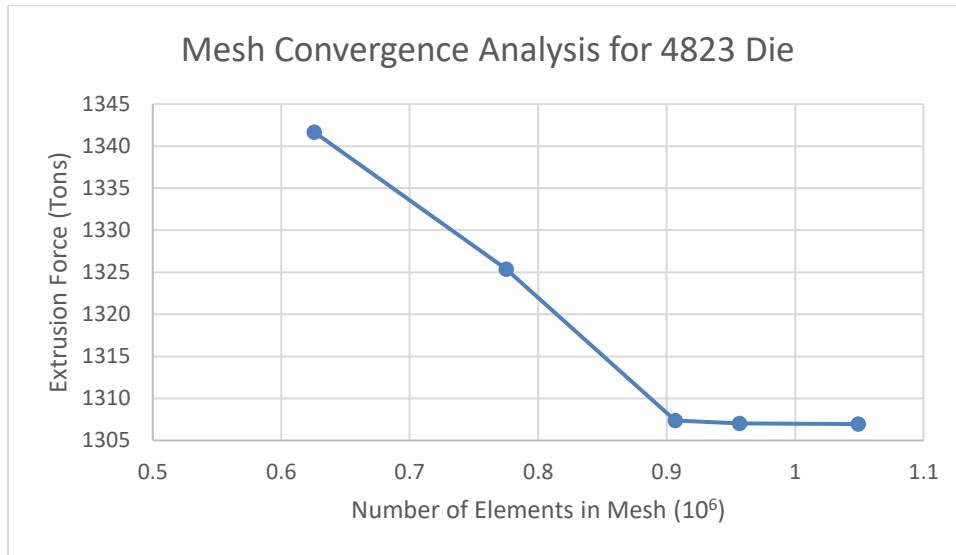


Figure 4.17: Mesh Convergence Analysis for 4823 Die.

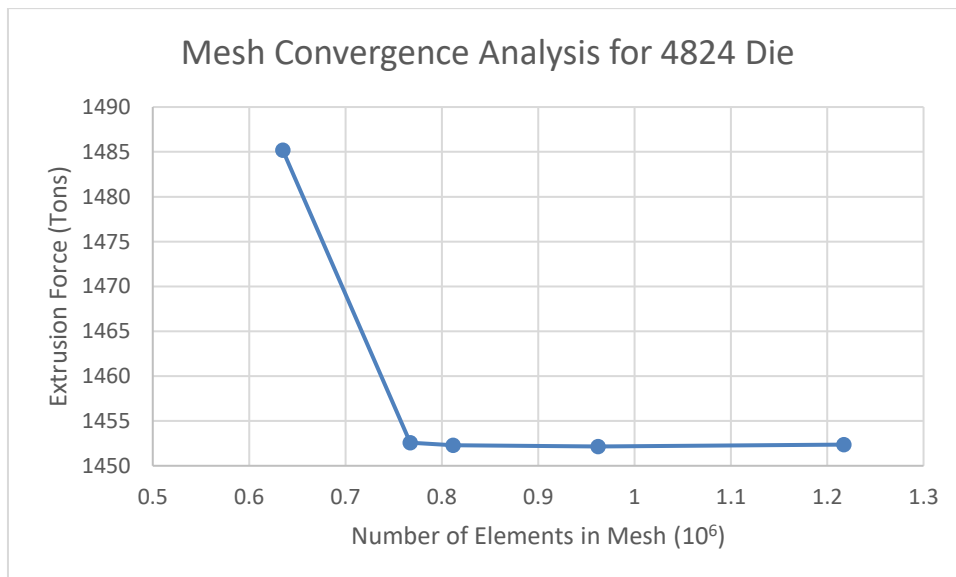


Figure 4.18: Mesh Convergence Analysis for 4824 Die.

4.4 Simulation Results

Extrusion process simulation is carried out to identify whether the process parameter has influences on the surface defects found on the samples and seek

for any improvement could be done to eliminate the defects. The results are obtained from the simulation are recorded and plotted into graph using Microsoft Excel. The process parameters to be investigated and discussed in this research are ram speed, initial metal billet temperature and initial die temperature. In order to capture and discuss the properties of the metal flow in the dies, the points captured in the simulation for 4823 die and 4824 die as shown in Figure 4.19 and Figure 4.20 respectively. There are total 13 points taken for each die. Point 1 to point 5 are located at the second step weld chamber and point 6 to point 13 are located at die bearing surface. The measured points at that particular sections are based on surface defects found on the extrudate samples given.

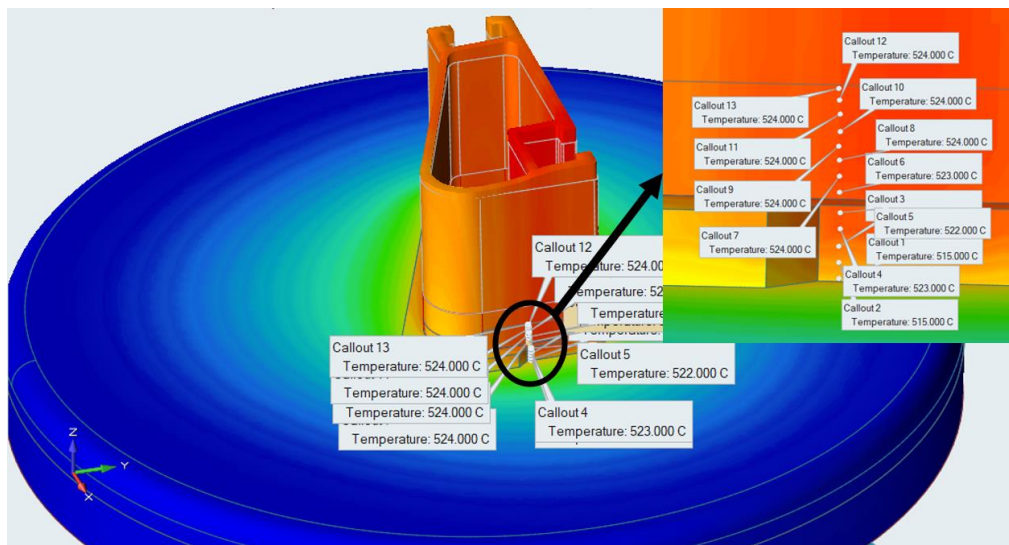


Figure 4.19: Measured Points on Metal Flow in Die 4823.

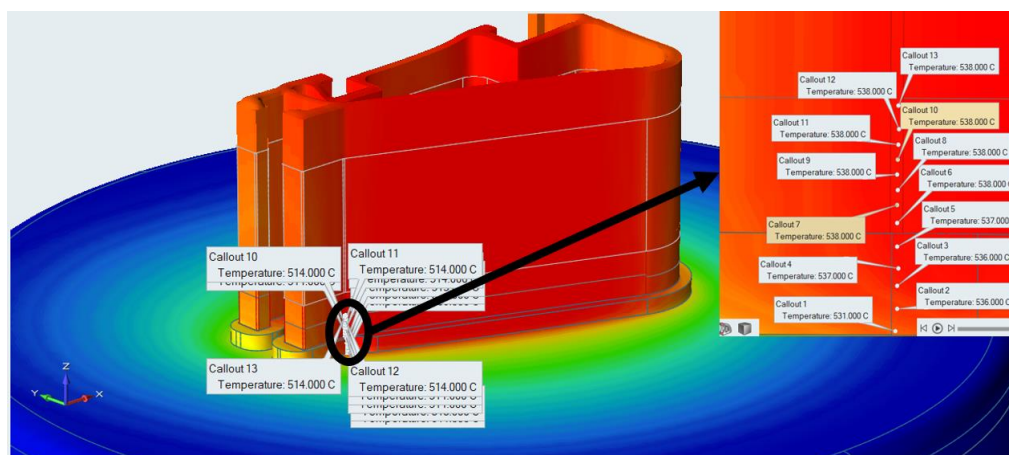


Figure 4.20: Measured Points on Metal Flow in Die 4824.

4.5 Effect of Ram Speed

Ram speed has great effect on the extrudate temperature and exit speed of extrudate. Higher ram speed can result in higher extrudate temperature and production output. However, the high temperature may lead to poor quality surface finish of extrudate and damage the die bearing surface severely. Thus, it is necessary to investigate the effect of ram speed on extrusion process and die wear behaviour by applying the modified Archard's Model. A series of ram speed of 1 mm/s, 2 mm/s, 3 mm/s, 4 mm/s and 5 mm/s are defined in the simulation. The distribution of field information is obtained based on the points measured for both dies which is discussed in previous section.

4.5.1 Temperature Distribution

From Figure 4.21 and Figure 4.22, it is noted that at second step weld chamber (from point 1 to point 5) the billet temperature increases gradually. This is due to the light of there are severe shear deformation and great friction between die and billet. Also, at die bearing surface (from point 6 to point 13), the billet temperature reaches maximum temperature, and remains relatively constant. This is because the billet experiences largest shear deformation and final shape of the profile is formed. Moreover, long heat exchange period between die and billet occurs at this area, so the maximum temperature can be obtained at die bearing surface. In addition, it is also noted that extrudate temperature at all measured points increases when ram speed increases. The billet temperature increases because at higher ram speed, greater plastic deformation occurs and more heat is generated due to friction between billet and die. Also, there is lesser time for the billet to dissipate heat to die since the it flows faster and more heat is restrained in billet during the extrusion process.

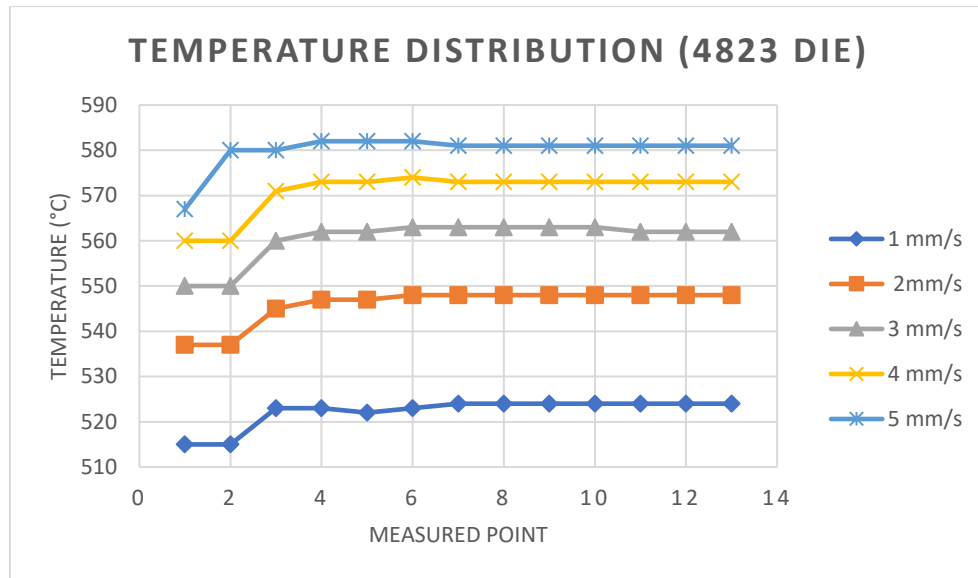


Figure 4.21: Temperature of Measured Points on 4823 Die at Different Ram Speed.

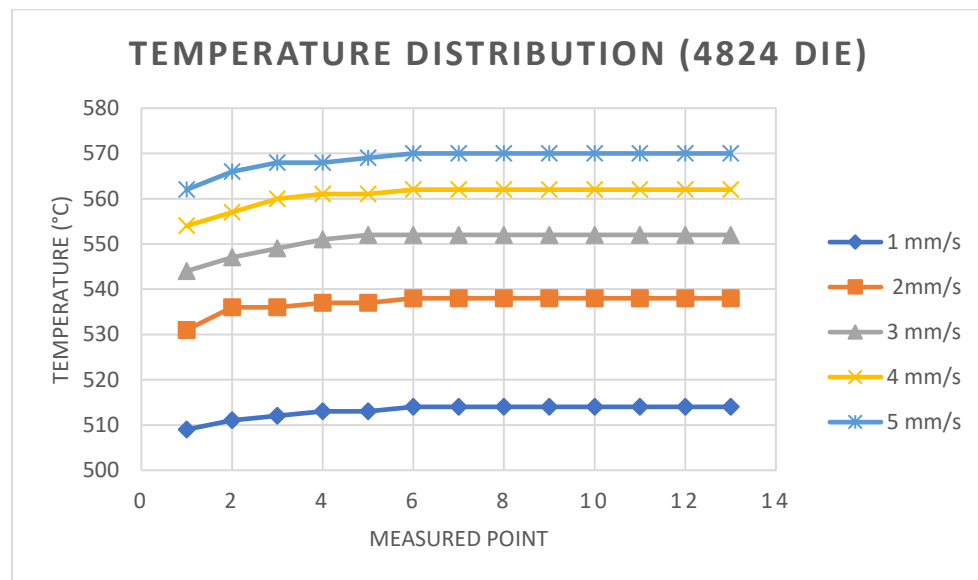


Figure 4.22: Temperature of Measured Points on 4824 Die at Different Ram Speed.

4.5.2 Average Temperature of Billet and Die

Figure 4.23 and Figure 4.24 are showing the average die temperature and billet temperature under various ram speed. From the figures, it noted that the billet temperature and die temperature increase with the ram speed. The rise of temperature is caused by the shear deformation occurs during the extrusion process and heat generated by friction as the ram speed increases. In addition, it

is also noted that the average billet temperature raises faster than average die temperature as ram speed. This is mainly due to time needed for the heat transfer from the billet to die is shorter when the ram speed. Thus, more heat energy is restrained in the billet.

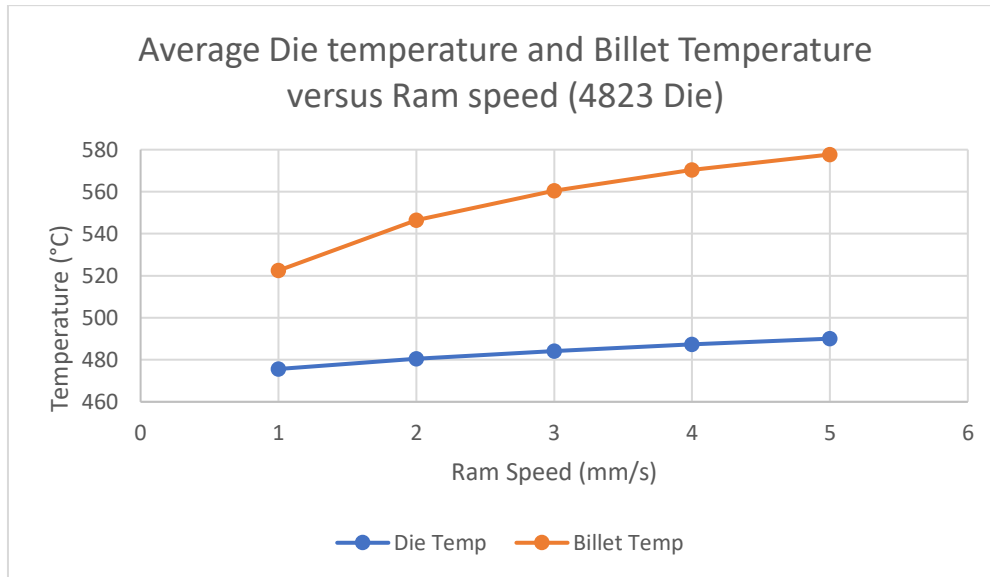


Figure 4.23: Average Temperature on Billet and Die Temperature at Different Ram Speed (4823 Die).

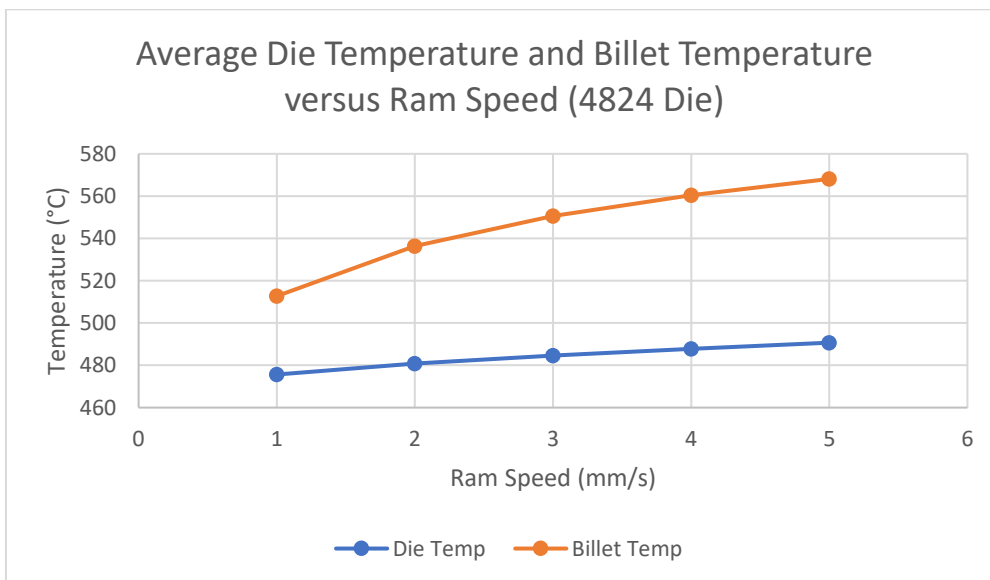


Figure 4.24: Average Temperature on Billet and Die Temperature at Different Ram Speed (4824 Die).

4.5.3 Pressure Distribution

From Figure 4.25 and Figure 4.26, it is noted that there is a spike at point 5. The pressure decreases from point 1 to point 5 because the material is flowing on the weld chamber wall and the flow stress can be lowered when it is at corner where it is away from the die orifice. At point 6, where the highest pressure is found. This is because the point is located at entrance of die orifice and there is an increase of hydro pressure at die orifice under high pressure and temperature. This can be explained that largest billet deformation occurs at point 6 when final profile is formed. After point 6, the pressure of the billet decreases gradually and remain constant at point 10 onwards as the billet moves forwards stably.

Furthermore, it is noted that the pressure in 4823 die doesn't vary much under different ram speed but there are some variations of pressure in 4824 die. In 4824 die, the pressure at point 5 is the lowest when the ram speed is 1 mm/s. This may be caused low extrusion force and results in low hydro pressure at low ram speed. Also, in 4824 die, pressure from point 7 to point 9 at 3 mm/s of ram speed are relatively low compare to the pressure for the same points obtained in other ram speed. Lower pressure can lower the die wear during the extrusion process.

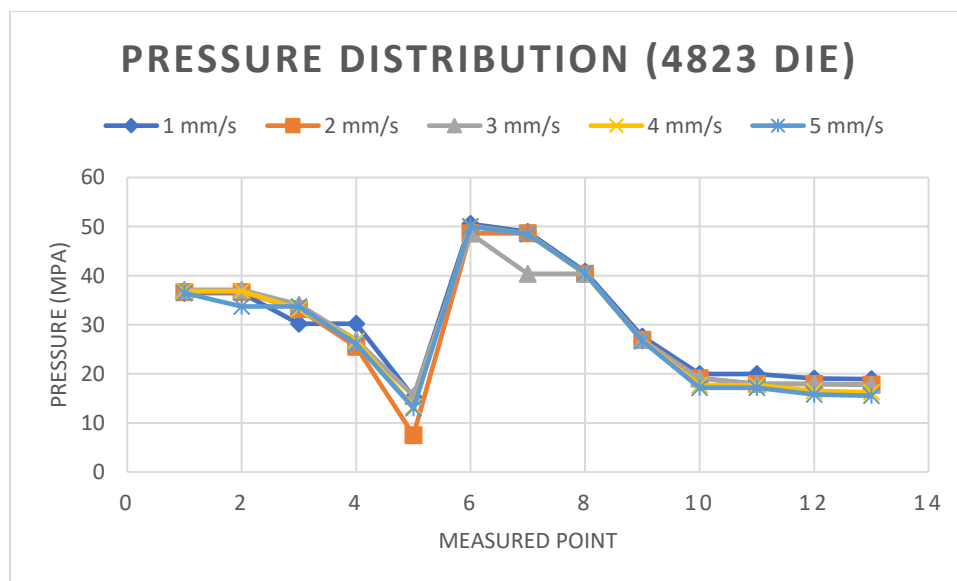


Figure 4.25: Pressure on the Measured Points at Different Ram Speed (4823 Die).

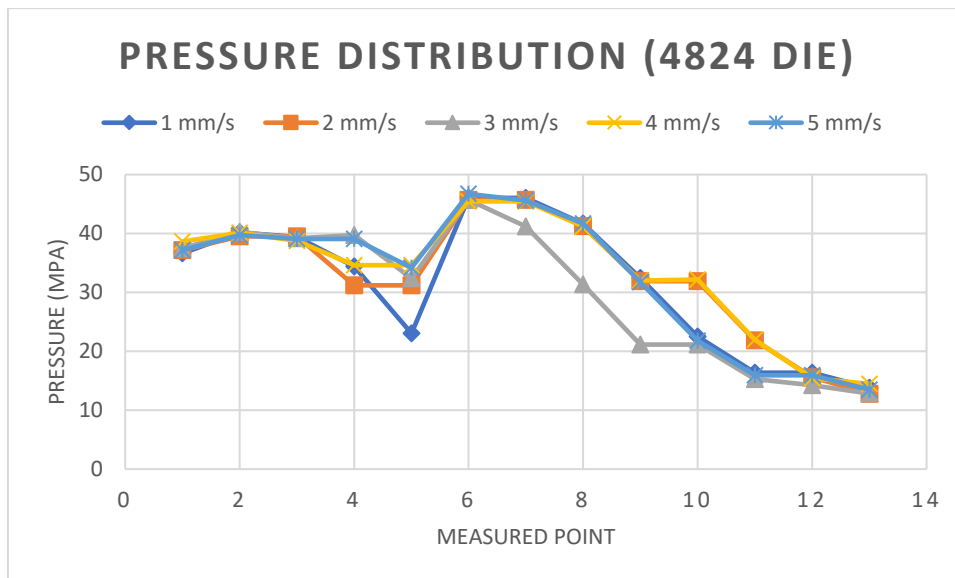


Figure 4.26: Pressure on the Measured Points at Different Ram Speed (4824 Die).

4.5.4 Extrusion Force

Figure 4.27 and Figure 4.28 show that the extrusion force increases when the ram speed increases. Higher ram speed can result in high billet flow stress in the die because greater deformation is required per unit time. According to the equation (3.6), the extrusion force is directly proportional to the extrusion constant. Average true stress is depending on the materials of the billet, temperature, flow stress, friction between extrudate and die and so on. Thus, greater extrusion force is required to extrude the billet through the die at higher ram speed because flow stress increases when ram speed is increasing. In addition, high extrusion force can lead to unbearable die wear, so extrusion force should be minimised as low as possible.

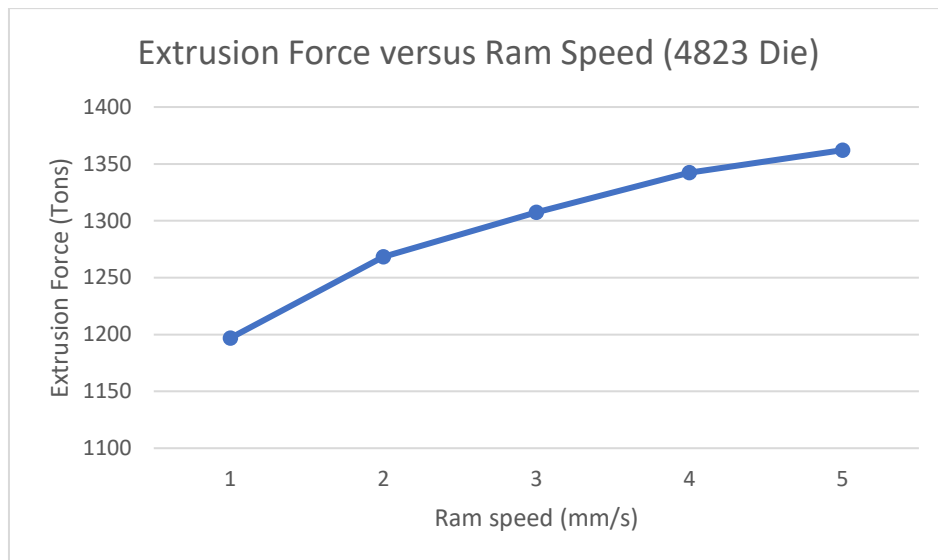


Figure 4.27: Extrusion Force at Different Ram Speed (4823 Die).

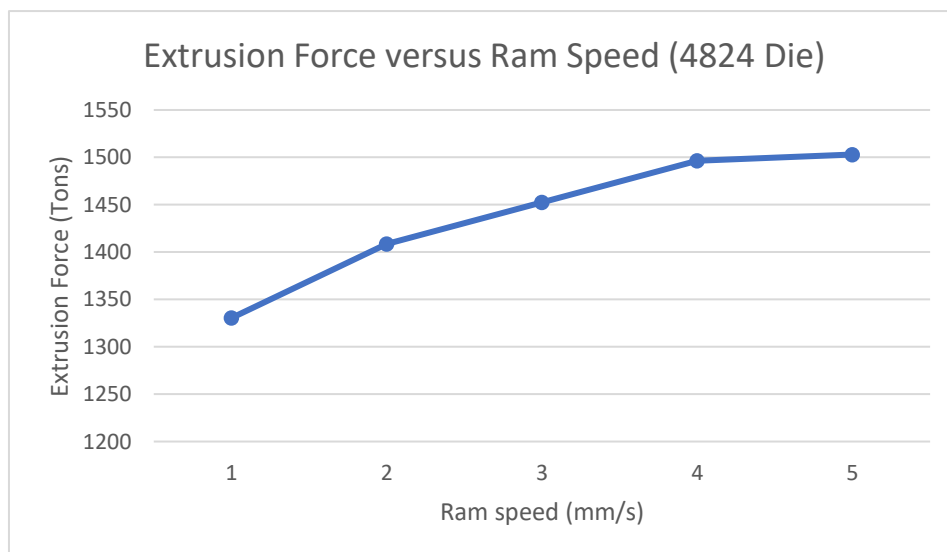


Figure 4.28: Extrusion Force at Different Ram Speed (4824 Die).

4.5.5 Wear Coefficient and Die Hardness

Average wear coefficient and average die hardness are calculated by using equation (3.3) and equation (3.4) respectively and listed in Table 4.1 for 4823 die and Table 4.2 for 4824 die. Both equations are depending on the temperature obtained earlier in temperature distribution section. The average wear coefficient increases when ram speed increases. From equation (3.3), it is noted that the wear coefficient is directly proportional to the temperature. Wear coefficient increases when the temperature increases due to heat generation from friction and deformation as the ram speed increases. On the other hand,

die hardness has the opposite reaction, the die hardness decreases when ram speed increases. This is because at higher ram speed can lead to higher temperature which can soften the die based on metallurgy science.

Table 4.1: Wear Coefficient and Die Hardness of 4823 Die at Different Ram Speed.

Ram Speed (mm/s)	Average Wear Coefficient (10^{-6})	Average Die Hardness
1	14.6	390.8
2	15.9	382.2
3	16.6	377.2
4	17.2	373.6
5	17.6	370.7

Table 4.2: Wear Coefficient and Die Hardness of 4824 Die at Different Ram Speed.

Ram Speed (mm/s)	Average Wear Coefficient (10^{-6})	Average Die Hardness
1	14.1	394.3
2	15.4	385.4
3	16.1	380.5
4	16.7	377.1
5	17.1	374.4

4.5.6 Die Wear Behaviour

Surface defect found on the aluminium extrudate may be caused by excessive wear occurs on the die bearing surface. Thus, it is important to investigate the die wear behaviour occurs along the metal flow in the die especially at bearing surface where the final profile is be formed. According to equation (3.5), die wear depth can be calculated at measured points by fetching the wear coefficient and die hardness value obtained in previous section, 4.5.5. Figure 4.29 and Figure 4.30 are showing the die wear depth calculated at respective measured points. From the calculated value of die wear depth, it is noted that the die wear

depth decreases gradually along weld chamber (point 1 to point 5) and increases sharply at bearing entrance (point 6). The die wear depth decreases gradually after bearing entrance and remains relatively constant towards exit edge of bearing surface (point 10 to point 13). Bearing entrance (point 6) has the deepest bearing wear depth in both dies because the severest deformation and highest temperature happened at bearing entrance. Li, et al. (2013) had also found that bearing entrance has the severest wear by using numerical simulation, DEFORM-3D because of the largest resistance and the largest deformation happens which can lead to greater pressure and worse die wear depth. Thus, area around point is most likely cause die failure and surface defects on the extrudate. However, it should be alerted that the results attained are not considering the surface treatment done to the die (such as nitriding) and in actual process, the die wear depth should be lower than predicted using numerical simulation.



Figure 4.29: Distribution of Die Wear Depth on Measured Points at Different Ram Speed (4823 Die).

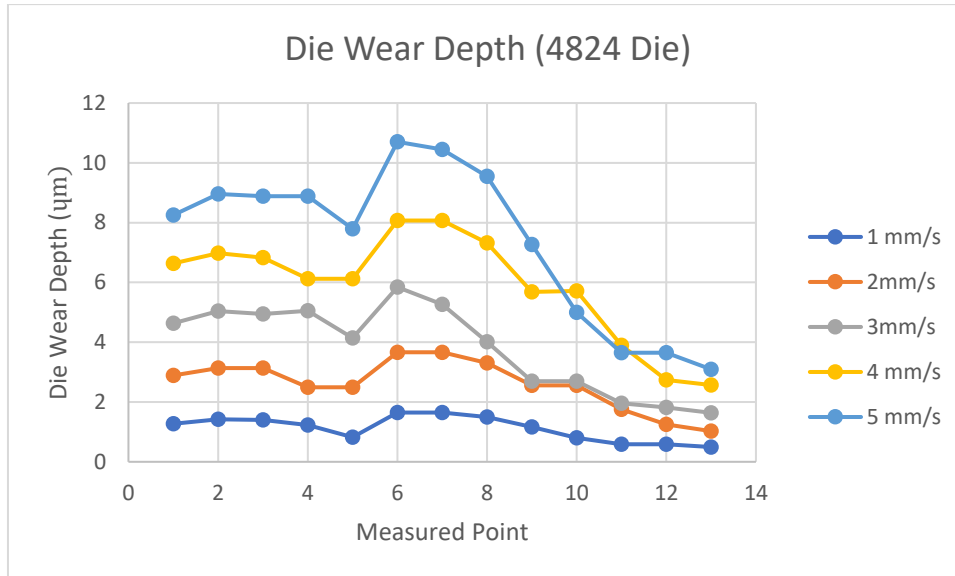


Figure 4.30: Distribution of Die Wear Depth on Measured Points at Different Ram Speed (4824 Die).

4.5.7 Maximum Extruded Profile Length

Die wear not only leads to surface defects on the aluminium extrudate. It also can lead to unacceptable dimension tolerance where the dimension is beyond scope. Therefore, die wear depth on the bearing surface should be well governed. Both dies tolerance were given at 0.15 mm. Number of maximum cycles can be carried out before the die tolerance out of range can be calculated by using equation (4.1). W_{max} is the maximum wear depth on the bearing surface per cycle at bearing entrance which is obtained from previous section, 4.5.6, T_{max} is the maximum tolerance for the die and x is the maximum number to cycle.

$$x = \frac{T_{max}}{W_{max}} \quad (4.1)$$

Also, by applying equation (4.2), the maximum extruded profile length, L (m) can be calculated by using based on the number of cycles could be done, x , billet length, L_{billet} (m) and extrusion ratio, R . The billet length is given at 650 mm for 4823 die and 670 mm for 4824 die. The extrusion ratio is given at 73.93 for 4823 die and 64.83 for 4824 die. The maximum extruded profile length for 4823 and 4824 is calculated and listed in Table 4.4 and Table 4.5 respectively.

$$L = (x)(L_{billet})[\ln(R)] \quad (4.2)$$

Both equation (4.1) and equation (4.2) are developed by myself and these equations are verified based on an article. Zhao, et al. (2013) obtained maximum number of cycles can be carried out and maximum extruded profile length through extrusion simulation by using DEFORM-3D. Unfortunately, Inspire Extrude Metal doesn't have this function to calculate. The Table 4.3 shows the percentage error between calculated values by using own-developed equations and the values from the articles obtained through numerical simulation. There are some parameters obtained from the article for this calculation purpose, such as, the maximum wear depth is $0.621 \mu m$, extrusion ratio is 12.57, die tolerance is 0.5 mm and billet length is 33.578 mm (Zhao, et al., 2013). Since the percentage error for both number of cycles and maximum extruded profile length are 0 %, both equation (4.1) and equation (4.2) are verified and can be applied to calculate the number of cycles and maximum extruded profile length in this work.

Table 4.3: Results Verification for Own-developed Equations.

	Number of cycles	Maximum Extruded Profile Length (m)
Values from Zhao, et al (2013)	805.2	68.44
Value calculated by using own-developed equations	805.2	68.44
Percentage error (%)	0	0

From Table 4.4 and Table 4.5, it is found out that the maximum extruded profile length for both profiles are decreasing when the ram speed increases. This is because die wear depth increases with ram speed which is caused by the greater pressure and temperature at higher ram speed. Li, et al. (2013) had also found that maximum extruded profile length decreases when the wear depth on

bearing surface increases. However, the results obtained should be lower than practical extrusion process as surface treatment which could enhance wear resistance on the die bearing surface (such as nitriding) for the dies was not considered in this numerical simulation.

Table 4.4: Maximum Extruded Profile Length for 4823 Die.

Ram Speed (mm/s)	Wear Depth of Bearing per Cycle, W_{max} (μm)	Number of Cycles, x	Maximum Extruded Profile Length, L (m)
1	1.9	79.3	221.8
2	4.1	36.8	103.0
3	6.5	23.1	64.6
4	9.3	16.1	45.0
5	1.2	12.5	35.0

Table 4.5: Maximum Extruded Profile Length for 4824 Die.

Ram Speed (mm/s)	Wear Depth of Bearing per Cycle, W_{max} (μm)	Number of Cycles, x	Maximum Extruded Profile Length, L (m)
1	1.6	91.0	254.5
2	3.7	40.9	114.4
3	5.8	26.7	71.8
4	8.1	18.6	52.0
5	1.1	14.0	39.2

Surface treatment such as salt bath nitrocarburizing or gas nitriding is usually done to hot extrusion die to enhance the wear resistance and hardness. The wear resistance and hardness are related to the surface treatment parameter. Higher temperature of treatment can lead to thicker nitriding layer which can improve the wear resistance and hardness as shown in Figure 2.17 (Krishnaraj, et al., 1998). However, salt bath nitrocarburizing process should be carried out at optimum temperature to have minimum die wear rate because too high treatment temperature can lead to die loss of core strength, resulting in die

deformation and inability to maintain dimensional accuracy of extruded products (Krishnaraj, et al., 1998).

4.6 Effect of Initial Billet Temperature

In hot extrusion process, metal billet is pre-heated before undergoing extrusion in order to soften the metal at elevated temperature. Softening the metal billet can help in improving its plasticity and lowering flow resistance which can lead to better flowability in the extrusion process. However, initial metal billet temperature has great impact on the die wear as there is great heat exchange between die and metal billet during extrusion which could lead to lower die hardness and die wear resistance. Therefore, it is also important to investigate effect of initial billet temperature on the extrusion process as well. A series of initial billet temperature: 440 °C, 460 °C, 480 °C, 500 °C and 520 °C were defined in simulation. The simulation is carried out with container temperature same as initial billet temperature and die temperature is 30 °C according lower than initial billet temperature. Ram speed was following default parameter value given by the local aluminium extrusion company at 3 mm/s. In this section, only extrusion force and die wear depth will be discussed as it is more informative to the die wear behaviour. Other information can be obtained in appendix A, B and C.

4.6.1 Extrusion Force

As discussed earlier, the purpose of pre-heating metal billet before extrusion process is to improve plasticity and lower flow resistance. It is expected the extrusion force required can be decreased with increasing initial billet temperature as shown in Figure 4.31 and Figure 4.32. For both dies, the extrusion drops almost 600 tons about 34.6 % when initial billet temperature increases from 440 °C to 520 °C. Decreasing trend of extrusion force required for the extrusion process seems good as the pressure on the die can be reduced as well and lead to lower friction. However, die wear is not only affected by the pressure on the die but also the temperature. Hence, next section will reveal the die wear behaviour at various initial billet temperature.

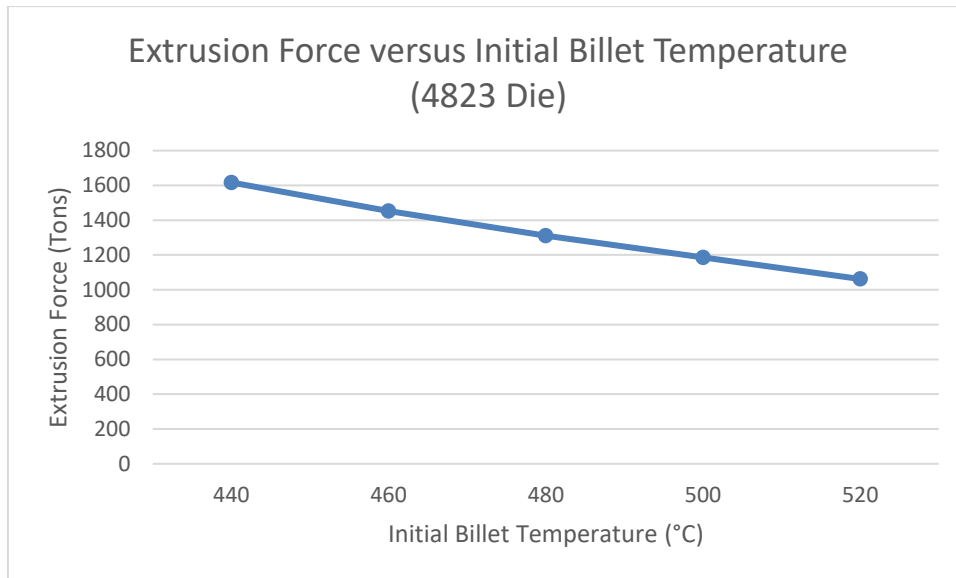


Figure 4.31: Extrusion Force at Different Initial Billet Temperature for 4823 Die.

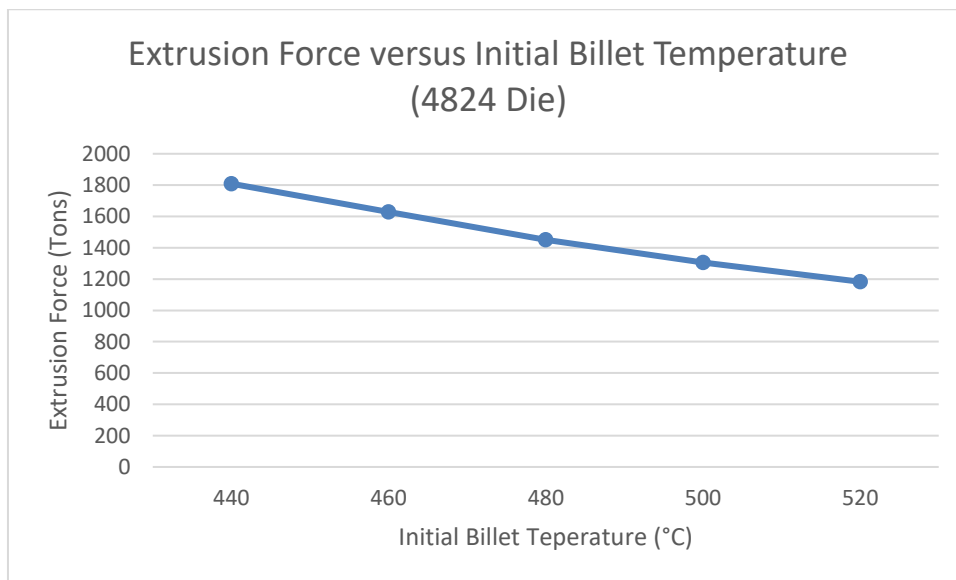


Figure 4.32: Extrusion Force at Different Initial Billet Temperature for 4824 Die.

4.6.2 Die Wear Behaviour

Figure 4.33 and Figure 4.34 are showing the die wear depth calculated at respectively measured point. From these figures, it is found that the die wear depth decreases gradually along weld chamber (point 1 to point 5) and increases sharply at bearing entrance (point 6). The die wear depth decreases gradually after bearing entrance and remains relatively constant towards exit edge of

bearing surface (point 10 to point 13). It is noted that die wear depth is not increasing much. This is mainly because the heat generated from friction and deformation have been shielded by increased billet temperature. The wear depth increases slightly due to the heat exchange between extrudate and die. Zhao, et al. (2013) pointed out that temperature has several effects on the die wear, but initial billet temperature has no direct impact on the die bearing wear depth. Therefore, it can be concluded that die wear depth is not sensitive to initial billet temperature.

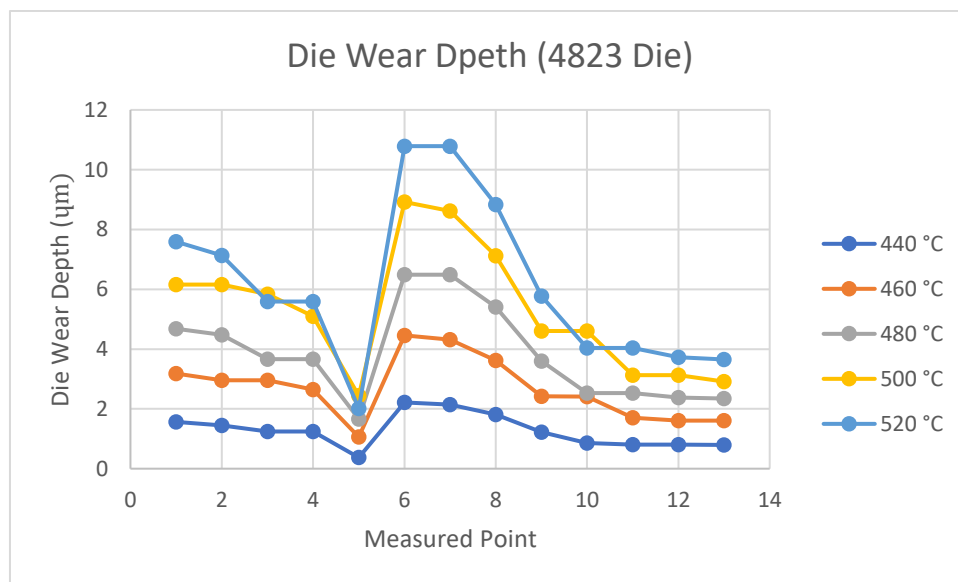


Figure 4.33: Distribution of Die Wear Depth on Measured Points at Different Initial Billet Temperature (4823 Die).

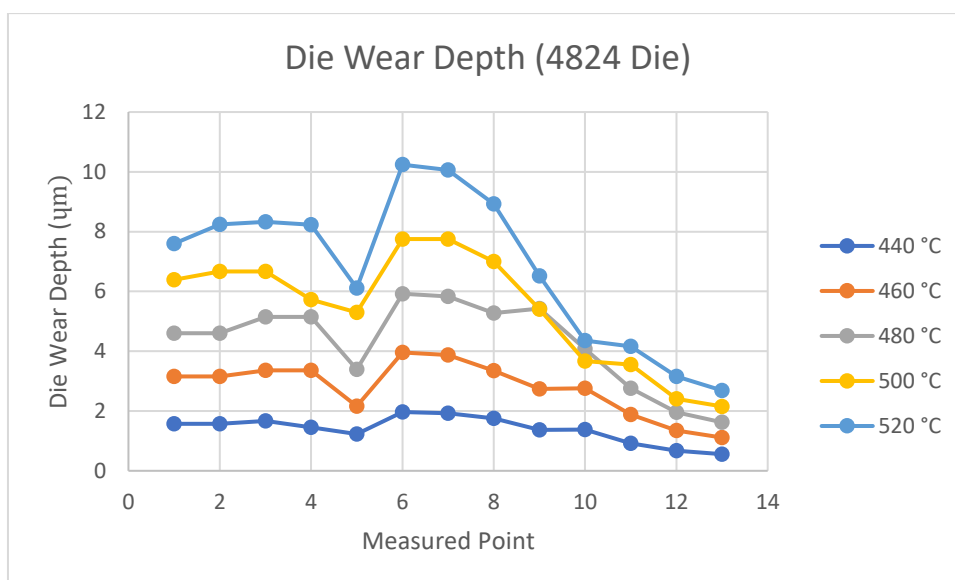


Figure 4.34: Distribution of Die Wear Depth on Measured Points at Different Initial Billet Temperature (4824 Die).

4.7 Effect of Initial Die Temperature

Initial die temperature may also affect the die wear as the wear is not only dependence on the pressure but temperature. So, a series of initial die temperature (390 °C, 420 °C, 450 °C, 480 °C and 510 °C) is defined in the simulation to study effect of initial die temperature on the extrusion process for both dies. Initial billet temperature and container temperature are defined as 480 °C which is according to the default parameter value given by the local aluminium extrusion company. Ram Speed is also following default parameter value at 3 mm/s. In this section, only extrusion force and die wear depth will be discussed as it is more informative to the die wear behaviour. Other information can be obtained in appendix D, E and F.

4.7.1 Extrusion Force

Throughout the simulation and analysis, it is found that the extrusion force required for extrusion process decreases when initial die temperature increases for both dies, as shown in Figure 4.35 and Figure 4.36. The extrusion force has decreased at about 11.98% for 4823 die and 13.51% for 4824 die when the initial die temperature increases from 390 °C to 510 °C. This is due to the light of heat transfer between die and metal billet occurs during extrusion process. Heat

could be transferred from die to metal billet, causing the metal billet to have better flowability as it can be softened at elevated temperature.

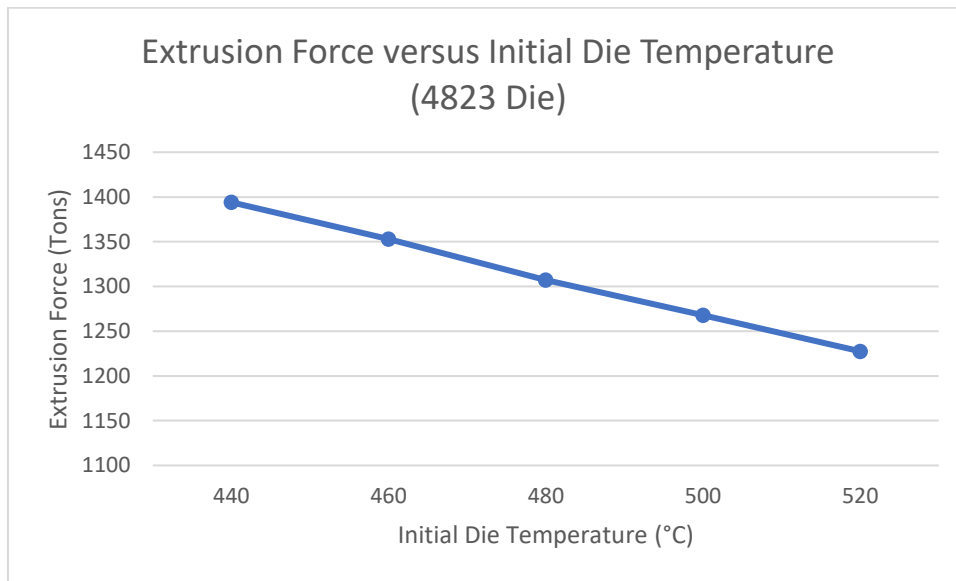


Figure 4.35: Extrusion Force at Different Initial Die Temperature for 4823 Die.

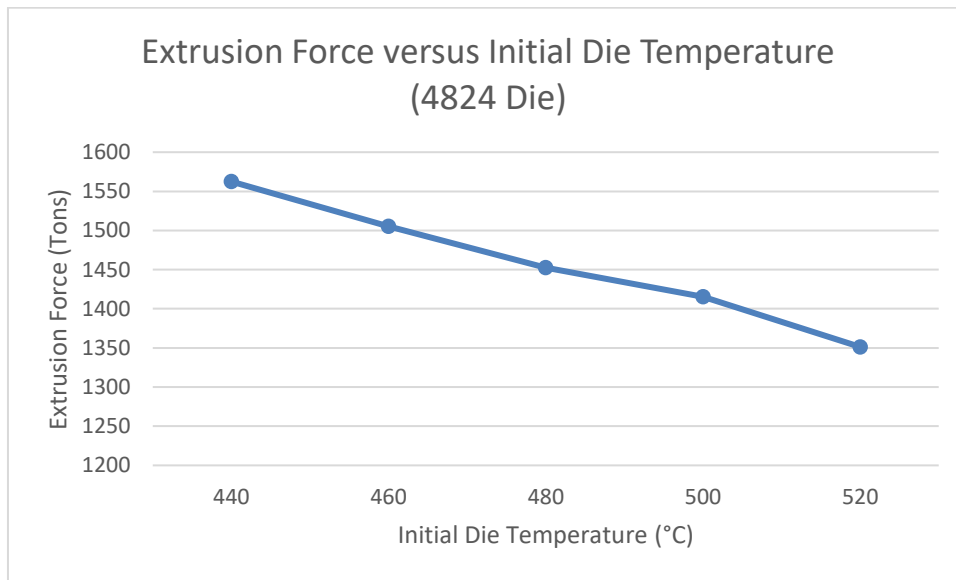


Figure 4.36: Extrusion Force at Different Initial Die Temperature for 4824 Die.

4.7.2 Die Wear Behaviour

As discussed earlier the die wear depth is affected by both pressure and temperature. Hence, it is crucial to investigate effect of die temperature on the die wear depth although extrusion force decreases when initial die temperature increases which is a good sign because pressure on die can be decreased. In

Figure 4.37 and Figure 4.38, it is clearly noted that maximum die wear depth increases when initial die temperature for both dies is increased. Maximum die wear depth is located at bearing entrance for both dies. This is because die wear depth is highly depending on the both die temperature and pressure. The die temperature has direct impact on the wear coefficient and die hardness. When the die temperature increases, the wear coefficient increases and die hardness decreases. This case is different from the effect of initial billet temperature on the die wear behaviour because billet temperature doesn't have much influence on the die temperature, whereas die temperature has the greatest influence on the die wear. Zhao, et al. (2013) had done simulation for effect of die temperature on the die wear for aluminium alloy 7075 tube extrusion and they figured out die wear can be decreased when initial die temperature is lower than initial billet temperature and increases when initial die temperature is higher than initial billet temperature. Therefore, it can be concluded that initial die temperature would be lower than initial die temperature in order to reduce die wear depth on the bearing surface.

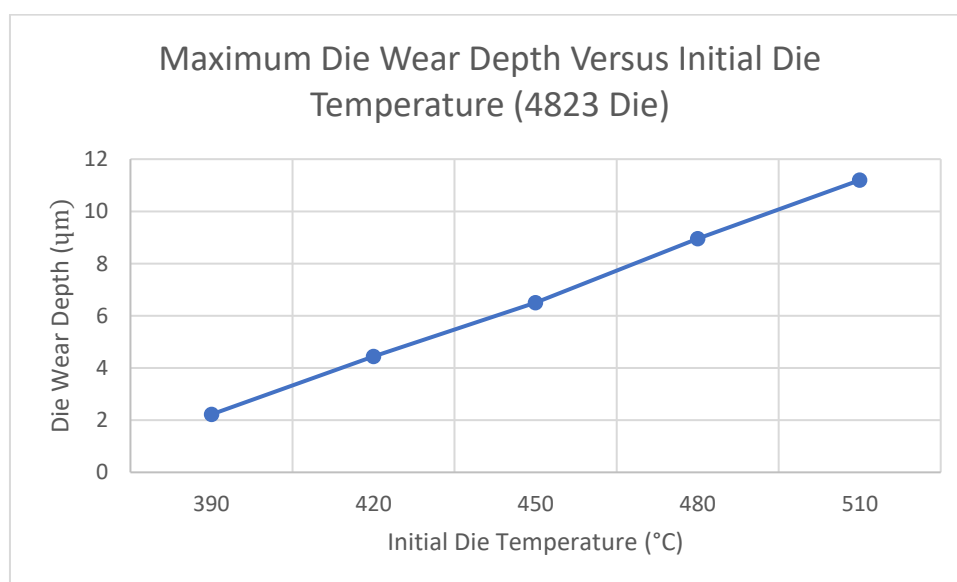


Figure 4.37: Maximum Die Wear Depth at Different Initial Die Temperature for 4823 Die.

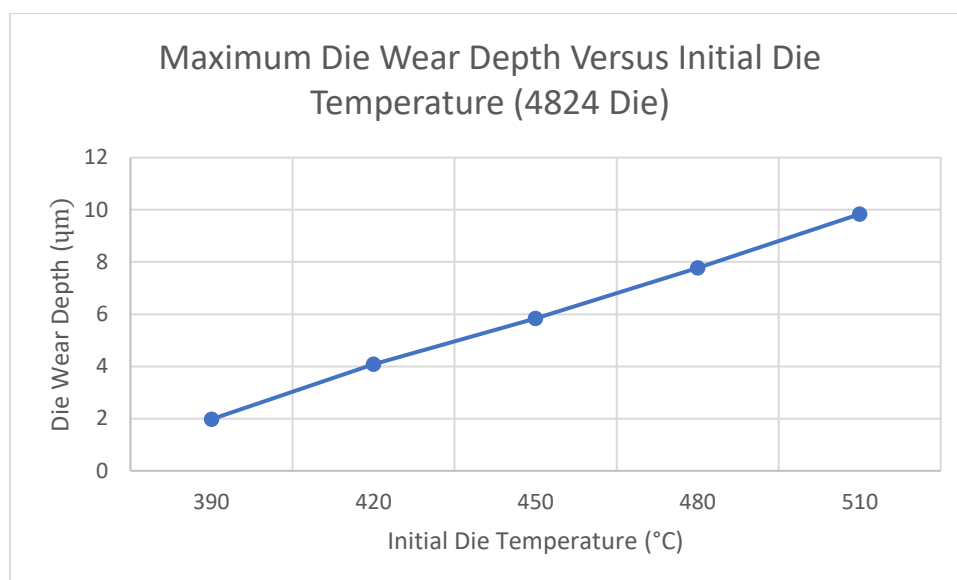


Figure 4.38: Maximum Die Wear Depth at Different Initial Die Temperature for 4824 Die.

4.8 Causes and Preventions of Pick-up Defect

There are some factors that could cause pick-up defect on aluminium extrudate such as, high exit temperature. Minoda, et al. (1999) pointed out that pick up defects can be formed when the extrudate reached eutectic reaction provided the temperature and extrudate material has silicon content more than 0.27 %. In this research, the aluminium billet used is AA6005 and it has at least 0.58 % of silicon content (refer to Table 3.2), which exceeds 0.27 %. Additionally, the eutectic point for aluminium alloy AA6005 is 555 °C where the magnesium silicon, Mg_2Si can react with aluminium to form liquid (refer to Figure 4.39). By following default extrusion parameter given by the local aluminium extrusion company which is given in Table 3.3 and the results obtained in simulation, the exit temperature of extrudate is very near to the eutectic point of the aluminium alloy at 552 °C (refer to Figure 4.22, ram speed: 3 mm/s). Therefore, pick-up defect may be formed due to exit temperature exceed eutectic point (555 °C). In order to reduce pick-up defect happens on the aluminium extrudate, the ram speed should be reduced to below 3 mm/s, so that the exit temperature can be always lower than eutectic point (555 °C). In another way, the initial billet temperature can be decreased to below 480 °C, so that the exit temperature doesn't exceed the eutectic point (555 °C). However, it should be noted that decreasing initial billet temperature can lead to increasing of

extrusion force (refer to Figure 4.32) which may cause spalling of nitriding layer when the extrusion force is too high. This can result in other surface defects on aluminium extrudate such as die line. Hence, decreasing initial billet temperature is not encouraged.

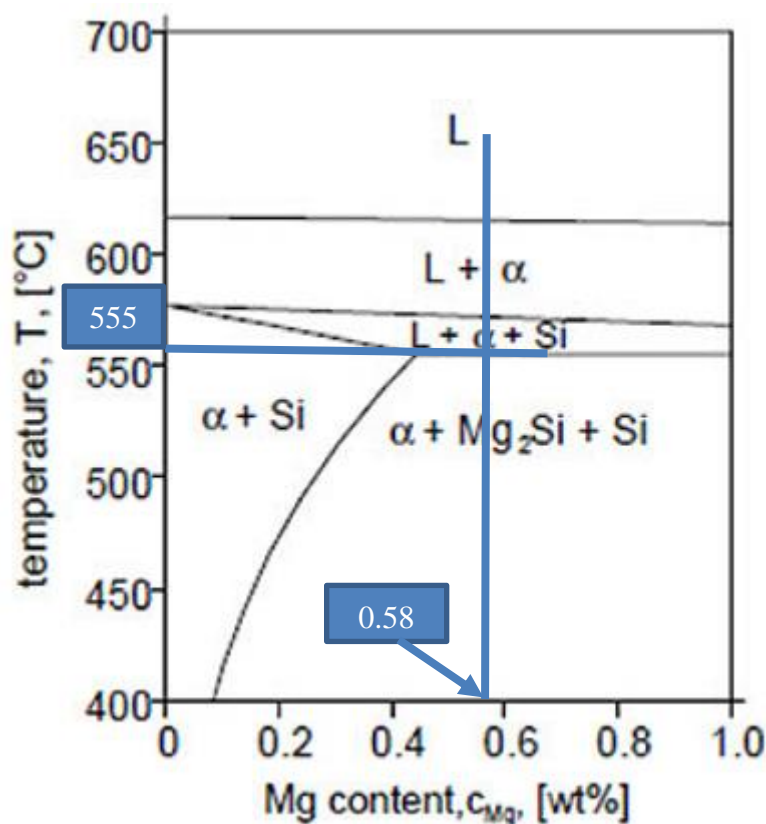


Figure 4.39: Phase Diagram for Aluminium Alloy AA6xxx with Magnesium Content (Total Materia, 2014).

Another possible cause of this pick-up defect is deterioration of die bearing condition. Deterioration of die bearing maybe due to wear over cycles of extrusion process. Occurrence of wear on die bearing surface can make the surface become uneven and scattered piece of die bearing surface or intermetallic particles and it could be the main cause of pick-up defect. To resolve this issue, re-nitriding process should be done properly to avoid premature wear by flecking and cracking. Also, proper die correction should have done as well such as polishing to ensure the die bearing surface is even and metal can flow smoothly during extrusion process (Arif, et al., 2009).

In addition, pick-up defect is caused by the accumulation and transfer of oxide on the die bearing surface due to presence of oxygen gas in the extrusion process (Montienzo, et al., 1983). Thus, in order to improve the extrusion environment. Nitrogen gas can be introduced to the extrusion process to deter the growth of oxide layer on the die bearing surface (Montienzo, et al., 1983). This method can also minimise the formation of pick-up defect on the aluminium extruded products.

Furthermore, quality of billet may be one of the factors for die pick-up formation. The aluminium billet should have sufficient homogenization where 95 % or more of $\beta - AlFeSi$ phase should be broken up to improve the workability (Fourmann, 2017). Sufficient homogenization of aluminium alloy can refine the coarse $AlFeSi$ particle and improve the metal flow during extrusion process. In addition, the iron (Fe) content of aluminium alloy is recommended to be lower than 0.18 % in order to have lesser $AlFeSi$ phase particle (Fourmann, 2017). The aluminium alloy AA6005 has maximum 0.25 % of Fe content which has exceeded 0.18 % (refer to Table 3.2). Thus, it is recommended to change to a better-quality of aluminium alloy billet which has sufficient homogenization and Fe content should be less than 0.18 %.

4.9 Causes and Prevention of Die Line Defect

Extrusion process parameter is playing vital on this die line defect especially those process parameters that can affect the extrusion force and pressure on the die bearing surface. Ram speed is one of the process parameters that has influence on the extrusion force. High extrusion force can lead to unbearable die wear and poor surface finish of extrudate (Zhao, et al., 2013). As discussed earlier, the nitriding layer can be spalled together with intermetallic material due to high pressure and force. Reducing ram speed can reduce the extrusion force (refer to Figure 4.27) and can reduce die wear depth (refer to Figure 4.29). Thus, the likelihood of spalling of nitriding layer can be reduced. It is suggested to reduce the ram speed to below 3 mm/s to reduce extrusion force as die line defect is formed on 4824 extrudate when ram speed is 3 mm/s and the extrusion force is rated at 1452.582 tons (refer to Figure 4.27). Furthermore, initial billet temperature has influence on the extrusion force as well. Increasing initial billet temperature can soften the aluminium alloy billet and reduce the extrusion force

(refer to Figure 4.31). Therefore, the spalling of nitriding layer can be minimised. However, initial billet temperature shouldn't be too high because it can affect exit temperature and exit temperature should not be higher than eutectic point (555 °C) as it can form another surface defect such as pick-up defect. It is not encouraged to increase the initial billet temperature when the ram speed is 3 mm/s as the exit temperature of extrudate may exceed eutectic point (555 °C). In short, it is very important to balance both ram speed and initial billet temperature in the extrusion process to avoid exit temperature of extrudate exceeds eutectic point (555 °C) and avoid extrusion force exceeds 1452.582 tons.

In addition, initial die temperature may also affect the deterioration of die bearing and result in spalling of nitride layer and die line. Overheating the die may result in higher chance to get surface defect on aluminium extrudate as the die bearing wears faster at higher temperature (refer to Figure 4.38). The initial die temperature should be lower than initial billet temperature (480 °C) because it can reduce die wear depth on the die bearing surface.

There are few other factors that could form die line on the aluminium alloy extrudate surface such as, occurrence of die bearing wear. Die bearing wear that could form die line is abrasive wear which has been discussed in previous section, 4.2.4. This abrasive wear can lead to pitting on the die bearing surface where nitriding layer is removed together with the intermetallic particle during the extrusion process. This issue can be resolved by polishing to improve the die bearing surface, so the die bearing surface could be even and flat (Arif, et al., 2009). Also, re-nitriding process should be done properly to avoid premature wear by flecking and cracking.

Furthermore, quality of billet may be one of the factors for die line formation. The aluminium billet should have sufficient homogenization where 95 % or more of $\beta - AlFeSi$ should be broken up to improve the workability (Fourmann, 2017). Sufficient homogenization of aluminium alloy can refine the coarse $AlFeSi$ particle and improve the metal flow during extrusion process. In addition, the iron (Fe) content of aluminium alloy is recommended to be lower than 0.18 % in order to have lesser $AlFeSi$ phase particle (Fourmann, 2017). The aluminium alloy AA6005 has maximum 0.25 % of Fe content which has exceeded 0.18 % (refer to Table 3.2). Thus, it is recommended to change to a

better-quality of aluminium alloy billet which has sufficient homogenization and Fe content less than 0.18 % to prevent $AlFeSi$ phase particles adhere to the die surface.

4.10 Summary

Pick-up defect is found on 4824 aluminium extrudate and die line defect is found on 4823 aluminium extrudate. Pick-up defect has a tear drop shape appearance and it is temperature sensitive defect. This defect is formed due to the accumulation of aluminium and transfer of oxide to the adhering aluminium layer and it occurs at interface of adhering aluminium layer on the bearing surface and extrudate. Die line is a streak of black line on the extrudate and is usually formed due to imperfection of die bearing surface such as spalling of nitriding die due to extensive force or pressure exert on the die bearing surface. Pick-up defect is sensitive to temperature. According to the process parameter given by the local aluminium extrusion company, the exit temperature of extrudate obtained from FEM can reach 553 °C which is very close to aluminium alloy AA6005 eutectic point (555 °C). Therefore, this defect can be eliminated and minimised by decreasing the ram speed to below 3 mm/s or initial billet temperature to below 480°C to reduce the exit temperature to below eutectic point. On the other hand, Die line mainly due to imperfections of die bearing surface because of spalling of nitriding layer due to high pressure or force exert on die bearing surface. In order to reduce the pressure or force applied on the die bearing surface, ram speed can be reduced to below 3 mm/s or increase initial billet temperature to minimize this defect. However, changing initial billet temperature has significant effect on the exit temperature of extrudate and extrusion force. Thus, it is very important to balance both ram speed and initial billet temperature to avoid exit temperature of extrudate exceeds eutectic point (555 °C) and avoid extrusion force exceeds 1452.852 tons in order to minimise the surface defects. In addition, re-nitriding and polishing of die and using better billet quality are suggested to eliminate or minimise both defects.

CHAPTER 5

CONCLUSIONS AND RECOMMENDATIONS

5.1 Conclusions

After going through the study in Chapter 4, surface defects on the aluminium extrudate were identified and their formation mechanism was studied as well. Also, effect of extrusion process parameters on extrusion process that would affect quality of extrudate was studied by using FEM. Besides, causes and preventions of the surface defects were discussed to minimise the surface defects. Hence, there are several conclusions can be made.

Pick-up defects and die line are found on the samples' extrudate surface. These defects have a specific appearance and characteristics. From these samples, die line defects can be found on 4823 extrudate surface and pick-up defects can be found on 4824 extrudate surface. Pick-up defect has a tear drop shape appearance and it is temperature sensitive defect. This defect is formed due to the accumulation of aluminium and transfer of oxide to the adhering aluminium layer and it occurs at interface of adhering aluminium layer on the bearing surface and extrudate. Die line defect is a streak of black line on the extrudate and is usually formed due to imperfection of die bearing surface such as spalling of nitriding die due to extensive force or pressure exert on the die bearing surface.

Pick-up defect is only found on 4824 extrudate sample and this defect is sensitive to temperature. According to the process parameter given by the local aluminium extrusion company, the exit temperature of extrudate obtained from FEM can reach 553 °C which is very close to aluminium alloy AA6005 eutectic point (555 °C). Therefore, this defect can be eliminated and minimised by decreasing the ram speed to below 3 mm/s or initial billet temperature to below 480 °C to reduce the exit temperature to below eutectic point (555 °C). However, decreasing initial billet temperature will lead to increase of extrusion force and it may affect the die wear. Therefore, it is very important to balance both process parameters to minimise the surface defects on aluminium extrudates. This defect is also due to the accumulation of aluminium and transfer of oxides, forming

aluminium oxide which will scratch the flowing aluminium extrudate. This oxidation can be minimised by introducing nitrogen gas to the extrusion process to minimise the present of oxygen gas and oxidation.

Die line is only found on 4823 extrudate sample and this defect is mainly due to imperfections of die bearing surface. Imperfections of die bearing surface may be spalling of nitriding layer due to high pressure or force exert on die bearing surface. In order to reduce the pressure or force applied on the die bearing surface, extrusion force should be reduced to below 1452.582 tons. The ram speed can be reduced to below 3 mm/s or increase initial billet temperature to minimize this defect. However, initial billet temperature shouldn't be too high because it can affect exit temperature and the exit temperature should not be higher than eutectic point (555 °C) as it can form another surface defect such as pick-up defect. Thus, it is very important to balance both process parameters to minimise the surface defects on aluminium extrudates.

Additionally, there are some improvements could be done to eliminate or minimize the defects which are not related to extrusion process parameter such as die bearing surface. Polishing and re-nitriding of die can be done to prevent flecking and cracking which can affect surface quality of the extrudate. Besides, quality of aluminium billet also may affect the extrudate surface quality. The aluminium should have sufficient homogenization where 95 % or more of $\beta - AlFeSi$ should be broken up to improve the workability and iron (Fe) content less than 0.18 % to have lesser $AlFeSi$ phase particle which can affect extrudate surface quality.

5.2 Recommendations for future work

In this research, dies were not provided for investigation on die bearing surface condition. Thus, it is recommended to further investigate on surface defect for different die bearing condition. The die bearing surface condition can determine the wear mechanisms happened to form the surface defect on extrudate surface. Also, there might be any improvement could be done to die construction to prolong the die service lifetime.

Investigation on surface defects for different homogenization conditions of aluminium alloy billet is recommended for future work. Homogenization

condition of aluminium alloy billet has influence on the types and size of the second phase particles. Therefore, it can be used to further establish the influence of billet quality on the surface defects found on the aluminium extrudate surface.

REFERENCES

Ahmad, M., Ismail, K.A. and Mat, F., 2013. Convergence of Finite Element Model for Crushing of a Conical Thin-walled Tube. *Procedia Engineering*, 53, pp.586-593.

Arai, T., 2015. The Thermo-reactive Deposition and Diffusion Process for Coating Steels to Improve Wear Resistance. *Thermochemical Surface Engineering of Steels*, pp.703-735.

Arif, A.F.M, Sheikh, A.K., Qamar, S.Z. and Raza, M.K., 2002. *Product Defect in Aluminium Extrusion and Its Impact on Operational Cost*. IN: Administrative Commission for Saudi Students Clubs, 6th Saudi Engineering Conference. Dammam, Saudi Arabia, 13 October 2002. London: Administrative Commission for Saudi Students Clubs.

Bishopp, J., 2005. Surface Pretreatment for Structural Bonding. *Handbook of Adhesives and Sealants*, 1, pp.163-214.

Bjork, T., Westegard, R. and Hogmark, S., 2001. Wear of Surface Treated Dies for Aluminium Extrusion — a case study. *Wear*, 249(3-4), pp.316-323.

Borowski, J. and Wendland, J., 2015. The Phenomenon of Durability Variable Dies for Aluminium Extrusion Profile. *Metalurgija*, 55(2), pp.229-232.

Bombac, D., Terčelj, M., Perus I. and Fajfar, P., 2013. The progress of degradation on the bearing surface of nitride dies for aluminium hot extrusion with two different relative lengths of bearing surface. *Wear*, 307(1-2), pp.10-21.

Budinski, K. G. and Budiskin, M. K eds., 2002. *Engineering Materials: Properties and Selection* 7th Edition. New Jersey: Prentice-Hall International Inc.

Butdee, S., Noomtong, C. and Tichkiewitch, S., 2008. A Process Planning System with Features Based Neural Network Search Strategy for Aluminium Extrusion Die Manufacturing. *Asian International Journal of Science and Technology in Production and Manufacturing Engineering*, 1(1), pp.27-52.

Clode, M.P and Sheppard, T., 1990. Formation of Die Lines During Extrusion of AA6063. *Material Science and Technology*, 6(8), pp.755-763.

Davis, J.R., 2011. Aluminium and Aluminium Alloys. *ASM International*, pp.351-416.

Fourmann, J., 2017. *Extrusion Defects Fundamentals & Solutions for Optimum Finish*. Ohio: Rio Tinto.

Guo, L. and Yang, H., 2014. Deformation Rules and Mechanism of Large-Scale Profiles Extrusion of Difficult-to-Deform Materials. *Comprehensive Materials Processing*, 5, pp.219-319.

Industry Reseach. 2019. Global Aluminum Extruded Products Market 2019 By Manufacturer, Regions, Type and Application, Forecast to 2024. [online] Available at: <https://www.industryresearch.biz/global-aluminum-extruded-products-market-13813711> [Accessed: 2nd March 2020]

Kalpakjian, S. and Schmid, S., 2010. *Manufacturing Engineering and Technology*. 6th edition. Chicago: Pearson.

Kang, J.H., Park, I.W., Jae, J.S. and Kang, S.S., 1999. A Study on a Die Wear Model Considering Thermal Softening: (I) Construction of The Wear Model. *Journal of Materials Processing Technology*, 96(13), pp.53-58.

Krishnaraj, N., Srinivasan, B.P., Iyer, K.J.L. and Sundaresan S., 1997. Optimization of compound layer thickness for wear resistance of nitrocarburized H11 steels. *Wear*, 215(1-2), pp.123-130.

Lee, R.S. and Jou, J.L., 2003. Application of Numerical Simulation for Wear Analysis of Warm Forging Die. *Journal of Materials Processing Technology*, 140(3), pp.43-48.

Lefstad, M. and Reiso, O., 1996. Metallurgical speed limitations during the extrusion of AlMgSi-alloys, *Procc. of the 6th Int. Aluminium Extrusion Technology Seminar*, pp.11–21.

Lefstad, M. and Reiso, O., 1996. Temperature Measurements in Extrusion Dies. *Materials Science Forum*, 217–222, pp.409–414.

Li, T., Zhao, G., Zhang, C., Guan, Y., Sun, X., and Li, H., 2013. Effect of Process Parameters on Die Wear Behaviour of Aluminium Alloy Rod Extrusion. *Material and Manufacturing Processes*, 28(3), pp.312-318.

Market Research Future., 2019. Aluminium-Extruded Products Market Research Report – Forecast to 2025. [online] Available at: <https://www.marketwatch.com/press-release/global-aluminum-extruded-products-market-share-size-2019---industry-future-demand-worldwide-research-top-leading-players-emerging-trends-region-by-forecast-to-2024-2019-11-13> [Accessed: 2nd March 2020]

Matienzo, L.J. and Holub, K.J., 1983. An Investigation on Surface Defects Produced During Extrusion of Some Aluminium Alloys. *Application of Surface Science*, 15(1), pp.307-320.

Minoda, T., Hayakawa, H. and Yoshida, H., 1999. A Mechanism of Pick-up Formation on 6063 Aluminium Alloy Extrusions. *Journal of Japan Institute of Light Metal*, 49(6), pp.253-257.

Mori, T., Takatsuji, N., Matsuki, K., Aida T., Murotani K. and Uetoko, K., 2002. Measurement of pressure distribution on die surface and deformation of extrusion die in hot extrusion of 1050 aluminium rod. *Journal of Material Processing Technology*, 130-131, pp.421-425.

Oamar, S.Z., Pervez, T. and Chekotu, J.C., 2018. Die Defects and Die Correction in Metal Extrusion. *Metals*, 8(380), pp1-18.

Ohta, Y., Sugimoto, Y. and Arai, T., 1995. Low Temperature Salt Bath of Chromium Carbonitride Coating Method. *Journal of The Surface Finishing Society of Japan*, 46(12), pp.1119-1124.

Ouwerkerk, G.V., 2009. CAD Implementation of Design Rules for Aluminium Extrusion Dies. PhD. University of Twente.

Pearson, C.E. and Parkins, R.N. eds., 1960. *The Extrusion of Metals*. 2nd Edition. New York: John Wiley & Sons.

Pérez, M. and Belzunce, F.J., 2016. A comparative study of salt-bath nitrocarburizing and gas nitriding followed by post-oxidation used as surface treatments of H13 hot forging dies. *Surface & Coatings Technology*, 3015(15), pp.146-157.

Peris, R.G., 2007. *Effects of Extrusion Conditions on "Die Pick-up" Formed During Extrusion of Aluminium Alloy AA6060*. Master. Auckland University of Technology.

Qamar, S.Z., 2010. Shape Complexity, Metal Flow, and Dead Metal Zone in Cold Extrusion. *Materials and Manufacturing Processes*, 20(5), pp.1454—146.

Saha, P., 2000. *Aluminium Extrusion Technology*. Ohio: ASM International.

Schey, J.A. 1999. *Introduction to Manufacturing Processes*. 3rd Edition. New York: McGraw-Hill.

Shahriar, A., Torgei, W., and Sigurd, S., 1996. *Interface Mechanisms on the Bearing Surface in Extrusion*. IN: Aluminium Association, 6th International Extrusion Technology Seminar. Chicago, United State, 14-17 May 1996. Washington: Aluminium Association.

Tempelman, E., Shercliff, H., and Eyben, B.H., 2014. Extrusion of Metals. *Manufacturing and Design*, pp.69-83.

Terčelj, M., Kugler, G., Turk, R., Cvahte P., and Fajfar P., 2005. Measurement of Temperature on Bearing Surface of Industrial Die and Assessment of Heat Transfer Coefficient in Hot Extrusion of Aluminium. *International Journal of Vehicle Design*, 39(1-2), pp.93-109.

Terčelj, M. and Kugler, G., 2017. An approach to increasing the service lifetime of nitrided dies for aluminium hot extrusion: A case study. *Wear*, 376-377(B), pp.1779-1788.

Terčelj, M., Smolej, A., Fajfar, P. and Turk, R., 2007. Laboratory assessment of wear on nitrided surfaces of dies for hot extrusion of aluminium. *Tribology International*, 40, pp.374-384.

Tong, K.K., Yong, M.S., Fu, M.W., Muramatsu, T., Goh, C.S., and Zhang, X.S., 2005. CAE enabled methodology for die fatigue life analysis and improvement *International Journal of Production Research*, 43(1), pp.131-146.

Total Materia., 2014. AlMgSi Alloys. [Online] Available at: <https://www.totalmateria.com/page.aspx?ID=CheckArticle&site=ktn&NM=348> [Accessed: 10 September 2020]

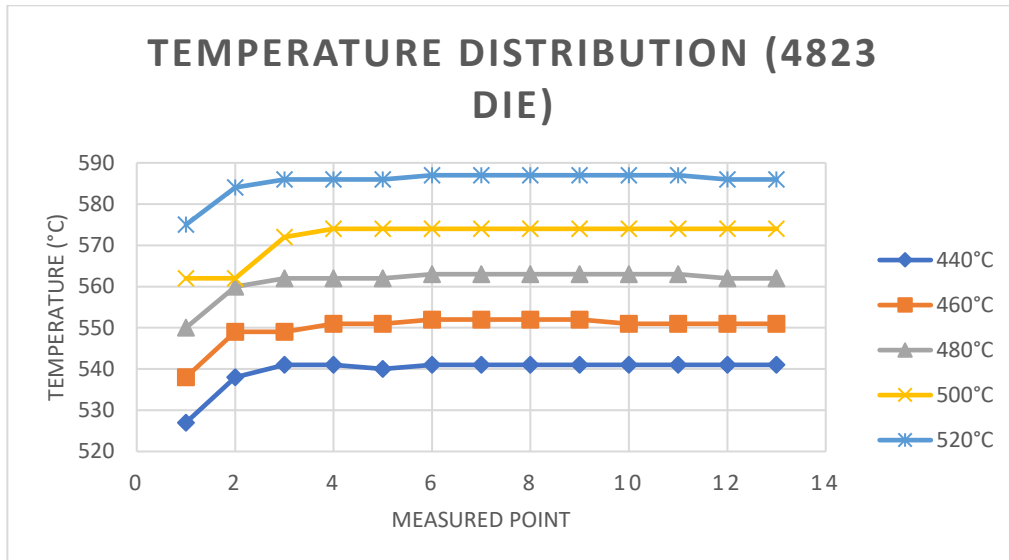
Trumony Aluminium Limited., 2020. Micro Multiport Tube Aluminium Extruded Profiles for Air Conditioning Heat Exchangers. [Online] Available at: <http://www.aluminiumfoilroll.com/sale-11814214-micro-multiport-tube-aluminium-extruded-profiles-for-air-conditioning-heat-exchangers.html> [Accessed: 2nd March 2020]

Zhang, C., Zhao, G., Chen, Z., Chen, H. and Kou, F., 2011. Effect of Extrusion Stem Speed on Extrusion Process for a Hollow Aluminium Profile. *Material Science and Engineering: B*, 177(19), pp.1691-1697.

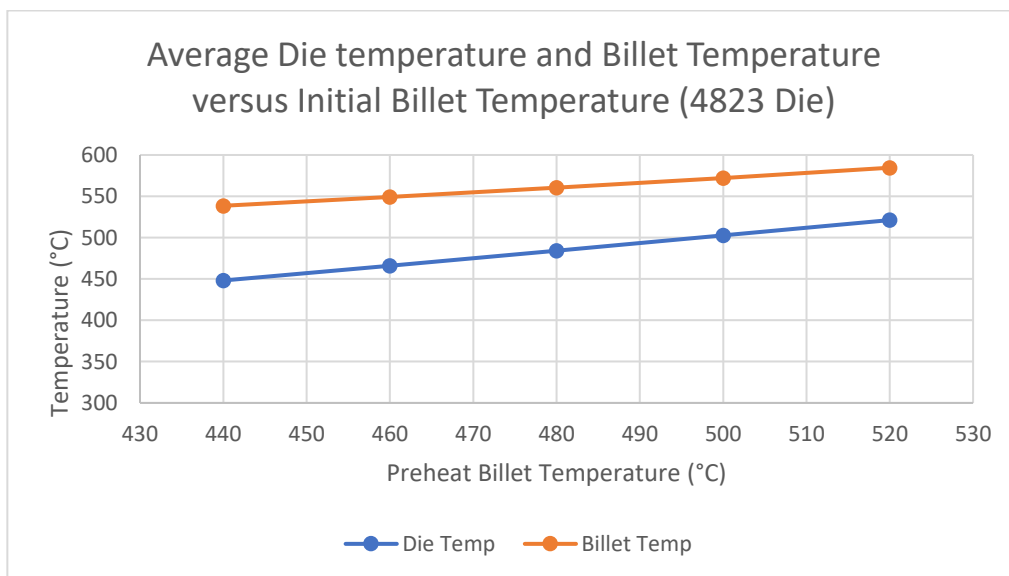
Zhao, G., Li, T., Guan, Y. and Chen H., 2013. An Investigation of Die Wear Behaviour During Aluminium Alloy 7075 Tube Extrusion. *Journal of Tribology*, 135(1), pp.1-9.

APPENDICES

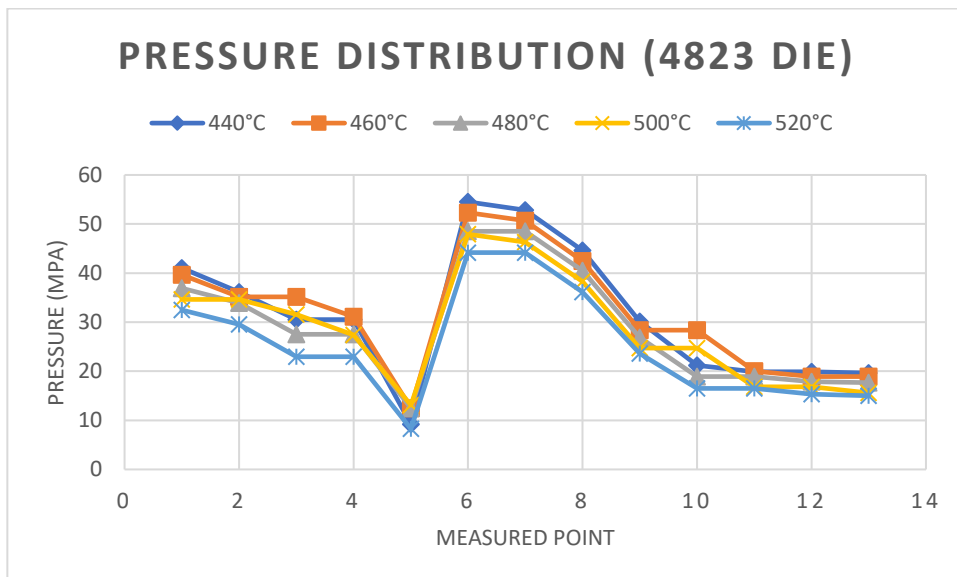
APPENDIX A: Graphs for Effect of Initial Billet Temperature (4823 Die).



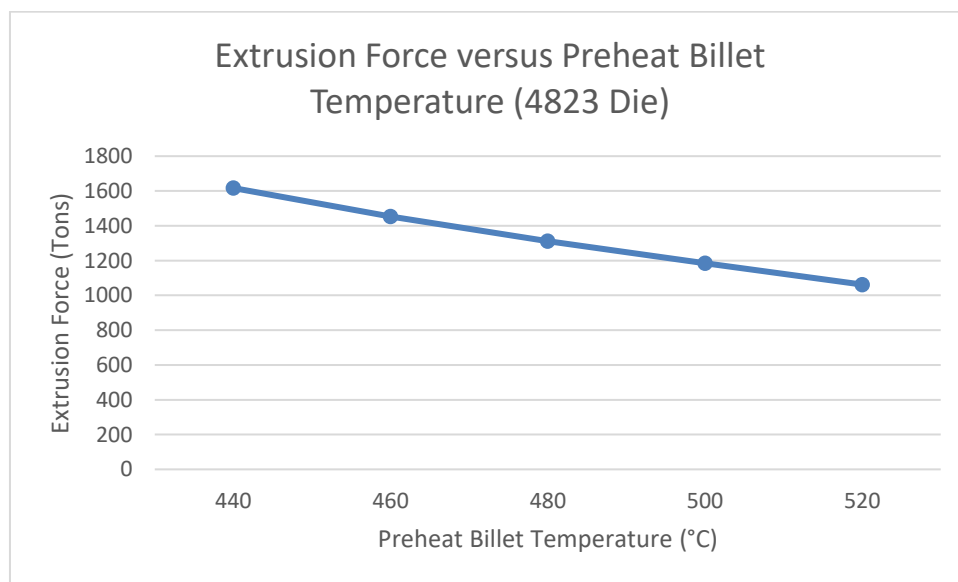
Graph A-1: Effect of Initial Billet temperature on Temperature Distribution at measured points (4823 Die).



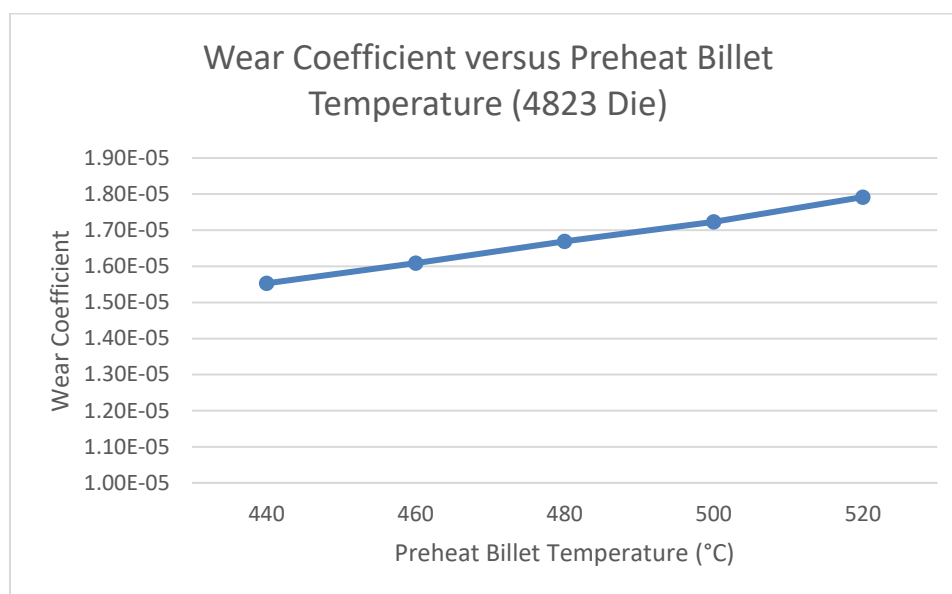
Graph A-2: Effect of Initial Billet Temperature on Average Die Temperature and billet Temperature (4823 Die).



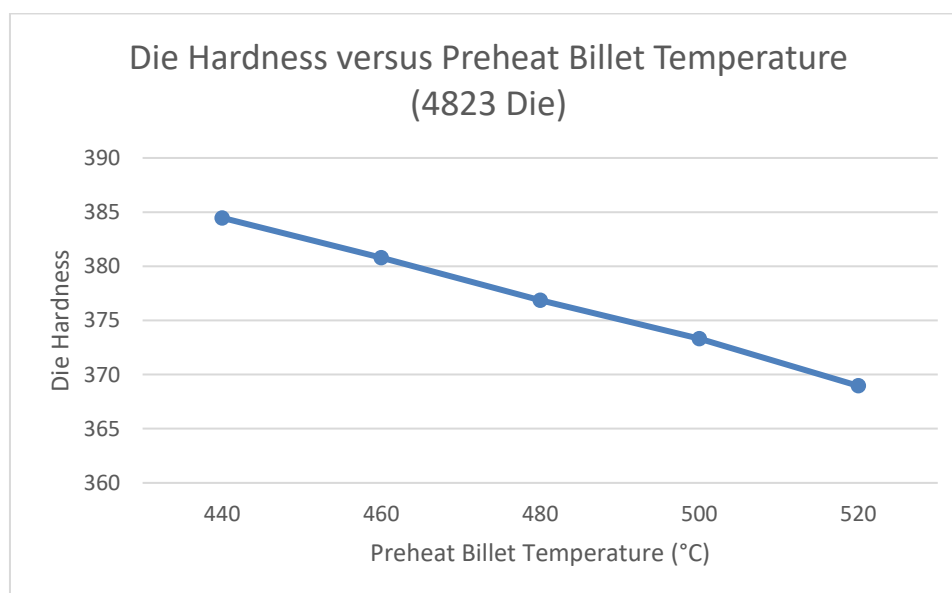
Graph A-3: Effect of Initial Billet Temperature on Pressure Distribution at Measured Points (4823 Die).



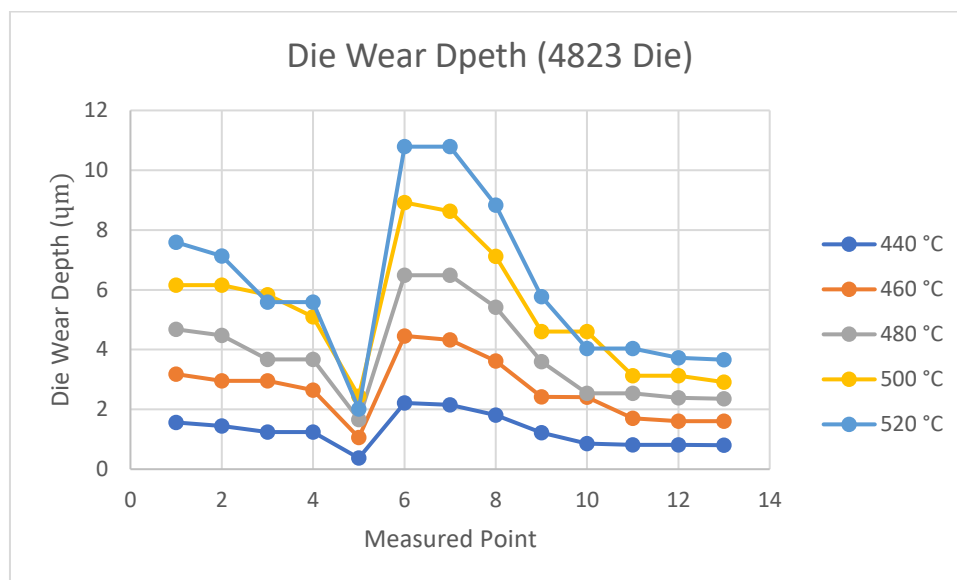
Graph A-4: Effect of Initial Billet Temperature on Extrusion Force (4823 Die).



Graph A-4: Effect of Initial Billet Temperature on Wear Coefficient (4823 Die).

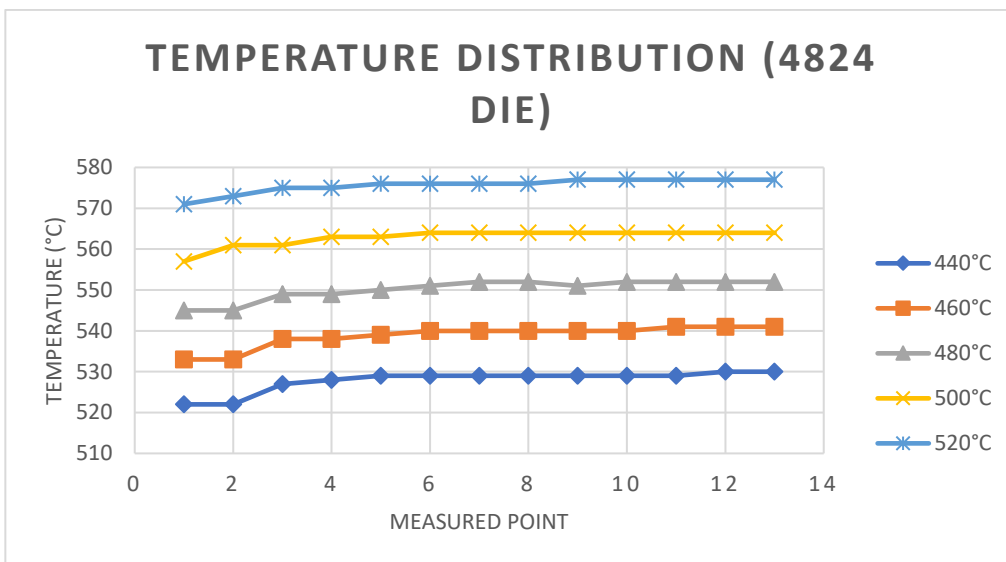


Graph A-5: Effect of Initial Billet Temperature on Die Hardness (4823 Die).

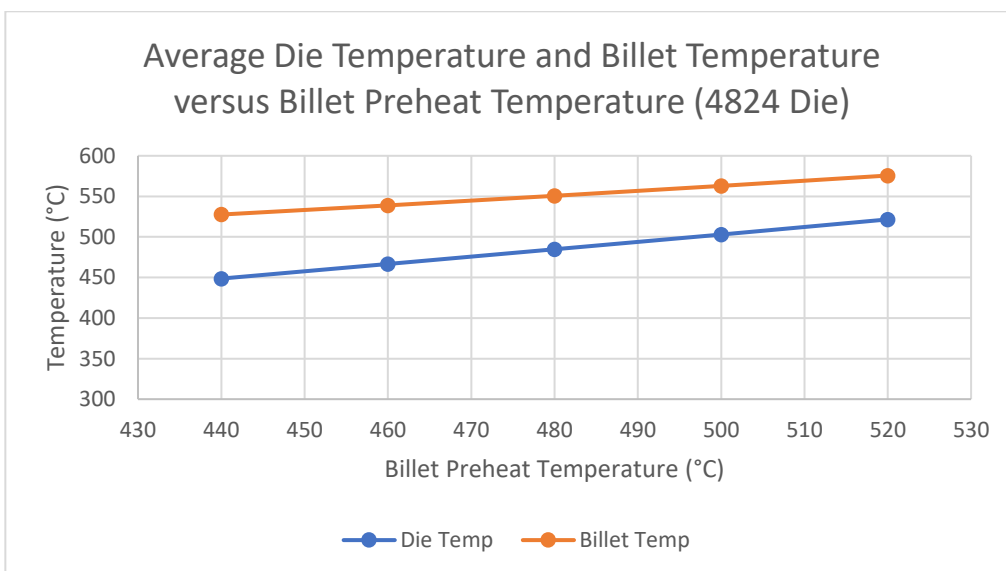


Graph A-6: Effect of Initial Billet Temperature on Die Wear Depth at Measured Points (4823 Die).

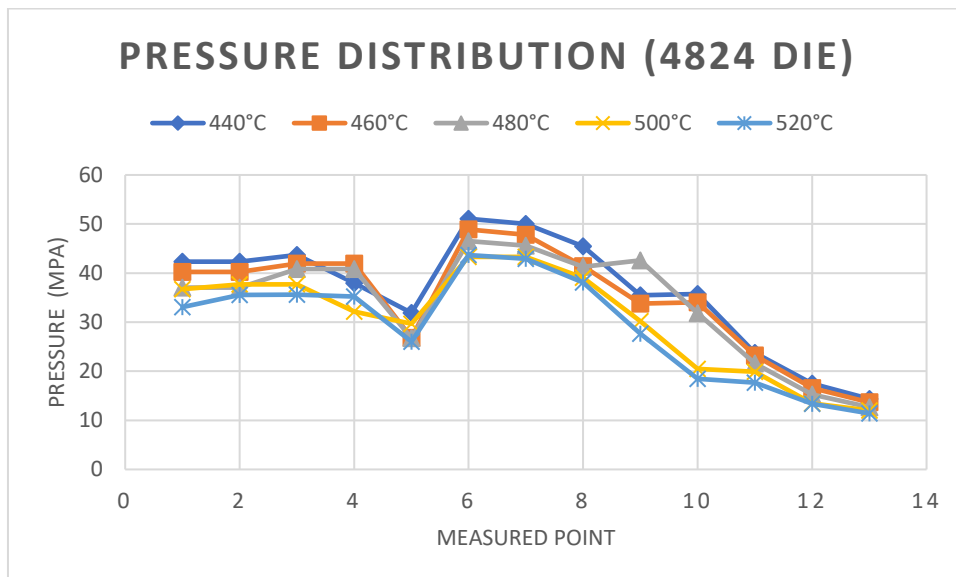
APPENDIX B: Graphs for Effect of Initial Billet Temperature (4824 Die).



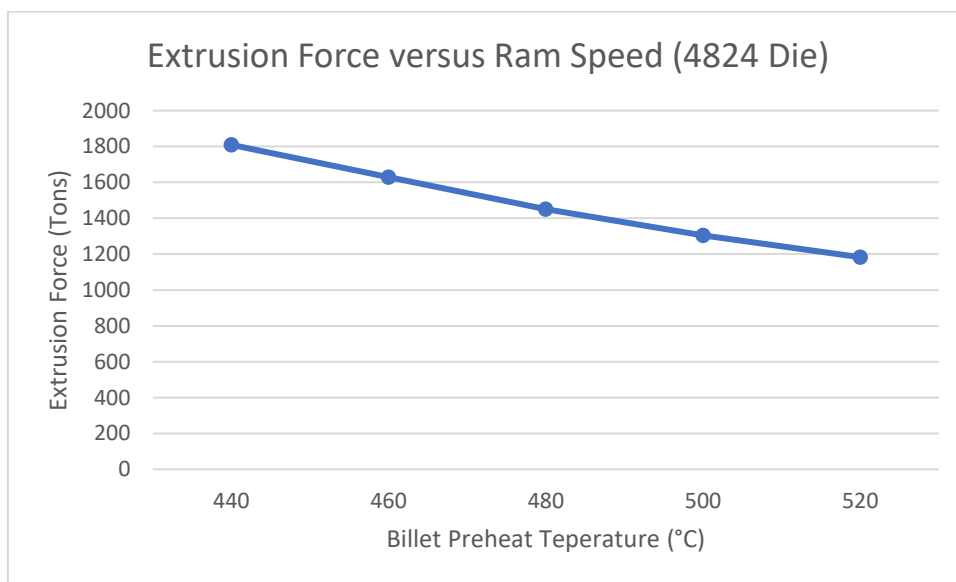
Graph B-1: Effect of Initial Billet temperature on Temperature Distribution at measured points (4824 Die).



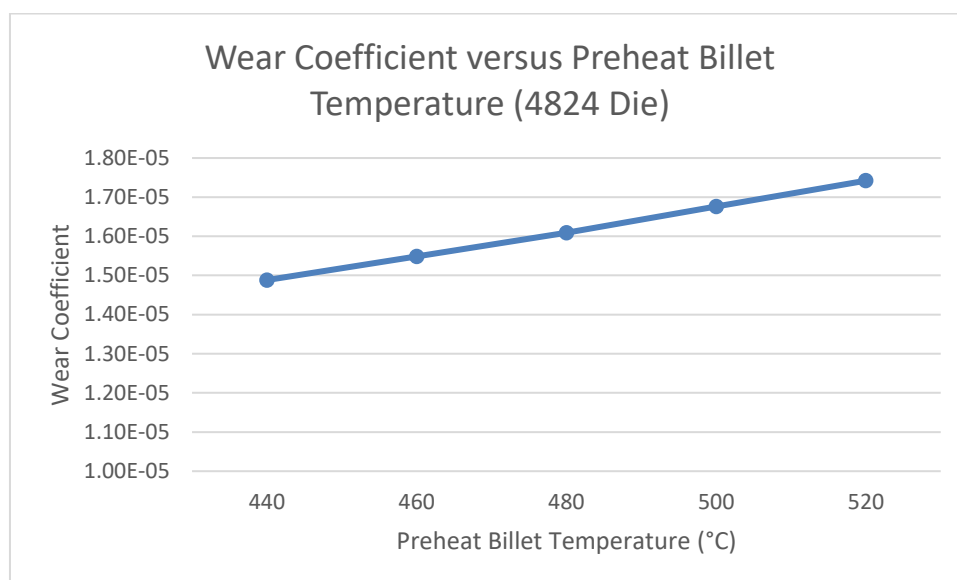
Graph B-2: Effect of Initial Billet Temperature on Average Die Temperature and billet Temperature (4824 Die).



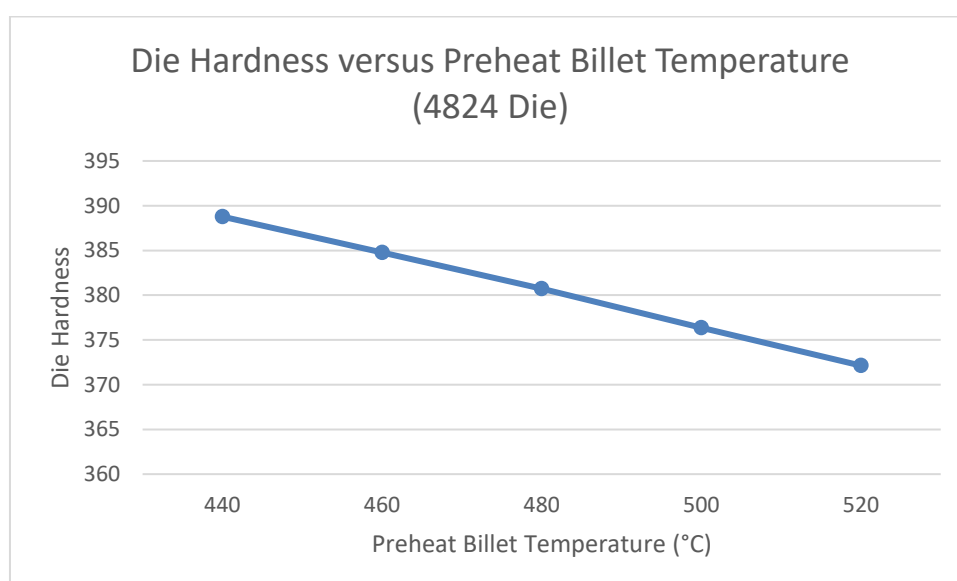
Graph B-3: Effect of Initial Billet Temperature on Pressure Distribution on Measured Points (4824 Die).



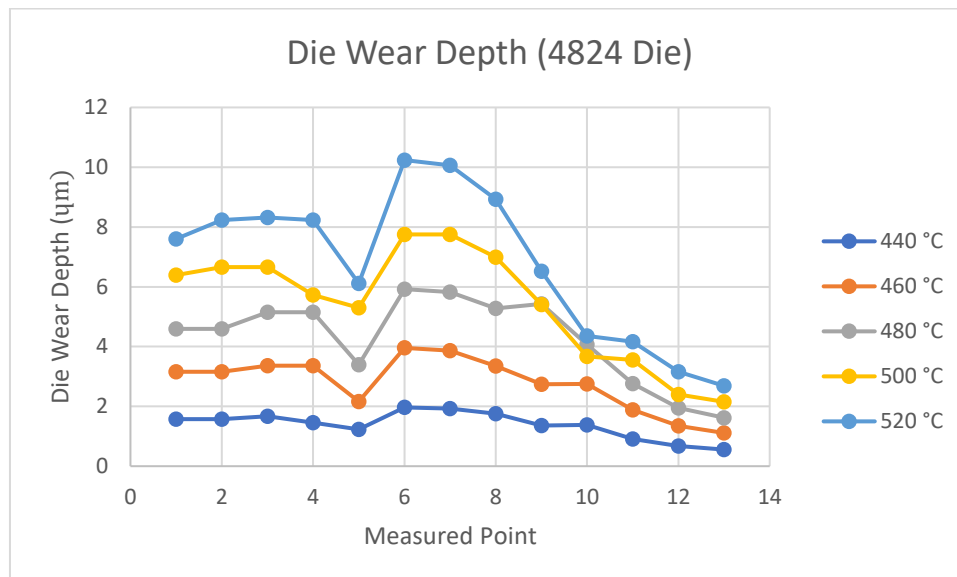
Graph B-4: Effect of Initial Billet Temperature on Extrusion Force (4824 Die).



Graph B-5: Effect of Initial Billet Temperature on Wear Coefficient (4824 Die).



Graph B-5: Effect of Initial Billet Temperature on Die Hardness (4824 Die).



Graph B-6: Effect of Initial Billet Temperature on Die Wear Depth at Measured Points (4824 Die).

APPENDIX C: Tables of Maximum Extruded Length Under Various Initial Billet Temperature (4823 Die and 4824 Die).

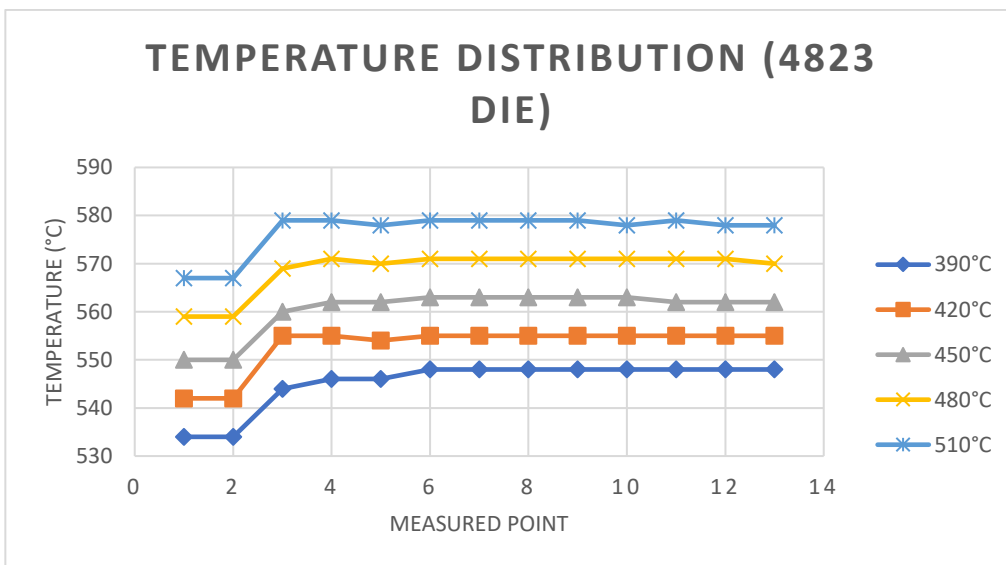
Table C-1: Effect of Initial Billet Temperature on Maximum Extruded Profile Length for 4823 Die.

Initial Billet Temperature (°C)	Wear Depth of Bearing per Cycle, W_{max} (m)	Number of Cycles, x	Maximum Extruded Profile Length, L (m)
440	2.216×10^{-6}	67.700	189.359
460	4.458×10^{-6}	33.645	94.107
480	6.487×10^{-6}	23.122	64.673
500	8.920×10^{-6}	16.816	47.035
520	1.079×10^{-6}	13.905	38.891

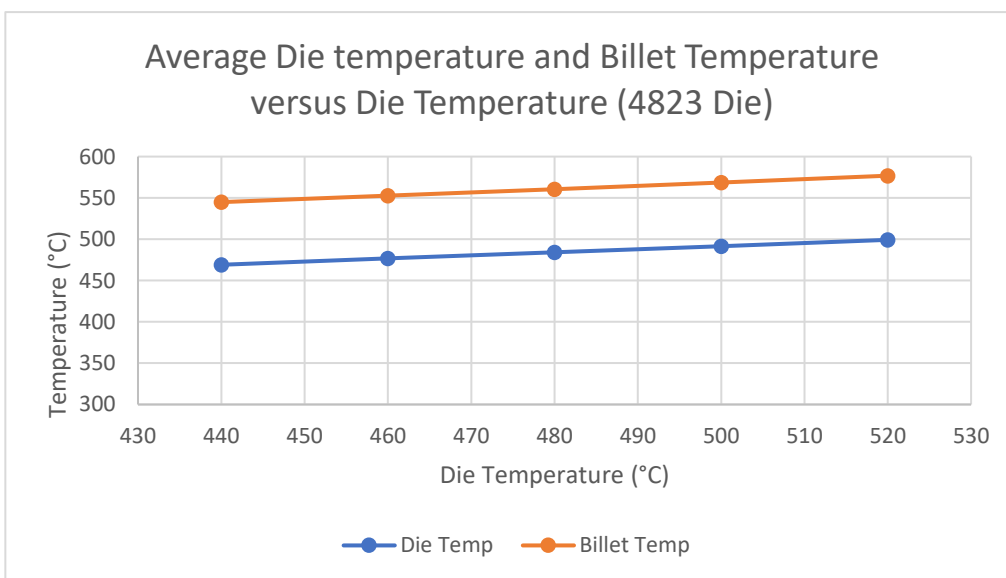
Table C-2: Effect of Initial Billet Temperature on Maximum Extruded Profile Length for 4824 Die.

Initial Billet Temperature (°C)	Wear Depth of Bearing per Cycle, W_{max} (m)	Number of Cycles, x	Maximum Extruded Profile Length, L (m)
440	1.966×10^{-6}	76.295	213.251
460	3.957×10^{-6}	37.907	105.954
480	5.922×10^{-6}	25.328	70.793
500	7.752×10^{-6}	13.350	54.086
520	1.024×10^{-6}	14.650	40.947

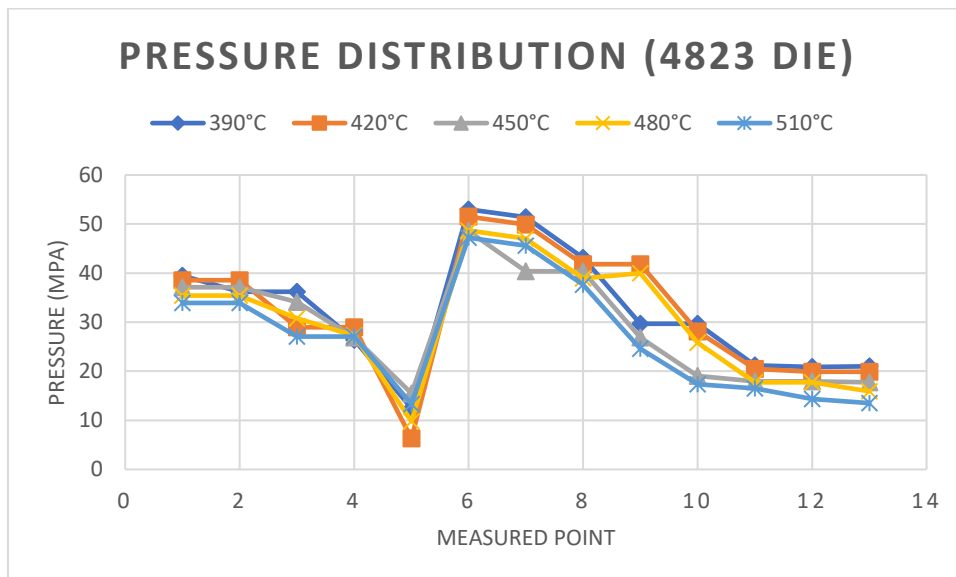
APPENDIX D: Graphs for Effect of Initial Die Temperature (4823 Die).



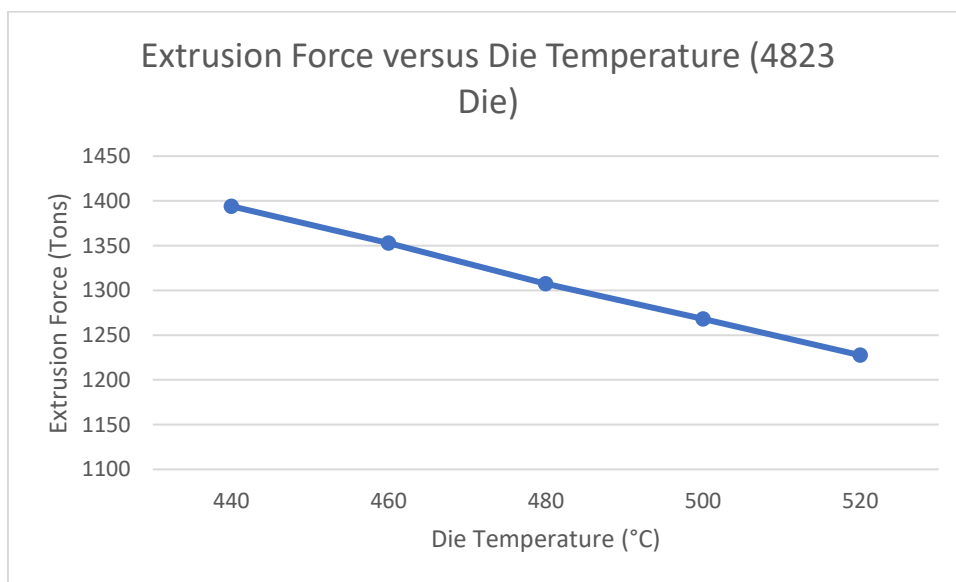
Graph D-1: Effect of Initial Die temperature on Temperature Distribution at Measured Points (4823 Die).



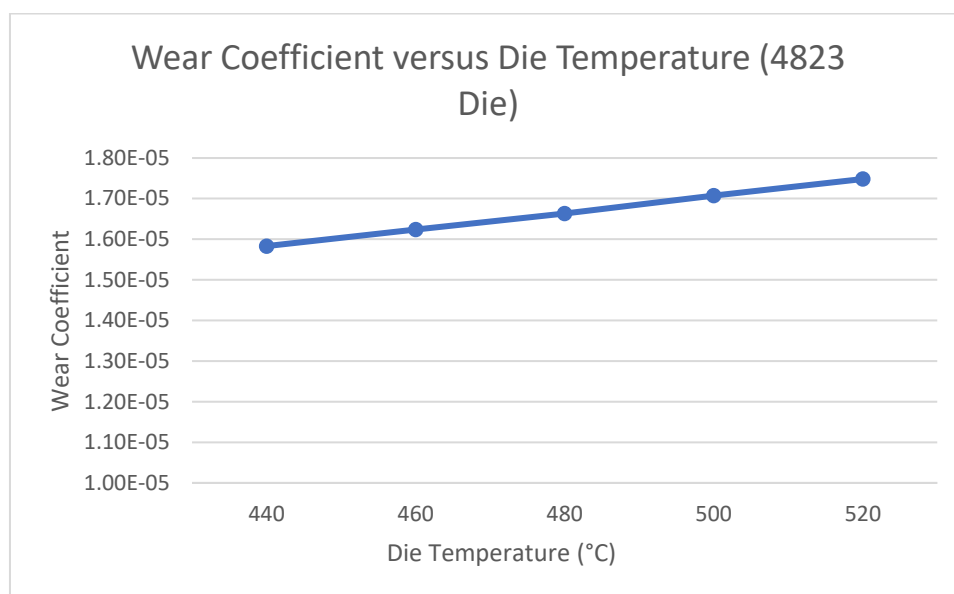
Graph D-2: Effect of Initial Die Temperature on Average Die Temperature and billet Temperature (4823 Die).



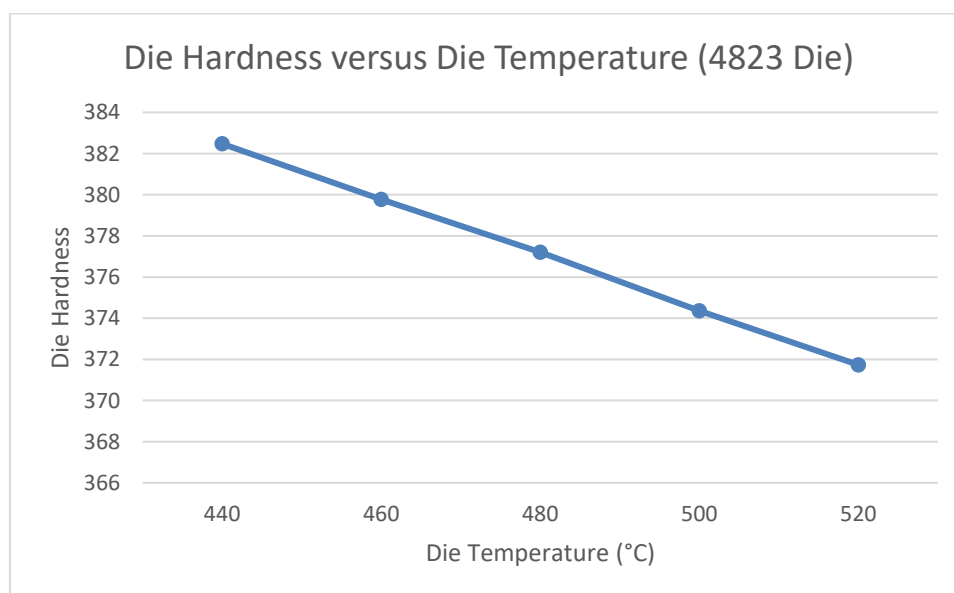
Graph D-3: Effect of Initial Die Temperature on Pressure Distribution at Measured Points (4823 Die).



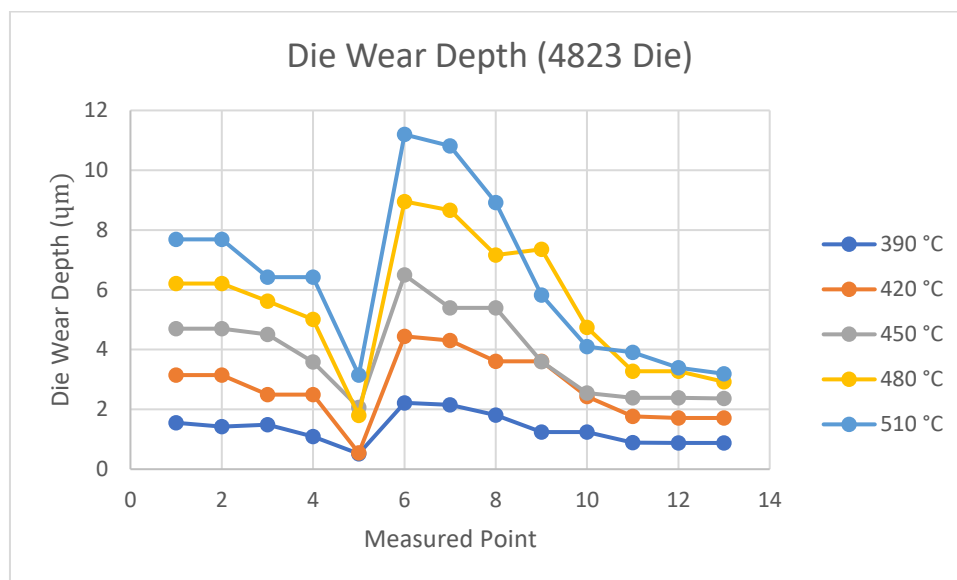
Graph D-4: Effect of Initial Die Temperature on Extrusion Force (4823 Die).



Graph D-5: Effect of Initial Die Temperature on Wear Coefficient (4823 Die).

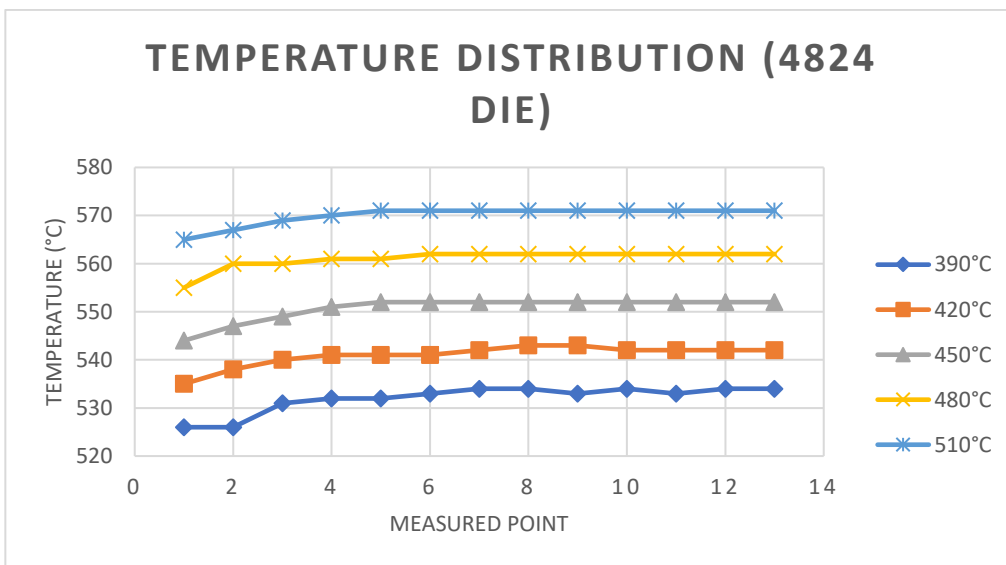


Graph D-6: Effect of Initial Die Temperature on Die Hardness (4823 Die).

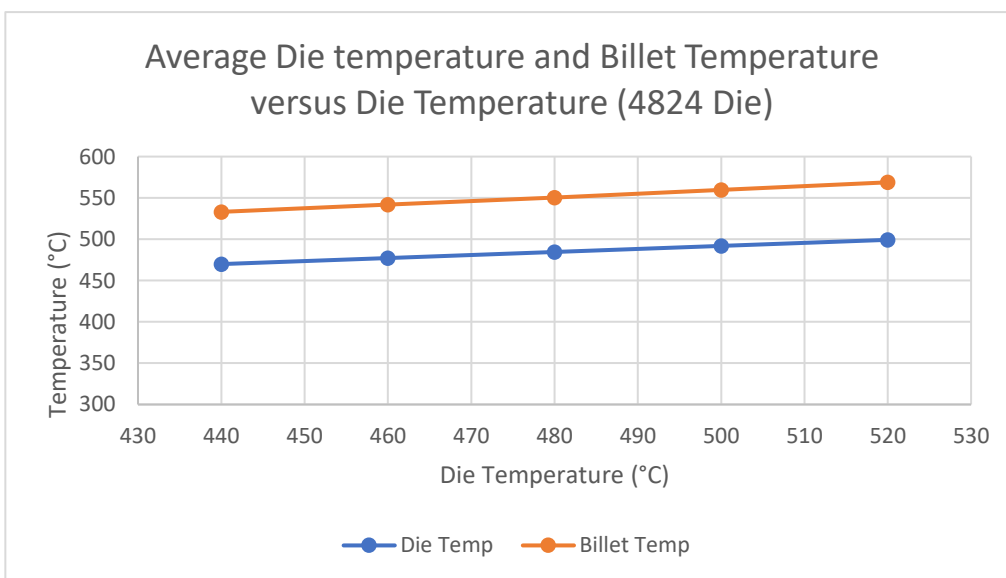


Graph D-7: Effect of Initial Die Temperature on Die Wear Depth at Measured Points (4823 Die).

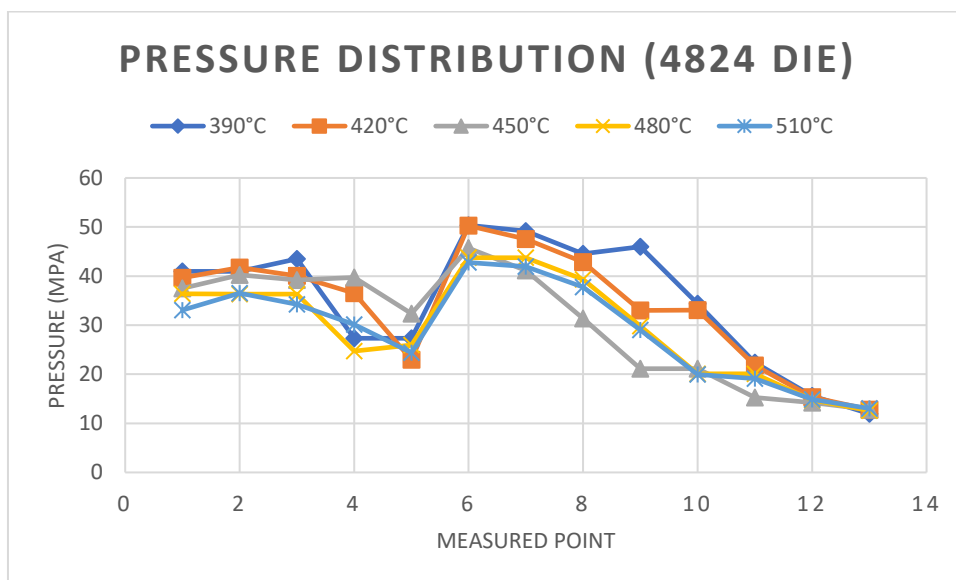
APPENDIX E: Graphs for Effect of Initial Die Temperature (4824 Die).



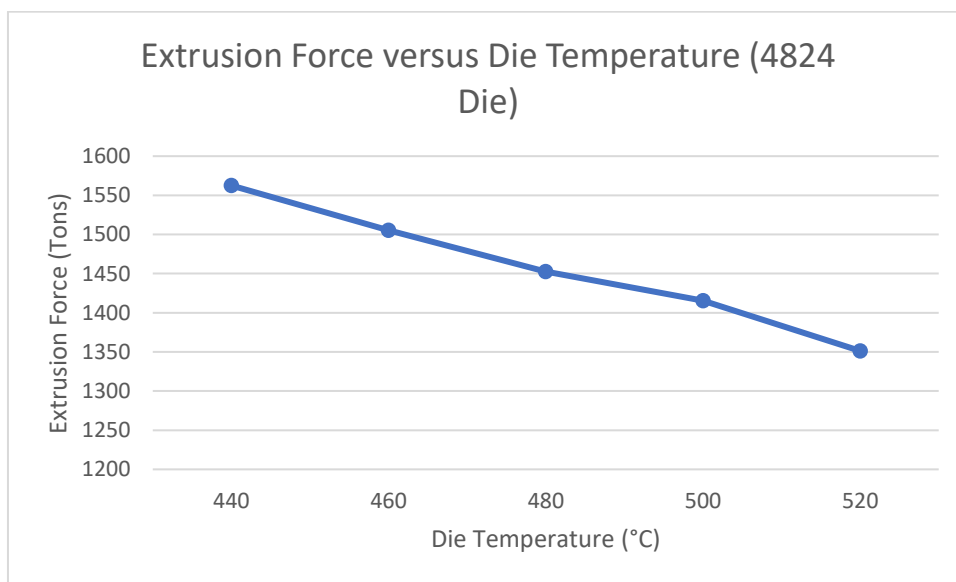
Graph E-1: Effect of Initial Die temperature on Temperature Distribution at Measured Points (48234 Die).



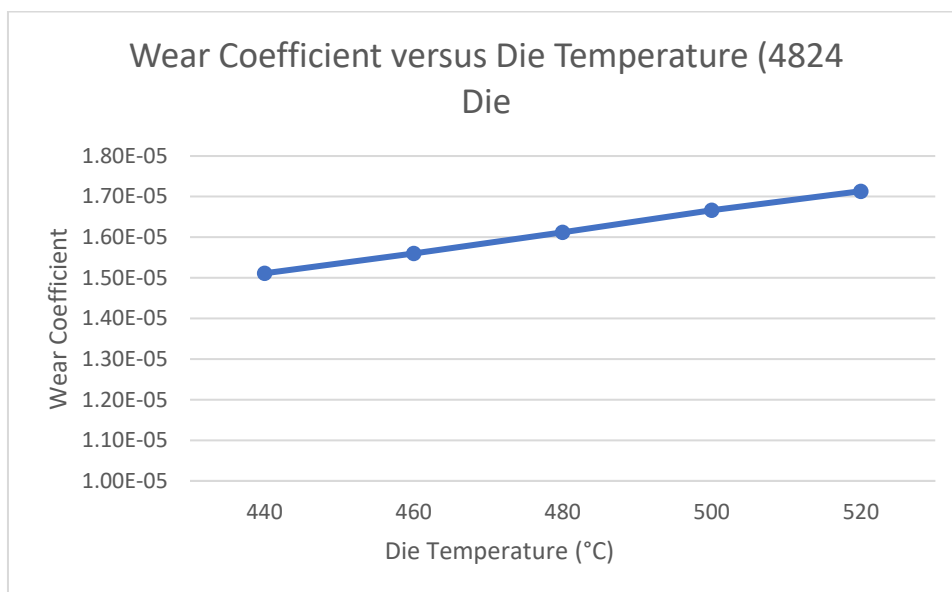
Graph E-2: Effect of Initial Die Temperature on Average Die Temperature and billet Temperature (4824 Die).



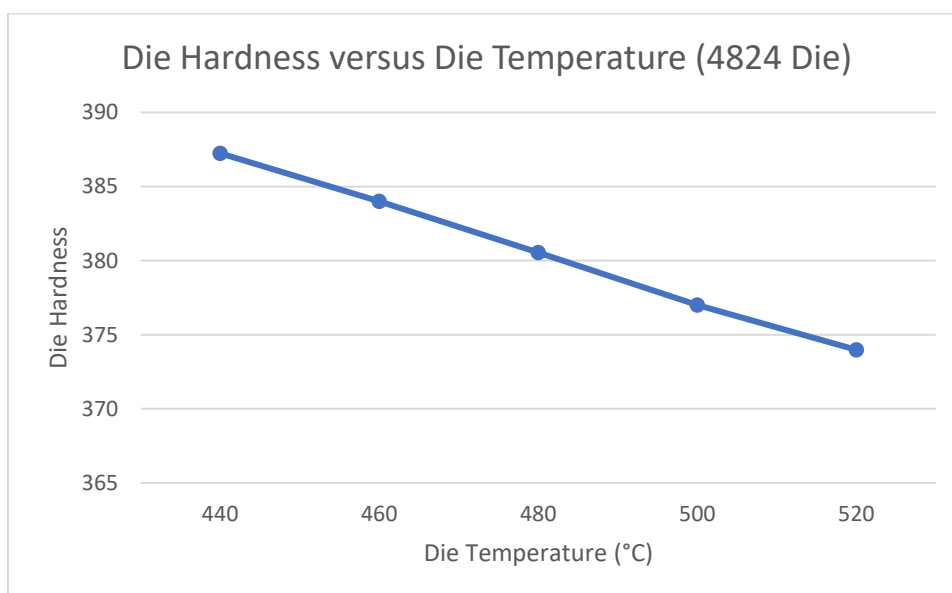
Graph D-3: Effect of Initial Die Temperature on Pressure Distribution at Measured Points (4824 Die).



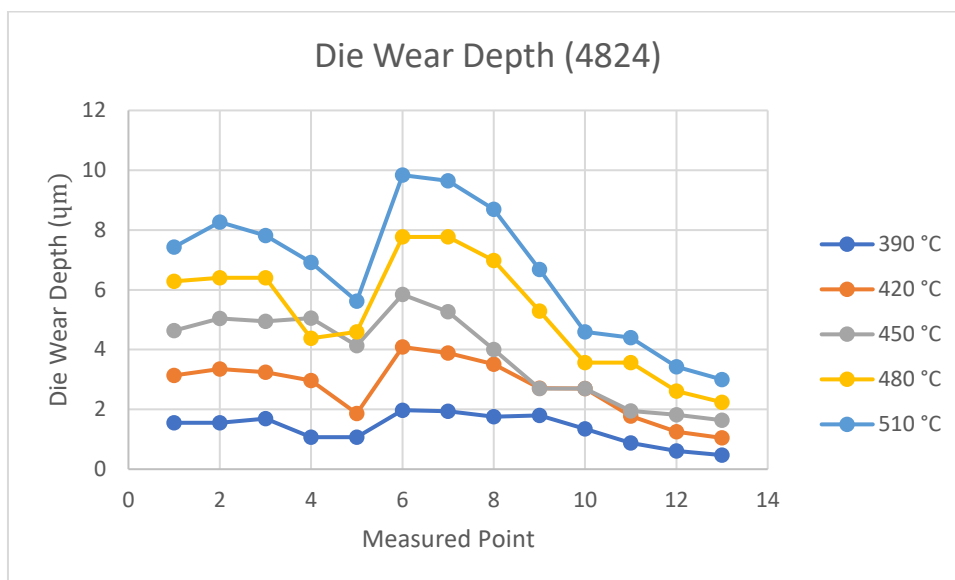
Graph E-4: Effect of Initial Die Temperature on Extrusion Force (4824 Die).



Graph E-5: Effect of Initial Die Temperature on Wear Coefficient (4824 Die).



Graph E-6: Effect of Initial Die Temperature on Die Hardness (4824 Die).



Graph E-7: Effect of Initial Die Temperature on Die Wear Depth at Measured Points (4824 Die).

APPENDIX F: Tables of Maximum Extruded Length Under Various Initial Die Temperature (4823 Die and 4824 Die).

Table F-1: Effect of Initial Die Temperature on Maximum Extruded Profile Length for 4823 Die.

Initial Die Temperature (°C)	Wear Depth of Bearing per Cycle, W_{max} (m)	Number of Cycles, x	Maximum Extruded Profile Length, L (m)
390	2.220×10^{-6}	67.573	188.826
420	4.444×10^{-6}	33.750	94.311
450	6.495×10^{-6}	23.093	64.532
480	8.956×10^{-6}	16.749	46.803
510	1.119×10^{-6}	13.399	37.442

Table F-2: Effect of Initial Die Temperature on Maximum Extruded Profile Length for 4824 Die.

Initial Die Temperature (°C)	Wear Depth of Bearing per Cycle, W_{max} (m)	Number of Cycles, x	Maximum Extruded Profile Length, L (m)
390	1.974×10^{-6}	75.970	212.344
420	4.087×10^{-6}	36.705	102.592
450	5.841×10^{-6}	25.680	71.776
480	7.768×10^{-6}	19.309	53.972
510	9.836×10^{-6}	15.251	42.6272